Republic of Iraq
Ministry of Higher Education and Scientific Research
University of Misan/Collage of Engineering
Department of Civil Engineering

STRUCTURAL BEHAVIOR OF SCREENED OPENINGS OF REINFORCED CONCRETE SHEAR WALLS

A thesis submitted in partial fulfillment of the requirements for the Master of Science degree in Civil Engineering
University of Misan

Prepared By
Ali Mahmoud Abbas
B.Sc. civil engineering, 2018

Supervisors: Prof. Dr. Sa'ad Fahad Resan

Assist. Prof. Dr. Hayder Al-Khazraji

November 2024

﴿اقْرَأْ بِاسْمِ رَبِّكَ الَّذِي خَلَقَ ۝١ خَلَقَ الْإِنْسَانَ مِنْ عَلَقٍ ۝٢ اقْرَأْ
وَرَبُّكَ الْأَكْرَمُ ۝٣ الَّذِي عَلَّمَ بِالْقَلَمِ ۝٤ عَلَّمَ الْإِنْسَانَ مَا لَمْ يَعْلَمْ ۝٥﴾

(العلق)

صَدَقَ اللهُ العَلِيُّ العَظيم

DEDICATION

❖ To whom stood beside me and took care of me over the years, to my parents, family, wife, my son and close friend.

❖ To all those who supported and helped me, made the difficult easy, especially to my supervisor

Prof. Dr. Sa'ad Fahad Resan

Assist. Prof. Dr. Hayder Al-Khazraji

I present my effort to them with all of my respect and appreciation.

ACKNOWLEDGEMENTS

First and foremost, I offer my sincere thanks to **Allah**, who guided me throughout the process of completing this work.

I would like to express my heartfelt gratitude and deep appreciation to my supervisors, **Prof. Dr. Saad F. Resan** and **Assist. Prof. Dr. Hayder Al-Khazraji**, for their invaluable guidance, advice, and constant support during the course of this study. Their encouragement played a crucial role in shaping this work.

I am also deeply grateful to **Prof. Dr. Abbas Oda Dawood**, Dean of the College of Engineering, and **Assist. Prof. Dr. Murtada Abass Abd Ali**, Head of the Civil Engineering Department, for their continuous support and assistance.

My heartfelt thanks go to **my family-my parents**, **my wife**, and my sons, **Hassan** and **Mohammed** -for their unwavering love, patience, and encouragement. I also extend my sincere gratitude to **my friends**, whose support and contributions were vital to the completion of this work.

A special thanks to **Mr. Abd Elkodous Joudah** for his invaluable assistance throughout this thesis.

Finally, I would like to express my sincere appreciation to **Prof. Dr. Ali Hameed Aziz** and **Assist. Prof. Dr. Nasser Hakeem Tu'ma** for their generous support and insightful contributions to this research.

SUPERVISOR CERTIFICATION

I certify that the preparation of this thesis entitled " **Structural Behavior of Screened Openings of Reinforced Concrete Shear Walls**" was presented by "**Ali Mahmoud Abbas**", and prepared under my supervision at The University of Misan, Department of Civil Engineering, College of Engineering, as a partial fulfillment of the requirements for the degree of Master of Science in Civil Engineering (Structural Engineering).

Signature:

Prof. Dr. Sa'ad Fahad Resan

Date:

Signature:

Assist. Prof. Dr. Hayder Al-Khazraji

Date:

In view of the available recommendations, I forward this thesis for discussion by the examining committee.

Signature:

Assist Prof. Dr. Murtada Abass Abd Ali

(Head of Civil Eng. Department)

Date:

EXAMINING COMMITTTEE'S REPORT

We certify that we, the examining committee, have read the thesis titled **(Structural Behavior of Screened Openings of Reinforced Concrete Shear Walls)** which is being submitted by **Ali Mahmoud Abbas**, and examined the student in its content and in what is concerned with it, and that in our opinion, it meets the standard of a thesis for the degree of Master of Science in Civil Engineering (Structures).

Signature:
Name: **Prof. Dr. Sa'ad Fahad Resan**
(Supervisor)
Date:

Signature:
Name: **Assist. Prof. Dr. Hayder Al-Khazraji**
(Supervisor)
Date:

Signature:
Name: **Prof. Dr. Ali Hameed Aziz**
(Chairman)
Date:

Signature:
Name: **Assist. Prof. Dr. Nasser Hakeem Tu'ma**
(Member)
Date:

Signature:
Name: **Assist Prof. Dr. Murtada Abass Abd Ali**
(Member)
Date:

Approval of the College of Engineering:

Signature:
Name: **Prof. Dr. Abbas Oda Dawood**
Dean, College of Engineering
Date:

ABSTRACT

This study investigates the impact of multiple openings on structural performance of reinforced concrete shear walls. An experimental program was conducted on nineteen square-shaped shear wall specimens, each with a 600 mm side length. The study examined the effect of opening size and shape (square and circular), wall thickness at 80, 100, and 120 mm, concrete strength at 30, 45, and 60 MPa, and the diagonal reinforcement pattern around the openings.

The results indicate that increasing the opening size in reinforced concrete shear walls leads to a reduction in ultimate load capacity. For opening ratios of 7.1%, 11.1%, 16.0%, and 21.8%, walls with square openings exhibit a decrease in load capacity of up to 81% at a 21.8% opening ratio, while circular openings reduce capacity by 76%. The shape of the opening plays a significant role, with circular openings showing a smaller impact on load capacity compared to square openings at lower opening ratios (7.1%, 11.1%, and 16.0%). Furthermore, increasing the wall thickness from 80 mm to 120 mm at a 16.0% opening ratio enhances load capacity by up to 39% for square openings and 58% for circular openings. Similarly, increasing concrete strength from 30 to 60 MPa improves load capacity by 33% for square openings and 17% for circular openings. These results suggest that walls with circular openings benefit more from increased thickness, while walls with square openings gain more from increased concrete strength in terms of load capacity.

Regarding ductility and energy absorption, the size and shape of the openings significantly affect these properties. At an opening ratio of 21.8%, square openings increase ductility by 23% and reduce energy absorption by 81%, while circular openings increase ductility by 10% and reduce energy absorption by 66%. Additionally, increasing wall thickness at a 16.0% opening ratio improves ductility

by 34% for square openings and 4% for circular openings, with energy absorption increasing by 160% and 104%, respectively. Moreover, increasing concrete strength from 30 to 60 MPa enhances ductility by 11% for square openings and 19% for circular openings, with energy absorption increasing by 77% and 29%, respectively. Additionally, the first model, which includes diagonal reinforcement around circular openings at a 7.1% opening ratio, shows a 12% increase in ductility and an 80% increase in energy absorption, demonstrating significant improvements compared to the second model.

The study also examines the impact of openings on shear stiffness. A square opening with a 21.8% ratio results in a 74% reduction in stiffness, while a circular opening with the same ratio decreases stiffness by 80%. Circular openings reduce stiffness less than square ones, particularly at opening ratios of 7.1%, 11.1%, and 16.0%. Increasing wall thickness at a 16.0% opening ratio enhances shear stiffness by 18% for square openings and 50% for circular openings. Similarly, increasing concrete strength boosts stiffness by 51% for square openings and 35% for circular openings when concrete strength increases from 30 to 60 MPa.

The study also evaluates the effect of diagonal reinforcement for walls with circular openings at a 7.1% ratio. Model 1, which includes two layers of conventional reinforcement with diagonal reinforcement, improves ultimate load capacity by 20% and slightly increases stiffness by 4%. In contrast, Model 2, with one layer of conventional reinforcement and diagonal reinforcement, shows a 2% increase in load capacity but a 5% decrease in stiffness compared to conventional reinforcement.

TABLE OF CONTANTS

LIST OF TABLES

LIST OF FIGURES

LIST OF SYMBOLES

f_{cu} Cube Compressive Strength in MPa

P_{cr} Cracking Load in kN

f_t Concrete Tensile Strength in MPa

$\emptyset$ Diameter of Reinforcement in mm

P_u Ultimate Load in kN

Δ_u Ultimate Displacement in mm

Δ_y Yield Displacement in mm

f_y Yield Strength in MPa

LIST OF ABBREVIATIONS

ACI	American Concrete Institute
ASTM	American Society of Testing and Material
BS	British Standard
ANSYS	Finite Element Computer Program
FEA	Finite element analysis
FEM	Finite element method
IQS	Iraqi Standard
LVDTs	Linear variable differential transformers
OPC	Ordinary Portland cement
R C	Reinforcement Concrete
R O	Reverse Osmosis
SP	Superplasticizer
tw	Wall Thickness
W/C	Water- cement ratio

CHAPTER ONE: INTRODUCTION

1.1 General

Tall buildings have attracted humans since the dawn of history. Since the 1880s, towering buildings have mostly served commercial and residential purposes due to urban population expansion and restricted space. A high-rise building is susceptible to axial and lateral loads. A building may experience lateral forces from a wind gust or the inertia of an earthquake. This force creates a state of instability within the structure, which then leads to failure within the building that may lead to the collapse of the structure [1].

Essentially, the requirements for stability (i.e., resistance against overturning moments) and rigidity (i.e., resistance to lateral deflection) grow increasingly significant. In a structure, these needs can be met in two different ways. The first is to enlarge members' sizes beyond and above the necessary strength. The second, advanced method of limiting deformation and enhancing stability is by changing the structure's form into one that is more rigid and stable. However, for structures higher than ten stories, the necessary lateral rigidity cannot be achieved by the frame action arising from the interactions of slabs and columns. It has become an uneconomical solution for tall construction as well. But shear walls, also known as structural walls, are so good at preserving the tall structures' lateral stability in high wind or seismic loads that they may be increased by positioning them strategically [2].

Shear walls have a major role in overall ductility, strength, and energy dissipation capability, in addition to lateral stiffness. Shear walls work by transferring the lateral loads acting on the building to the foundation, thus reducing the building's sway and minimizing the risk of structural failure during extreme

events like earthquakes or strong winds. They accomplish this by effectively resisting shear forces and bending moments induced by lateral loads [3].

In general, shear walls have a significant impact on the structural behavior of buildings, so many essential considerations should be taken when determining where to locate them. The best torsional resistance and stability for the entire structure may be achieved by placing the shear walls in the perimeter, intersection points, and core of the buildings, where Figure 1.1 shows several positions and types of shear walls[4]. Moreover, shear walls are erected around openings like windows, doors, and service openings to preserve structural integrity and avoid excessive distortion. However, based on seismic standards, building codes, structural research, and architectural considerations, the locations of these shear walls are carefully selected [5].

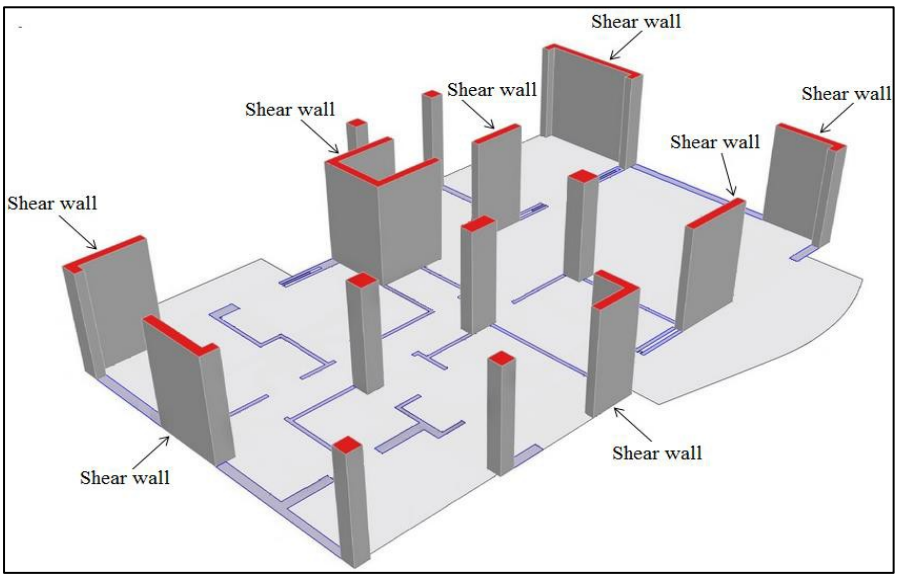

Figure 1.1 3-D view of a building with various shear wall locations and types.

Meanwhile, engineers must take into consideration cases in which shear walls need to have openings; this must be done in accordance with the engineering aims. However, there are some situations in which concrete shear walls without openings are unavoidable. These openings provide mechanical, plumbing, and electric

requirements in addition to architectural ones like installing windows and doors. On the other hand, structures with elevators and stairwells must have an opening that permits access to every part of the building. Though the size of the openings varies from one building structure to another, the effect of different opening sizes on a construction's stiffness is not consistent. A door-sized opening, for example, has a radically different effect on rigidity than a smaller opening, such as a window. Figure 1.2 displays many buildings with shear wall openings [6-8].

Figure 1.2 High-rise building with multiple openings in the shear walls.

The problem with openings is that engineers occasionally fail to consider how an opening will impact the structural responsiveness of the shear wall. In any case, it's critical to understand how openings impact the capacity of the shear wall to

withstand seismic activity and their overall performance. Figure 1.3 illustrates a shear failure mechanism that is not in favor [9, 10].

Figure 1.3 Shear failures of RC shear walls in Chile earthquake.

1.2 **Shear Wall Classification**

Many analyses and experimental studies have focused on the categorization of shear walls. Numerous studies concur that shear walls may be divided into various groups based on their (i) construction materials , (ii) aspect ratio and (iii) geometry[11, 12]:

1.2.1 **According to Construction Materials**

Shear walls are divided into several categories based on the structural materials they are built of. Some well-known varieties of shear walls include:

1. Steel plate shear walls
2. RC hollow concrete block masonry
3. Mid-ply shear wall
4. Wooden shear wall
5. Shear wall made of reinforced concrete.

Steel shear walls are primarily used in industrial structures due to their lower future costs compared to initial costs, offering a high strength-to-weight ratio. The

benefits of shear walls vary by location; timber walls are preferred in colder climates but are unsuitable for high-rise buildings due to their limited strength. Masonry shear walls are not recommended for buildings taller than four stories due to stability concerns. Meanwhile, RC shear walls are widely used in residential and commercial buildings, which explains the focus of many studies on this topic. Figure 1.4 illustrates the classification of shear walls according to structural materials.

Figure 1.4 Shear walls classification by material (A) steel plate, (B) reinforced concrete hollow block masonry, (C) mid-ply, (D) wooden, (E) reinforced concrete.

1.2.2 Based on the Aspect Ratio

The aspect ratio of a shear wall is the ratio between its height (H) and width (W), and it is crucial to structural engineering because it dictates how a shear wall will behave over time. The various kinds of shear walls that are available are categorized. Shear walls are typically thought of as being short when their aspect ratio is less than (1). Short walls, on the other hand, have always played a significant role in people's lives and have been since the 1920s, when they were primarily employed as a means of protection. Figure 1.5 shows shear wall classification according to the aspect ratio.

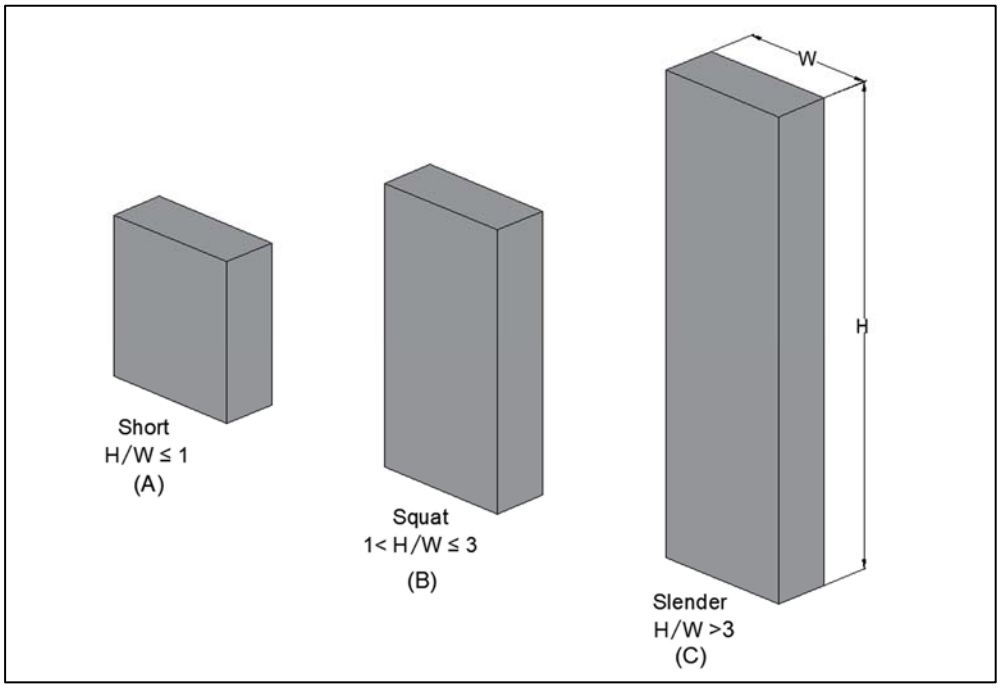

Figure 1.5 Shear wall classification according to aspect ratio (A) short shear wall, (B) squat shear wall, (C) slender shear wall.

In general, shear walls with an aspect ratio between (1) and (3) can be considered squat. According to Paulay and Priestley (1992), short, squat shear walls are undesirable as they are prone to brittle failure. Flexural behavior typically occurs in slender shear walls with an aspect ratio greater than (3) [13].

1.2.3 Geometry of Shear Wall

When studying the concept of geometric shear walls, it's important to note the variety of reinforced concrete shear walls available. Murthy (2004) identified several notable types, including core, column-supported, framed, coupled, flanged, rectangular, and bell-shaped shear walls. However, the most common and widely used types are flanged, bell-shaped, and rectangular shear walls [14].

1.3 Forces on Shear Wall

Shear and uplift forces are the two kinds of forces that shear walls resist. In stationary buildings, accelerations from ground movement as well as outside forces like wind and waves produce shear forces. Shear pressures are produced between the top and bottom shear wall connectors across the wall's height by this process. Shear walls experience uplift forces because the horizontal forces act on the wall's top. These uplift pressures aim to drive the wall's other end down while lifting the wall's upper end. The uplift force might occasionally be so great that it topples the wall [15].

1.4 Function of Shear Wall

The shear wall of a structure mainly resists lateral forces such as wind loads, seismic forces, and any other horizontal loads functioning perpendicular to the wall's plane. Shear walls are essential to a building's stability and strength. Here is an overview of the functions of shear walls: -

1. Lateral load Resistance: Shear walls are designed to withstand lateral forces that would cause the building to sway or deform. These forces are most typically experienced during windstorms, earthquakes, or other external loads that act horizontally on the building. Shear walls help to stabilize the building and avoid structural damage by resisting lateral loads.

2. Stiffness and Rigidity: Shear Walls provide large stiffness and rigidity to building in the direction of their orientation, which reduces lateral sway of the building and thus reduces damage to structure.

3. Withstanding shear and uplifting forces on the building.

4. Vertical Load Support: Shear walls support vertical loads from roofs, floors, and various other construction elements in addition to resisting lateral loads.

In general, the main purpose of shear walls is to ensure the structural integrity and safety of the structure by offering resistance to horizontal forces and lateral stability, particularly in areas where earthquakes or strong winds are common as shown in Figure 1.6 [16-19].

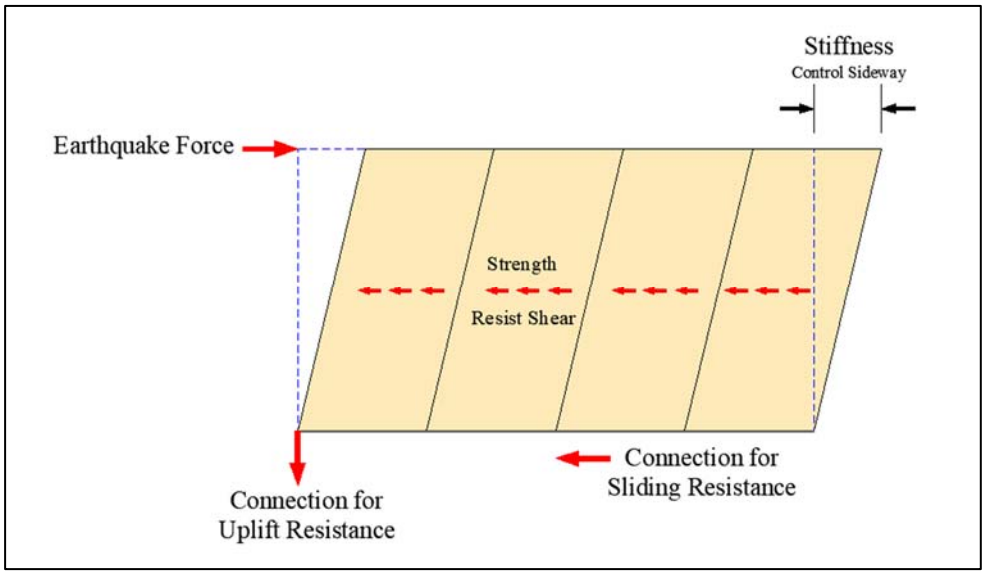

Figure 1.6 Functions of shear wall.

1.5 **Aim of Study**

This study aims to investigate the structural behavior of concrete shear walls with screen openings under various variables by testing nineteen specimens. The research will focus on examining the impact of different opening sizes and assessing how variations in opening size affect the structural performance of the walls.

Additionally, the study will explore the influence of different opening shapes on wall behavior.

The study will also evaluate the effects of various reinforcement patterns and their arrangements around the openings on the walls' efficiency. Furthermore, the impact of concrete strength variations on the structural properties of the walls will be assessed, along with the effect of wall thickness variations on their structural performance.

1.6 **Outline of Thesis**

The chapters of this study are as follows:

Chapter One: Covers the study's introduction, insights, aims, importance, and thesis structure.

Chapter Two: This chapter covers previous studies on the effect of many variables on concrete shear wall openings.

Chapter Three: Focuses on the experimental work; instruments, test procedures, characteristics of the tested shear wall, and testing and properties of the materials used in the investigation are all illustrated.

Chapter Four: Focuses on analyzing the data, study findings, and discussion.

Chapter Five: The final chapter of this thesis includes conclusions and recommendations for future works.

CHAPTER TWO: LITERATURE REVIEW

2.1 General

A concrete shear wall is a vertical structural element designed to resist lateral forces, such as those caused by wind and earthquakes that act on a building. These walls are particularly favored in high-rise structures like apartments, condominiums, and office buildings. However, to meet functional needs like windows and doors, shear walls often include various openings. From an architectural and functional perspective, the size and location of these openings can vary significantly. In many apartment buildings, the placement and dimensions of shear wall openings are often determined with little consideration for their effect on the building's structural performance.

2.2 Experimental Works

In 1988, Lin and Kuo conducted a comprehensive study on the ultimate strength of shear walls with openings subjected to lateral loads, utilizing both finite element analysis and experimental testing. They constructed and tested to failure a total of 13 shear wall panels, as illustrated in Figure 2.1. The specimen dimensions, shown in Figure 2.2, were approximately two-thirds the size of a prototype shear wall. Except for variations in opening size and reinforcement patterns around the openings, all wall units had identical boundary element dimensions and reinforcement details. When reinforcing bars were interrupted by an opening, various reinforcement configurations with differing amounts were applied around the openings, as depicted in Figure 2.1. The study’s findings indicated that the diagonal reinforcement around openings contributed up to 40% of its yield strength in shear strength, while the rectangular reinforcement configuration contributed only 20%. A strong correlation between the experimental results and the finite element

analysis was observed, especially when tensile stresses in the concrete were adequately relieved following section cracking. [20].

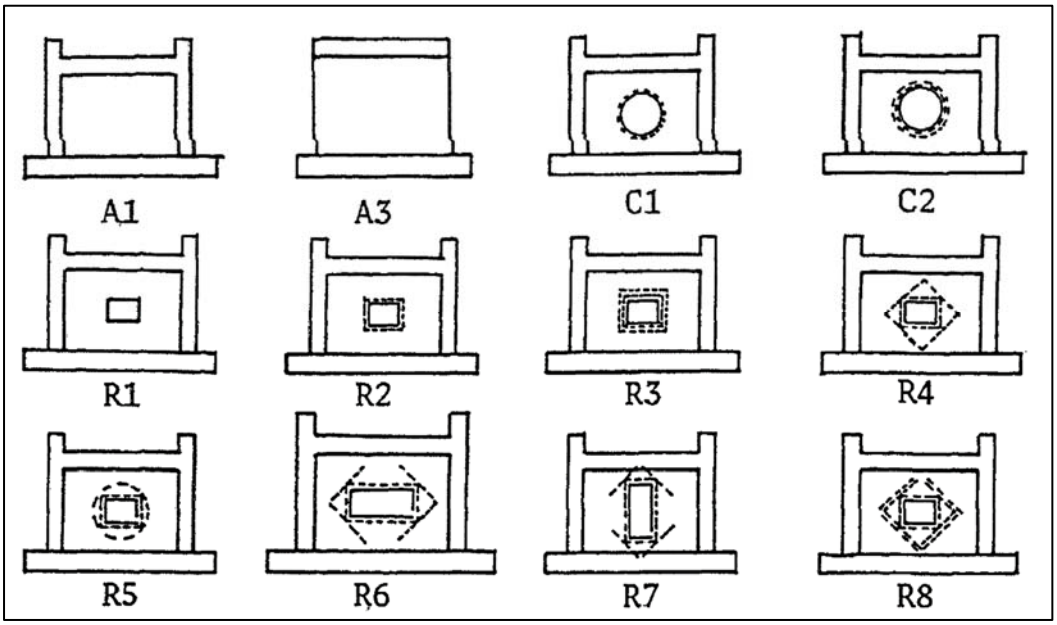

Figure 2.1 Test Specimens.

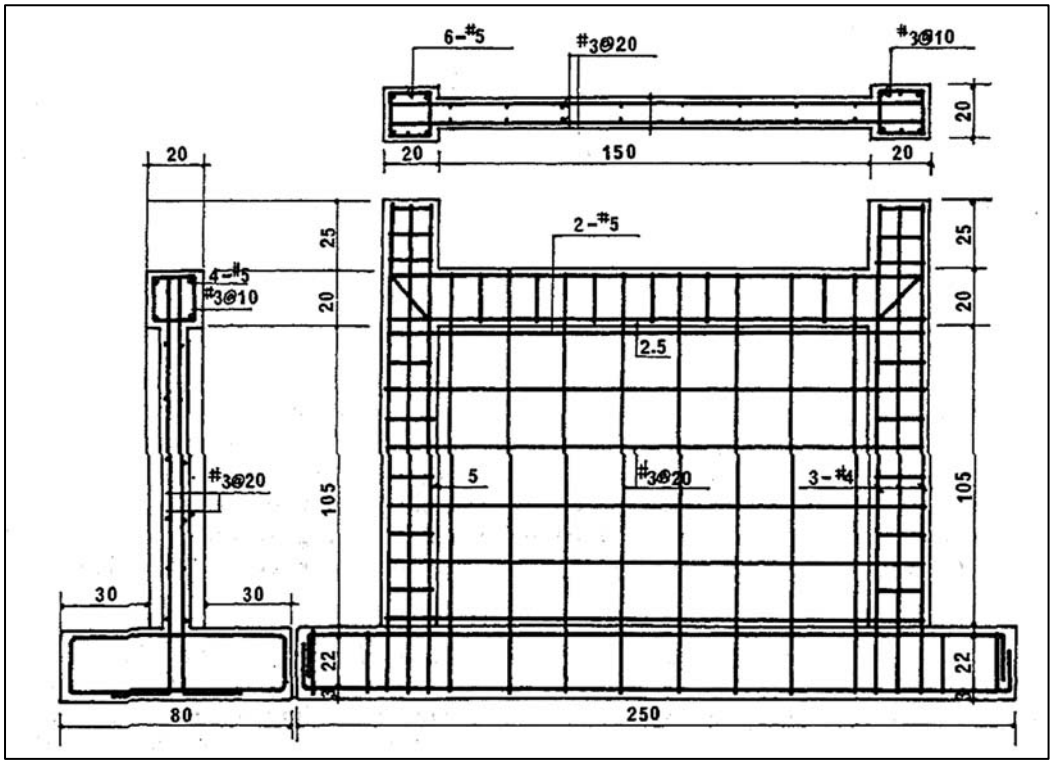

Figure 2.2 The dimension of test Specimen.

In 2012, Fragomeni et al. conducted a comprehensive experimental study on 47 reinforced concrete shear walls with various opening configurations, as shown in Figure 2.3. These walls were tested under both one-way and two-way loading conditions, as illustrated in Figure 2.4. The panels had slenderness ratios of 30, 35, and 40, and were subjected to a uniformly distributed axial load applied with an eccentricity of tw/6 (where tw denotes the thickness of the wall). The study included detailed descriptions of the experimental setup, failure modes, crack patterns, and load-displacement behavior of the panels. The design equation from the Australian Standard for walls was used to compare the experimentally observed failure loads with predicted values. The results indicated that both failure loads and crack patterns were significantly influenced by the opening configuration and support conditions. Notably, two-way panels with openings showed failure loads approximately two to four times higher than those of comparable one-way panels with openings. Furthermore, increasing the number of openings from one to two led to a reduction in failure loads. For one-way panels, a decrease in axial strength ratios was observed as the slenderness ratios increased from 30 to 40 [21].

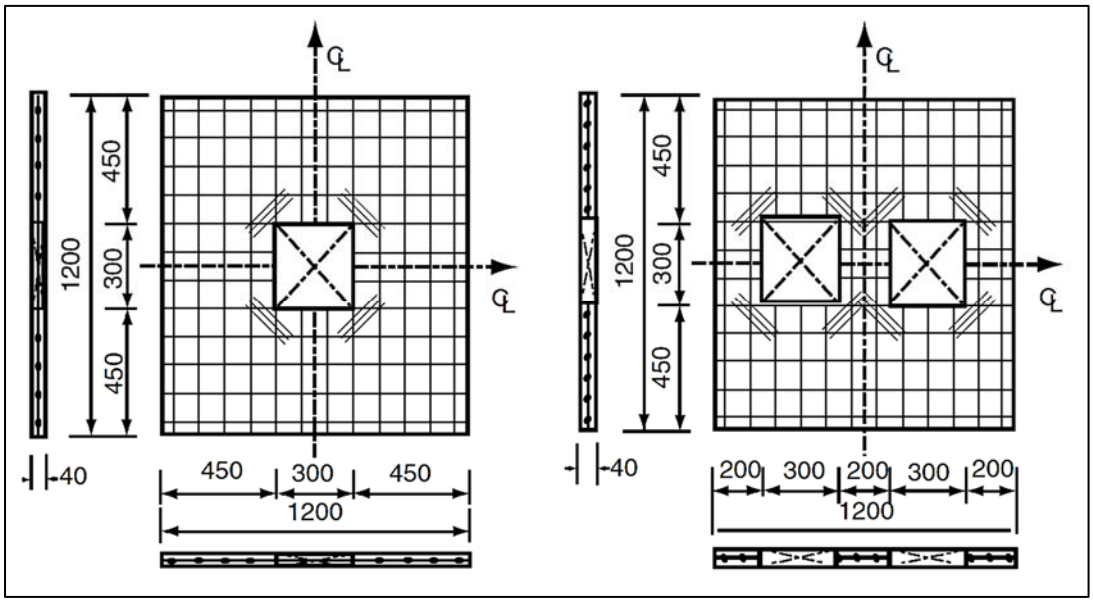

Figure 2.3 Details of typical test wall panels with one and two openings.

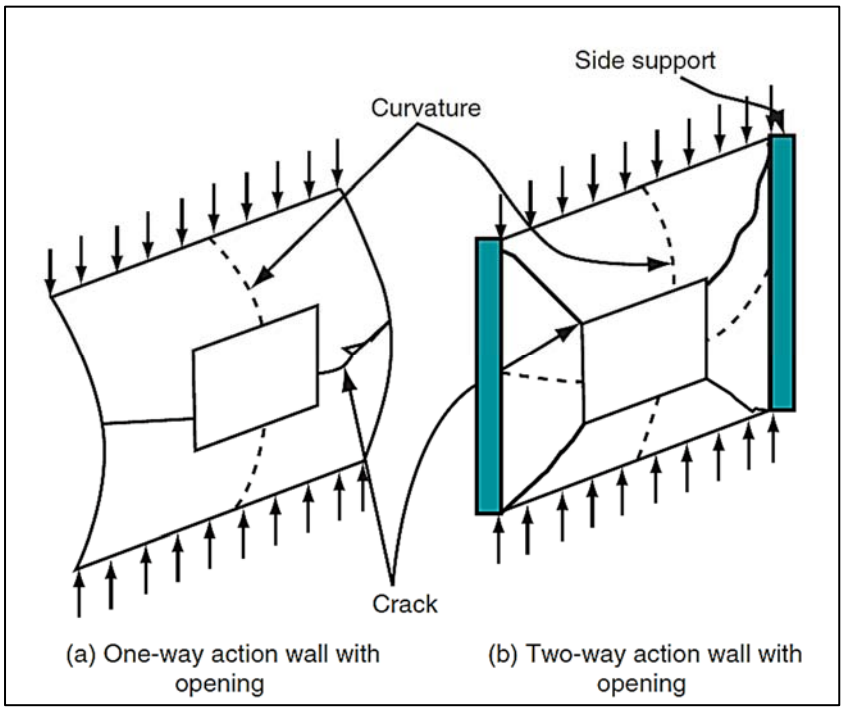

Figure 2.4 Walls with and without side supports (Doh and Fragomeni 2006).

In 2012, Wang J. et al. conducted tests on three scaled-down (40%) reinforced concrete (RC) structural walls with eccentric openings, as illustrated in Figure 2.5. Each wall spanned three stories and included a single opening with varying area ratios. These walls were subjected to lateral reverse cyclic loading until significant shear damage occurred. The primary aim of the tests was to assess the impact of different opening ratios on the cracking behavior and shear strength of structural walls under cyclic loading. All specimens were specifically designed to fail in shear rather than in flexure. The opening ratios for specimens S1, M1, and L1 were 0.3, 0.34, and 0.46, respectively. The results indicated that the shear strength of the structural walls varied with the loading direction due to the eccentric position of the openings. Loading from the side of the opening resulted in a significant increase in shear strength compared to loading from the opposite direction. Eccentric openings disrupt the shear transfer mechanism and can cause concrete damage at the corners of the openings, ultimately leading to wall failure [22].

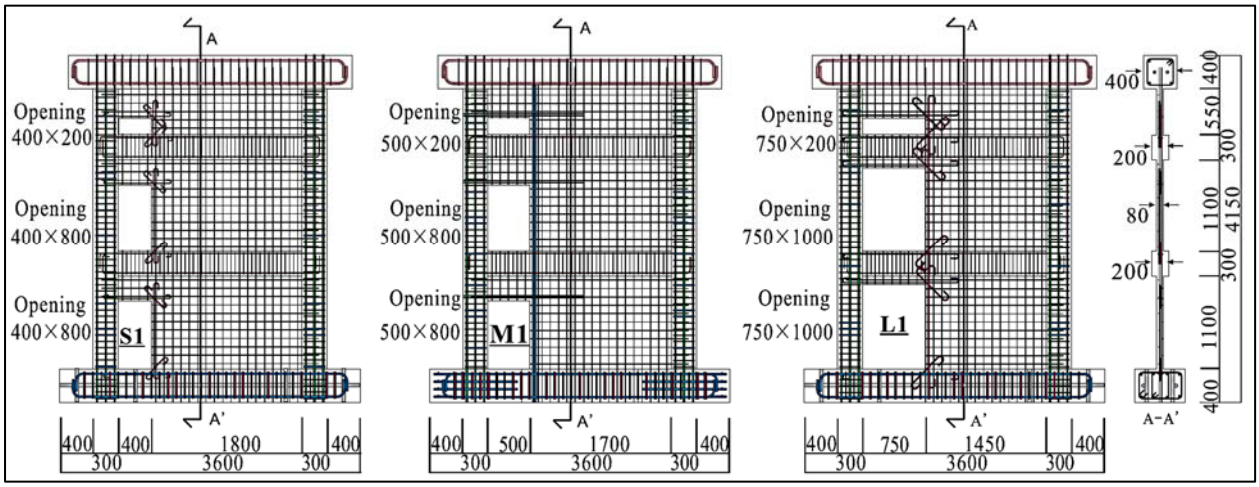

Figure 2.5 Dimensions and reinforcement arrangement (all dimensions in mm).

In 2015, Marsono A. K. and Hatami S., identified that rectangular openings were the most commonly used shape for shear wall openings in designs for windows, parking entrances, doors, stairwells, or elevators. To enhance the performance of coupling beams, they recommended using octagonal openings and adding haunches at the corners of rectangular openings. Their study investigated the behavior of coupling beams under cyclic loading, comparing shear walls with a single band of octagonal openings to those with rectangular openings.

To assess the effect of adding haunches to the corners of rectangular openings in shear walls, two 1:30 scale models were selected for laboratory testing: Model 1, a shear wall with a single band of rectangular openings, and Model 2, a shear wall with a single band of octagonal openings with haunches measuring 25 mm in width and 25 mm in height. The geometries of the specimens are shown in Figure 2.6. These models were specifically designed to capture the influence of opening shapes and haunches on the shear wall's behavior under cyclic loading.

The experimental results showed that coupling beams in shear walls with octagonal openings demonstrated higher strength compared to those in shear walls with rectangular openings [23].

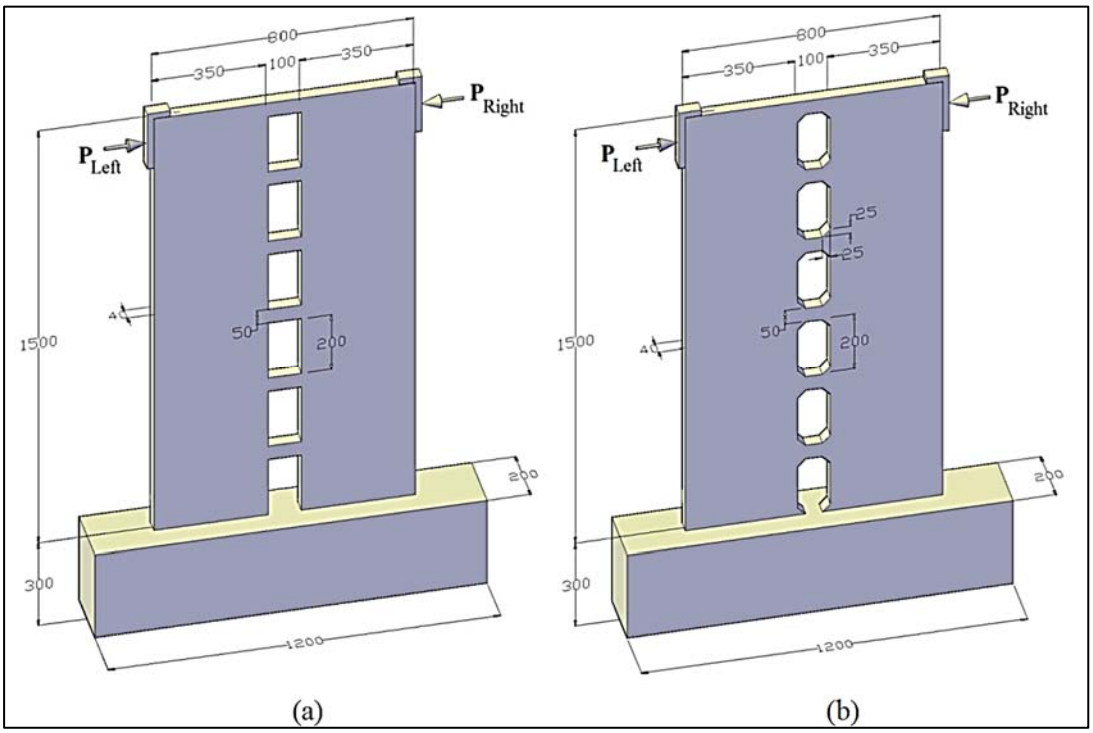

Figure 2.6 Layouts of shear walls with single band of a) rectangular openings (Model 1) b) octagonal openings (Model 2)

In 2015, Li, Bing, Pan, Zuanfeng, and their colleagues analyzed the earthquake performance of three lightly concrete shear walls with openings when exposed to cyclic loading. The study focused on three models: a solid wall as a control sample and two walls containing openings that were either regular or irregular. The results showed that all three models failed due to the rupture of the outer reinforcement bars and concrete crushing in the compression zone, leading to significant spalling near the base. The model with five openings exhibited a degradation in ultimate strength and stiffness similar to the control sample. On the other hand, the model with nine openings had lower ultimate strength but was more flexible, with a slower degradation in stiffness and an increase in shear contribution compared to the control sample. Furthermore, models for bracing and connections were developed to estimate the ultimate strength of the walls with openings, resulting in outcomes that aligned with the experimental observations [24].

In 2016, Popescu, Cosmin, Gabriel, and their colleagues studied the effect of openings on the axial strength of large concrete wall panels. The study included three half-scale shear walls with large and small door-shaped openings, as illustrated in Figure 2.7, which were subjected to slight eccentricity and a uniformly distributed axial load. The results indicated that the load-bearing capacity decreased by approximately 36% and 50% due to a reduction in the cross-sectional area of the solid shear wall by 25% and 50%, respectively, as a result of adding the small and large openings [25].

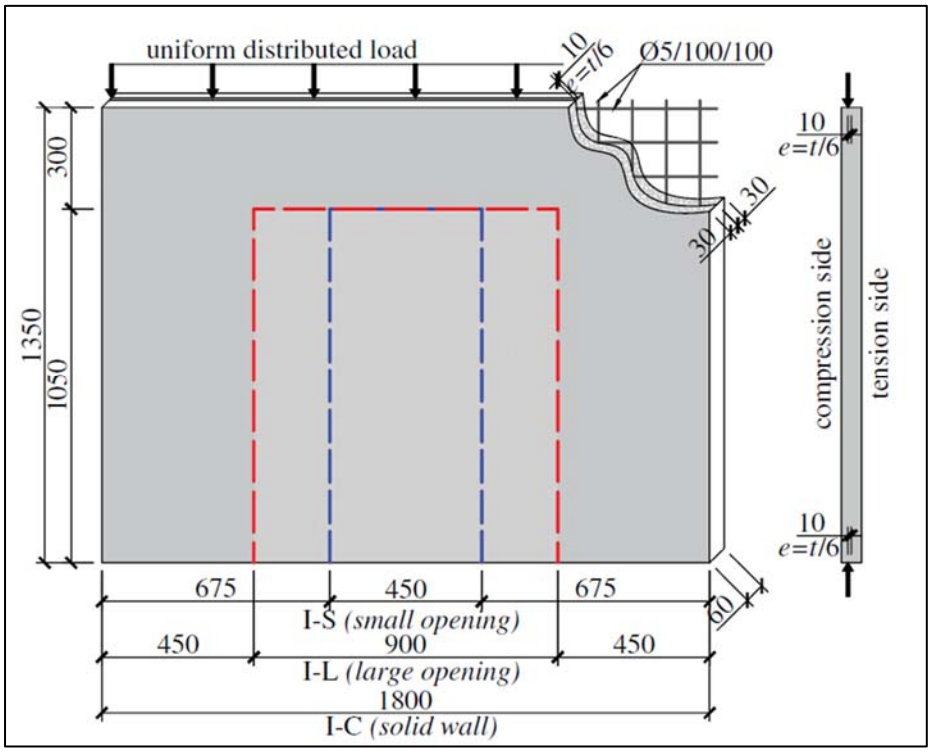

Figure 2.7 (Color) Configuration and details of the tested walls.

In 2018, Ali et al., conducted an experimental study to investigate the structural behavior of shear walls with axial loads containing openings. In this study, 26 shear walls with dimensions of 700 × 700 mm were cast and tested using the diagonal compression method, as illustrated in Figure 2.8. This study considers three variables: aspect ratio, opening size and opening inclination angle. The experimental

results show that thickness has a significant impact on the structural response of RC shear walls, especially those with openings. When the thickness of the sample increases from 100 mm to 150 mm, the maximum load increases by 18%, while the maximum load increases by 100% in samples with openings when the wall thickness is increased from 100 mm to 150 mm. Furthermore, the results indicate that the opening is the main reason for the reduction in maximum load in shear walls. When the opening size increases from 3% to 8%, the maximum load of the sample decreases by 48%. The effect of the inclination angle is less than that of the opening size. Cracks in samples with small openings start from the opening angle and propagate towards the support and load area, while cracks in samples with large openings start from the opening angle and grow towards the nearest edge. Also, the ultimate displacement for all models was recorded as shown in Figure 2.9, which illustrates the load-displacement curves for all models with openings at angles of 0, 15, 30, and 45 degree .In addition, compressive and tensile strains were also recorded for all models, as shown in Figures 2.10 to 2.13, shows the strain and load curves for all models with openings at angles of 0, 15, 30, and 45 degrees [26].

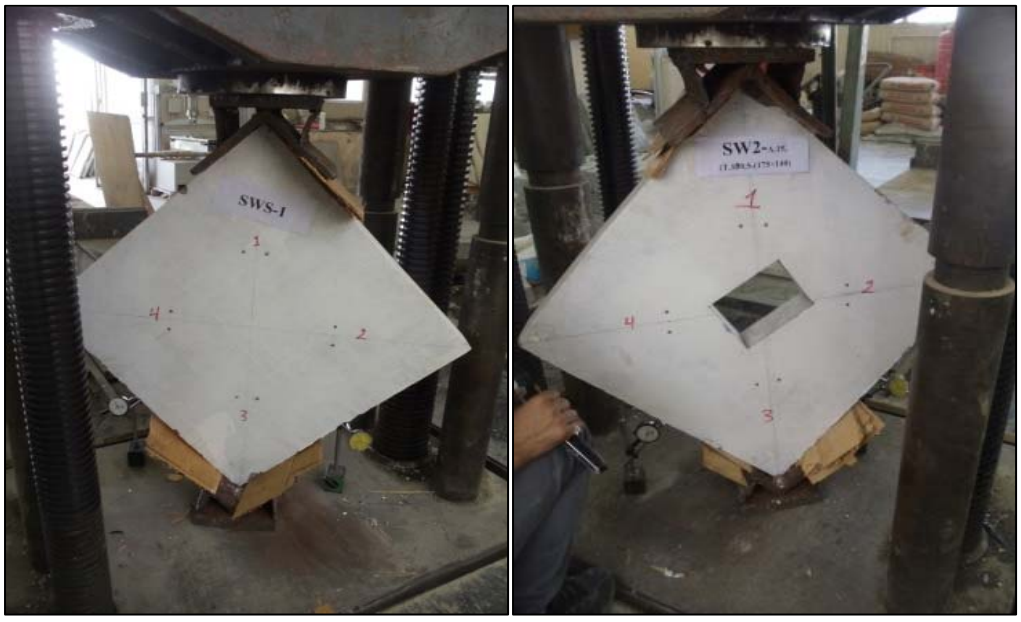

Figure 2.8 Method of testing models under diagonal compression.

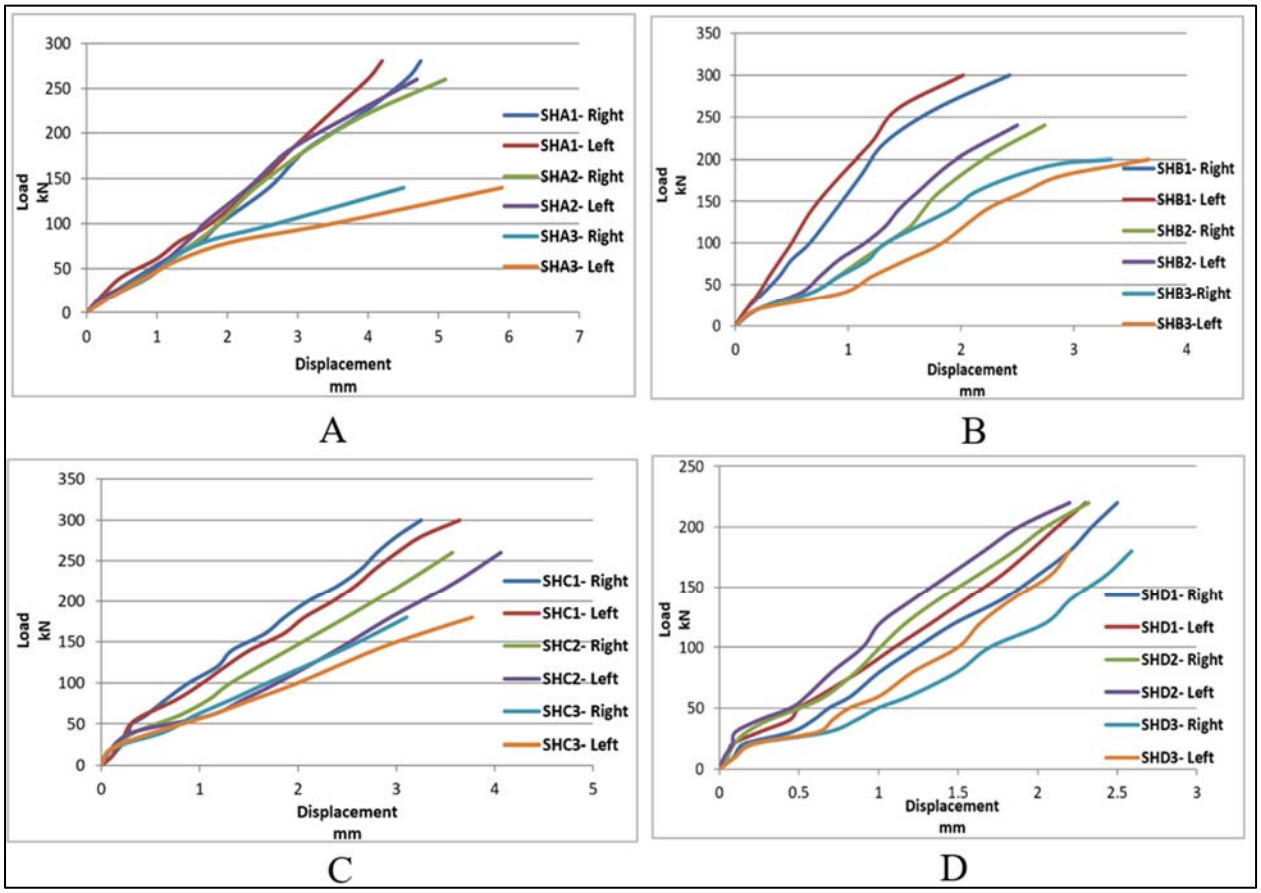

Figure 2.9 Load-displacement curves for shear walls with opening thickness 100 mm and angle (A-0°, B-15°, C-30°, and D-45°).

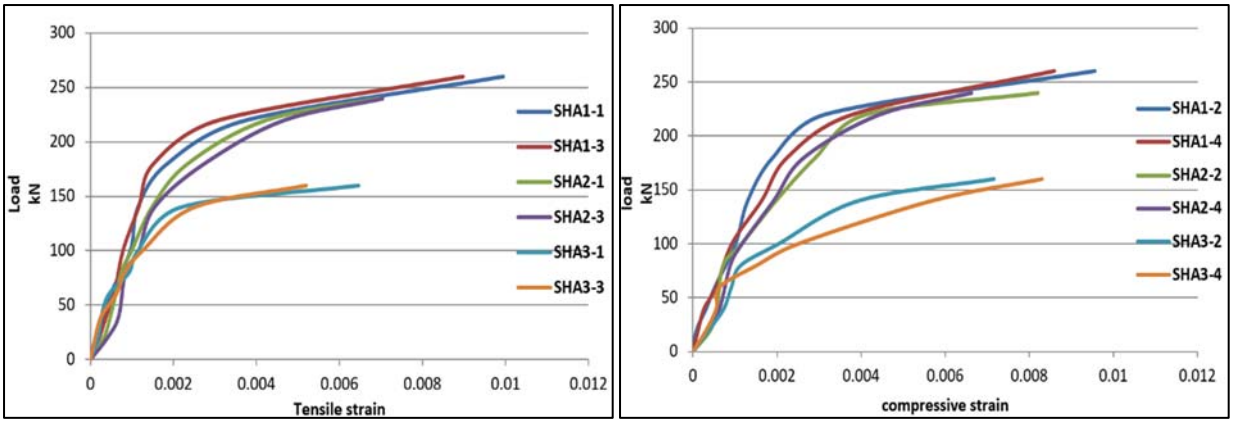

Figure 2.10 Tensile and compressive strain of shear wall with opening thickness 100 mm and angle 0°.

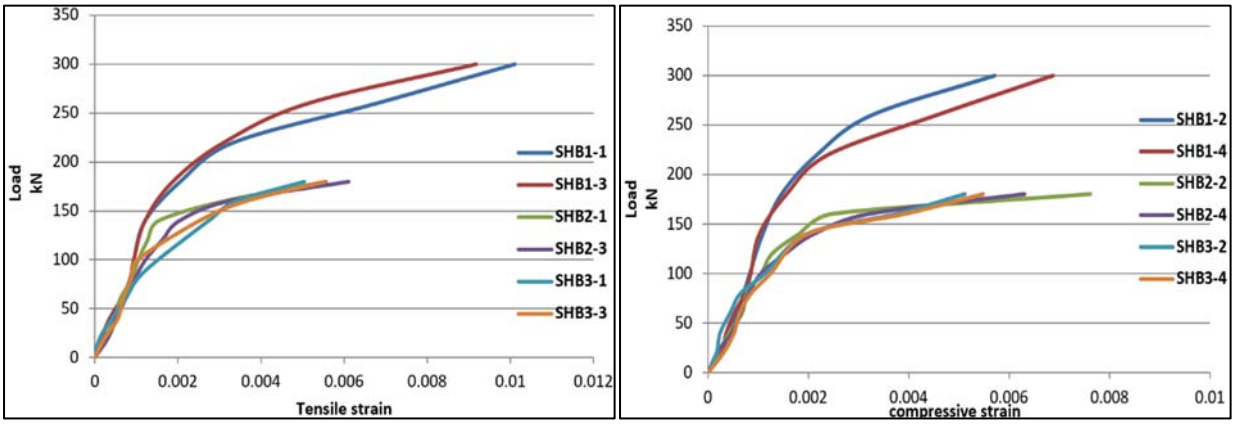

Figure 2.11 Tensile and compressive strain of shear wall with opening thickness 100 mm and angle 15°.

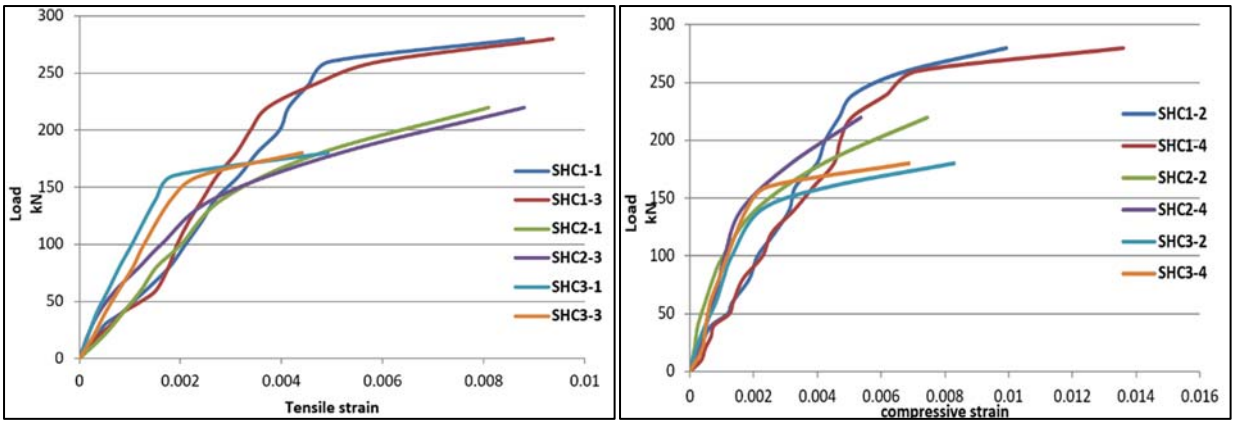

Figure 2.12 Tensile and compressive strain of shear wall with opening thickness 100 mm and angle 30°.

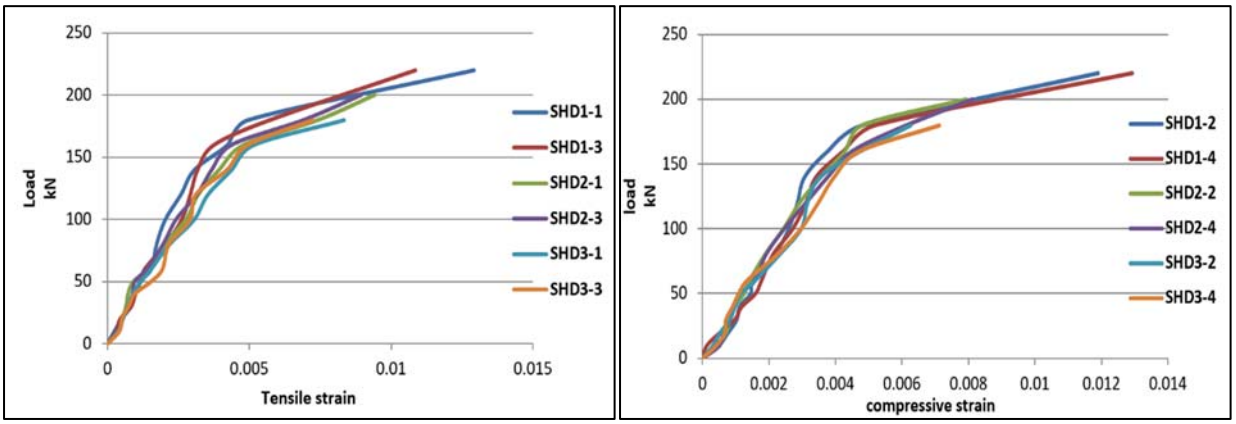

Figure 2.13 Tensile and compressive strain of shear wall with opening thickness 150mm and angle 45°.

In 2019, Massone, L. M. et al., conducted an experimental and numerical analysis on slender shear walls with central openings at the base, focusing on the influence of opening size and shape on structural performance. Four RC walls with dimensions of 2650 mm high, 900 mm long, and 150 mm thick were designed and constructed with an opening at the base, using common characteristics in Chilean construction. The openings varied between 15% and 30% of the wall's length and 11% and 22% of its height. The specimens were subjected to constant axial loads and cyclic lateral loads applied at the top. Results showed that while lateral strength remained consistent across all cases, displacement capacity decreased with increased opening size, particularly in specimens with wider openings, where displacement capacity was reduced by approximately 30%. Additionally, the width of the opening had a more significant effect on displacement capacity than its height. Numerical analysis using finite element modeling confirmed these findings, demonstrating that simplified flexural models can effectively capture the essential parameters of strength, stiffness, and displacement capacity [27].

In 2021, Hisham et al. investigated the effect of different openings in shear walls to determine the effectiveness of openings on the strength and stiffness of reinforced walls. The experimental program included four reinforced concrete shear walls with the same dimensions and reinforcing details. The dimensions of the walls were 1000 mm × 2000 mm with a thickness of 150 mm. These walls contained varying openings for lateral loads. The program was designed to investigate the impact of different opening sizes, reinforcement arrangements around the openings, and the locations of the openings. Lateral stiffness and horizontal displacements of the shear walls with openings were studied. According to the results, having two vertical openings in the center was found to be preferable to having a single central opening, as the latter reduces the stiffness of the wall. Moreover, the size of the openings had

a greater effect on the stiffness of the shear wall structure than the arrangement of the openings when the opening area was less than 20% of the shear wall area. However, when the opening area exceeded 20% of the total area of the shear wall, the configuration of these openings significantly affected the system's stiffness [28].

In 2022, Tafheem et al. conducted a study on the impact of openings in reinforced concrete (RC) walls on their stiffness and strength. The performance of RC walls is influenced by several factors, including the size, shape, and location of openings, the reinforcement around them, and the failure mode (whether flexural or shear). However, the individual effects of these factors on RC wall performance are not fully understood. This study focused on experimentally investigating the effects of two specific factors: the size of the opening and the additional reinforcement around the openings. Six RC wall specimens were tested using an innovative setup capable of applying pure cyclic shear loads, as shown in Figures 2.14 and 2.15.

The results indicated that strength decreases linearly with an increase in opening size, while initial stiffness follows a nonlinear trend, showing a significant drop in stiffness for larger openings. Additionally, the study found that additional reinforcement around the openings enhances the maximum strength of the walls but has a minimal effect on initial stiffness. The proposed analytical model for initial stiffness was validated against experimental results, showing good agreement with the tests.

Regarding failure, it involved sudden strength loss due to concrete crushing, with diagonal cracks starting at the corners of the openings and widening near the wall corners. Fewer but wider cracks were observed in specimens with larger openings, while specimens with additional reinforcement showed more cracks than those without [29].

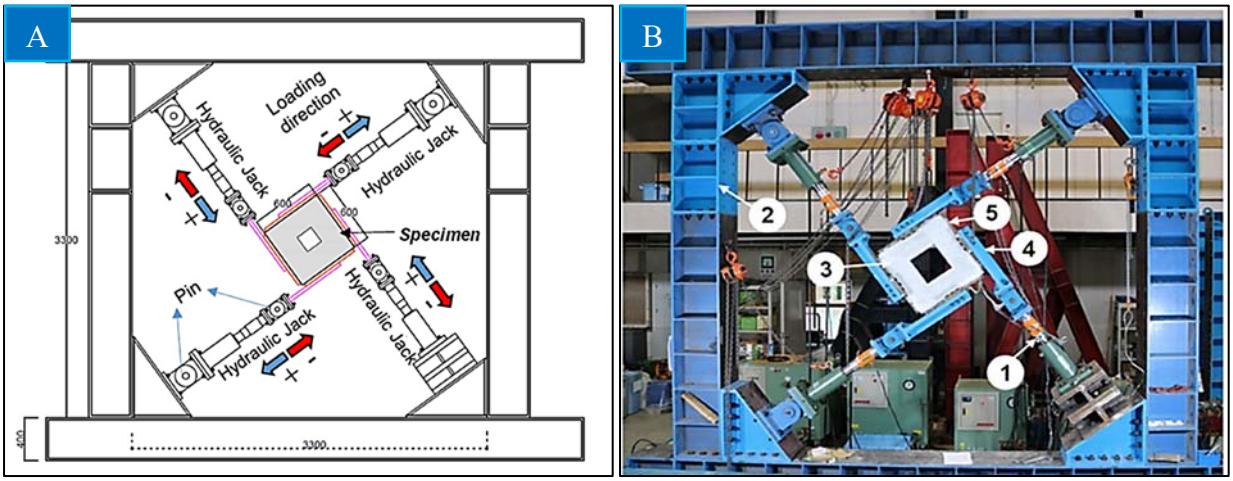

Figure 2.14 The machine used for testing in this study (A) schematic diagram of the test setup, (B) Photographic view of the test setup.

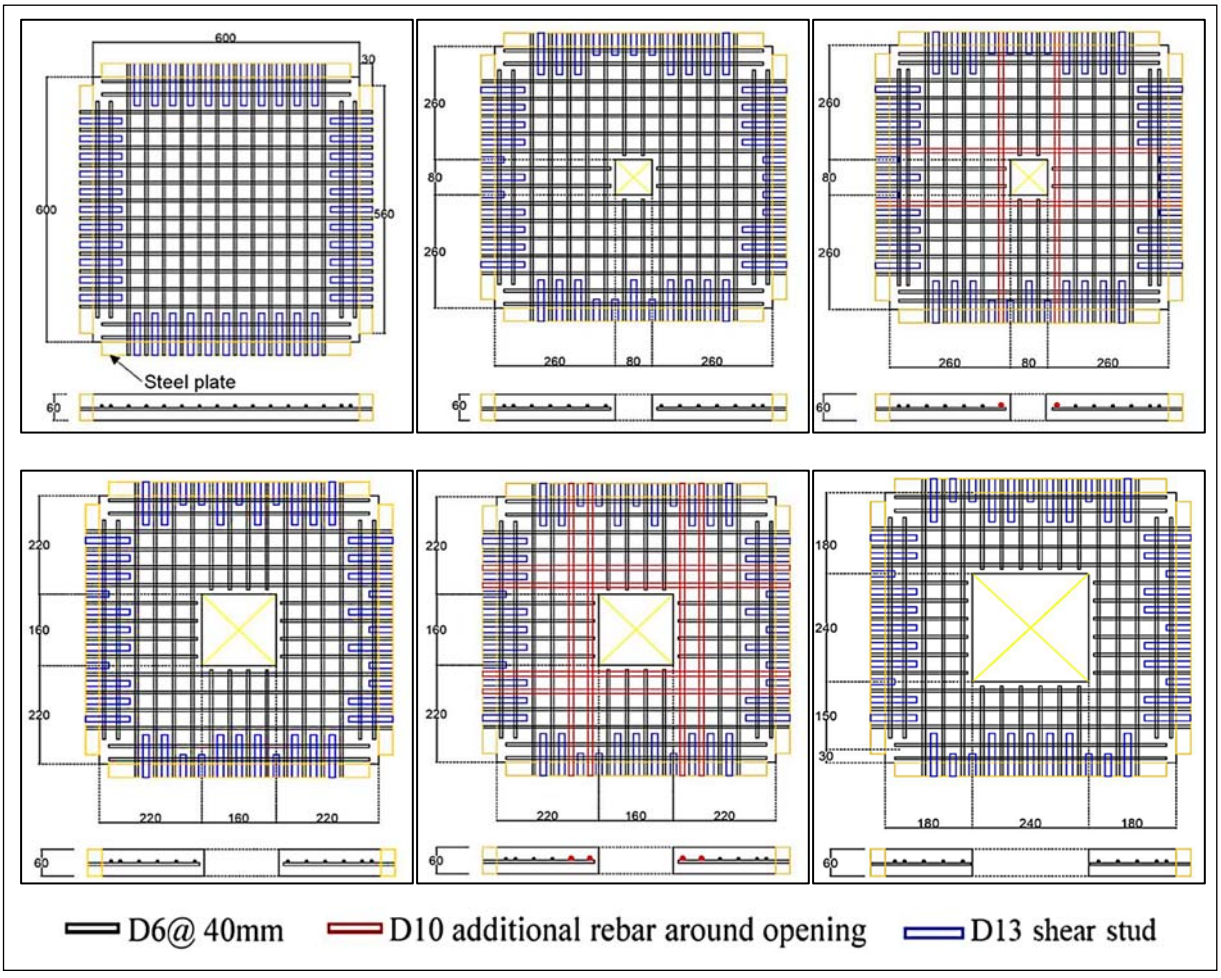

Figure 2.15 Dimensions and reinforcing details of six RC wall test specimens (in mm).

2.3 Analytical and Numerical Works

In 2008, Sakurai et al., studied the effects of varying the number and arrangement of openings on reinforced concrete (RC) shear walls. As illustrated in Figure 2.16, the study focused on assessing the impact of different opening configurations on shear resistance. They used the equivalent perimeter ratio of openings to evaluate shear resistance and applied the finite element method (FEM) to simulate the walls' behavior. Their findings showed that multiple openings complicate the failure mechanism and reduce the wall's resistance to seismic loads, especially due to stress redistribution at the base. This study highlights the importance of considering opening configurations in the design of RC shear walls [30].

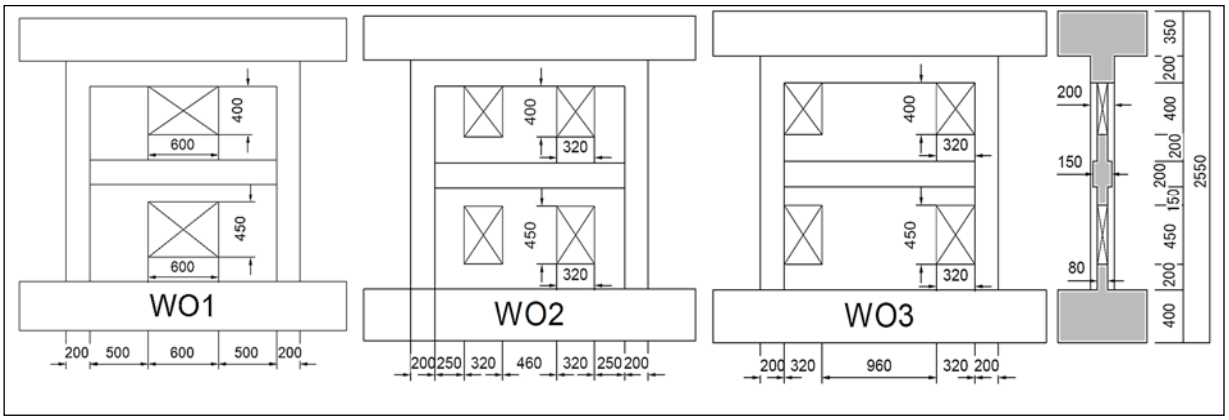

Figure 2.16 Test specimens.

In 2012, Khatami, S. M., et al., a three-dimensional building with a shear wall under two near-fault ground motions had its three structural systems was examined. In the first building study, SAP 2000 was used to select basal shears and lateral displacements as the comparative quantities. In a second study of almost square panel models (without and with openings), the top lateral displacement and the ultimate resisting lateral force were chosen using ANSYS. In the first study, the 3D building's entire shear wall was able to absorb more energy than other shear wall models with openings that were looked into. Openings reduce the lateral carrying

capacities of panels and shear walls. At the yielding load level, the second study also showed a deformation delay, this time for the panel with the opening rather than the entire panel. These details describe how shear walls and panels with openings behave and function, which lessens their ability to support lateral loads [31].

In the same year, Masood M. et. al., an attempt was made to determine the maximum base opening range that could be allowed without appreciably altering the stiffness and strength. The behavior of a planar and box shear wall with different percentages of base opening was compared to that of a shear wall without an opening. A package of finite element modeling was done with ANSYS. To help the designer choose the right opening width, a set of non-dimensional graphs with key variables was created. Researchers found that as the percentage of base opening increases, so do the deflection and stresses. Even so, the rate of deflection increase was only somewhat rapid, up to 60% base opening. The wall's stiffness dramatically reduces after a 60% base opening. It was proposed that, depending on the study's findings, a base opening of up to 50% of the wall's length might be a reasonable choice in high-rise construction [32].

In 2014, Hegde, P. et al., investigated the behavior of creating openings at the base of shear walls. Some high-rise buildings require parking openings at the base of RC shear walls. The study was conducted using the ANSYS software program to determine the impact of these openers on shear wall performance. A nonlinear static analysis was conducted considering two parameters: (a) the position of the base opening and (b) its ratio area relative to the shear wall. The results indicate that shear walls with an eccentric base opening exhibit a reduced load-carrying capacity compared to those with a symmetric base opening. Additionally, the load capacity of a shear wall decreases sharply when the base opening area exceeds 50% of the solid wall area [33].

In a 2015 study by Gandhi, B. H., conducted a study on six-story frame-shear wall buildings using equivalent static analysis and linear elastic analysis with STAAD PRO software, the results showed that the size and placement of openings in shear walls impact the stiffness and seismic response of structures. The study found that the maximum deflection occurred in an eccentric straight opening, while the minimum deflection occurred in an eccentric zigzag opening. The study also analyzed stresses related to various opening conditions and confirmed that stress increases rapidly after a 40% opening. Bottom stress increases proportionally up to a 40% opening and then rises significantly with a 50% opening [34].

In the same year, Sharma et al., examined the impact of openings in the shear walls of a 30-story building using the ETABS program. The analysis reveals that when the aspect ratio is high, the shape of the opening significantly influences displacement and drift, in addition to its size. Compared to shear walls without openings, the overall lateral displacement of the buildings increases from 0.58% to 20.95%, and the inter-storey drift rises from 1.04% to 23.63%. This increase is attributed to the varying sizes of the openings in the shear walls [1].

In 2015, Aarthi Harini, T., and colleagues used the Response Spectrum Method to investigate a seven-story frame shear wall structure using linear elastic analysis and the finite element software ETABS. The comparison findings demonstrated that the configuration of the openings affects displacement, base shear, period, and stress distribution surrounding the openings. Finally, as it satisfies both the seismic and architectural criteria, it was suggested that the staggered configuration for the shear wall openings be implemented in actuality [35].

In the same year, Hong A. Y., conducted a study to examine how the location and size of openings affect the behavior of structural shear walls under different static loading conditions, utilizing ANSYS 12.0 software for the analysis. The study

involved shear walls with different opening sizes and locations, denoted as SW2, SW3, SW4, SW5, SW6, SW7, and SW8, with SW1 serving as a solid reference wall. The analysis employed two types of loads: uniformly distributed axial loads and uniformly distributed lateral loads. The study compared cracking patterns and stress distributions across the shear walls under identical loading conditions. Key findings revealed that shear walls with larger openings exhibited reduced efficiency under both axial and lateral loads. Moreover, the distance of the opening from the support significantly affected the axial strength of the wall more than its lateral strength. Additionally, the effectiveness of the shear wall diminished as the opening approached the applied load [36].

In 2015, Vishal A. Itware., and colleagues explored the impact of shear wall openings on the seismic performance of buildings. Using STAAD Pro, they modeled 3D structures of 6 and 12-story buildings with typical floor dimensions of 35m by 15m and a height of 3m per floor. The analysis followed the guidelines of IS 1893 (Part 1): 2002. Their findings indicated that the size of the openings has a greater effect on the seismic response than their configuration. Additionally, when the opening area exceeds 20%, there is a noticeable reduction in the stiffness of the shear walls[37].

In 2016, Yasrebinia, Y., and colleagues conducted a study to investigate the influence of rectangular openings of varying sizes and locations on the behavior of concrete shear walls during near-fault seismic events. The study focused on factors such as ductility, base shear, maximum displacement, and energy dissipation. The analysis was performed using ABAQUS Finite Element Software, and the numerical findings were validated by comparing them with experimental results. The openings had sizes ranging from 0.1 to 0.3 in area and were placed in different positions on the shear wall, such as the center and near the edges. Subjected to near-fault

earthquake records, the results indicated that openings reduced the energy absorption capacity, base shear, and lateral load-bearing capacity of the walls. Additionally, the study highlighted the significant influence that the location of openings had on the overall behavior of the shear wall under seismic loads[38].

In the same year, Kankuntla A. et al., used finite element modeling to analyze shear walls with openings under seismic load action on member forces. The purpose of the study was to compare shear wall openings with the seismic performance of a fifteen-story building in an earthquake zone. The SAP2000v program was used for seismic analysis, and the results were compared. By changing the shear wall's opening sizes and shapes to accommodate all building models, the optimal location for the shear wall was established. A comparative study found that reinforced concrete buildings' shear walls with different opening sizes were cost-effective. The study also showed that altering the arrangement of openings in shear walls could improve the seismic performance of the building and reduce the negative effects of seismic loads [39].

In 2018, Montazeri E. et al., conducted a study to evaluate the performance of shear walls with staggered openings subjected to lateral loading. The dimensions and locations of these openings are illustrated in Figure 2.17. Using the ABAQUS program, the study analyzed the failure modes of RC shear walls with vertically aligned openings and three different opening angles under increasing lateral loads. The failure analysis revealed that walls with ordered openings experienced significant rigidity degradation due to coupling beam failure. Conversely, walls with staggered openings exhibited greater loading capacity and rigidity compared to their ordered counterparts. In terms of crack formation, the initial crack in walls with ordered openings appeared in the coupling beam, whereas in walls with staggered openings, it originated at the base of the compression piers. [40].

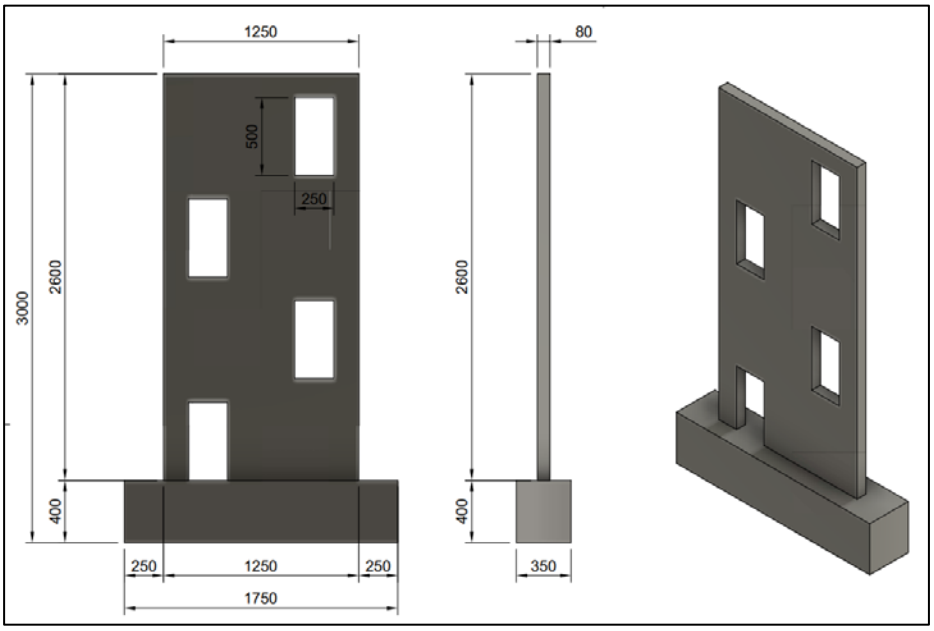

Figure 2.17 Shear wall dimensions.

In 2019, Morsy, A., and Ibrahim, Y., used the finite element method to study the behavior of walls containing openings. The research included determining the optimal shape of the openings, their orientation, aspect ratio, size, and location in reinforced concrete walls of varying thicknesses, with the aim of enhancing capacity and reducing cracks. A statistical analysis was conducted on 38 samples from the finite elements, and the results revealed the following points: [41]

1.The axial load capacity of a reinforced concrete wall with a vertical rectangular opening is higher than that of square and circular openings of the same size because the cross-sectional area around the rectangular opening is larger, allowing it to withstand higher axial loads.

2. The orientation of the opening greatly impacts the wall's ductility and axial capacity, as a vertical rectangular opening has a larger loaded cross-sectional area than a horizontal one of the same size.

3. The optimum opening location in the shear wall for axial load capacity is at the lower middle because it is away from the loaded edge and the axial load path.

4. R.C. walls with small openings of less than 7% of the total area do not affect shear wall capacity. On the other hand, if the opening is sufficiently large (size >7%), the amount of shear wall capacity.

In the same year, Alimohammadi et al., examined the seismic behavior of a concrete shear wall with a constant cross-section and openings of various shapes. Using 3D Abaqus software to model these case studies, the results showed that the strength is reduced more when an opening is situated near the wall's edge than when it is farther away. Additionally, an opening could decrease the seismic characteristics of the shear wall by up to 50% in terms of ultimate load, energy dissipation, and stiffness, although the extent of reduction in strength and ductility varies depending on the type and configuration of the openings [42].

In 2019, Chaudhary et al., the purpose of the study is to determine the stress distribution for various shear wall opening shapes. The ANSYS 16.0 software was used for the study. Scientific information was gleaned from a collection of openings with varying shapes by examining them. In terms of stress and strain, it can be observed that semicircular and rectangular openings perform better than triangular openings. It is also observed that there is a similar amount of deformation in all the shapes of the opening. The values only show a slight change. Only the shape of the opening is altered because all other dimensions remain the same. Thus, the overall analysis of the shape effect leads us to the conclusion that shape influences in addition to the location and size of the shear wall [43].

In 2021, Fares, A. M., provided a general conceptual understanding of the opening's effect, linear elastic analysis at SAP2000 is used to study openings at reinforced concrete shear walls. The modeling and behavior of concrete shear walls with openings are covered in this study. These openings are doors, as well as centrally located square windows. A matrix of variables that are anticipated to

impact the wall's lateral stiffness is looked for. The wall aspect ratio (H/B), opening type, and opening ratio are all included in this matrix. Both central openings and multiple central openings with varying wall heights are examined in terms of how openings affect the lateral deflection of the wall. The following succinctly summarizes the primary findings and conclusions: [44]

1. The opening size has a major impact on the stiffness and lateral displacement of the concrete shear walls.
2. The lateral displacement increased as the opening size in the shear walls increased, thereby reducing the structure's lateral stiffness.
3. It was discovered that a standard door, commonly used in practice with dimensions of 2 × 1 m, reduced the stiffness of a 3 × 3 m solid wall by 60%.

In 2022, Bush et al. conducted a study using ETABS software to analyze story drift, displacement, stiffness, and base shear in a 10-story asymmetric building. They examined the effects of staggered opening shapes (square, rectangular, and triangular) in shear walls compared to models with uniform openings and one without any openings. The study found that walls with staggered openings were stiffer than those with uniform openings, and walls without any openings performed best under seismic loads. Among the configurations tested, shear walls with staggered square and rectangular openings showed the least displacement and superior seismic performance [45].

In the same year, Kumar, M. et al., investigated the opening size and shape of openings that affect lateral deformations in a multistory-framed building. The shear wall includes triangular, square, and circular openings, with 20% and 25% of each shape considered. The SAP2000 software was used to analyze a ten-story building with different shear wall configurations under seismic loads. The outcomes were reached based on the findings of the study. Shear walls with 20% and 25% triangular

openings show significantly higher lateral displacements (19% and 24%) than those without openings. Triangular openings were found to have the lowest resistance to lateral deformation when compared to circular and square openings [46].

In 2022, Praveen K. et al., analyzed 11-story buildings using ETABS 2016. Five models are analyzed by varying the opening location and size as shown in Figure 2.18. The results are compared to determine the optimal opening position. Results compared include story drift, maximum displacement, and story shear. Comparing models with different opening patterns reveals that openings have an impact on the behavior of the shear wall component. The study also highlights the significance of opening locations and sizes. This study suggests that zigzag patterns are best suited for openings [47].

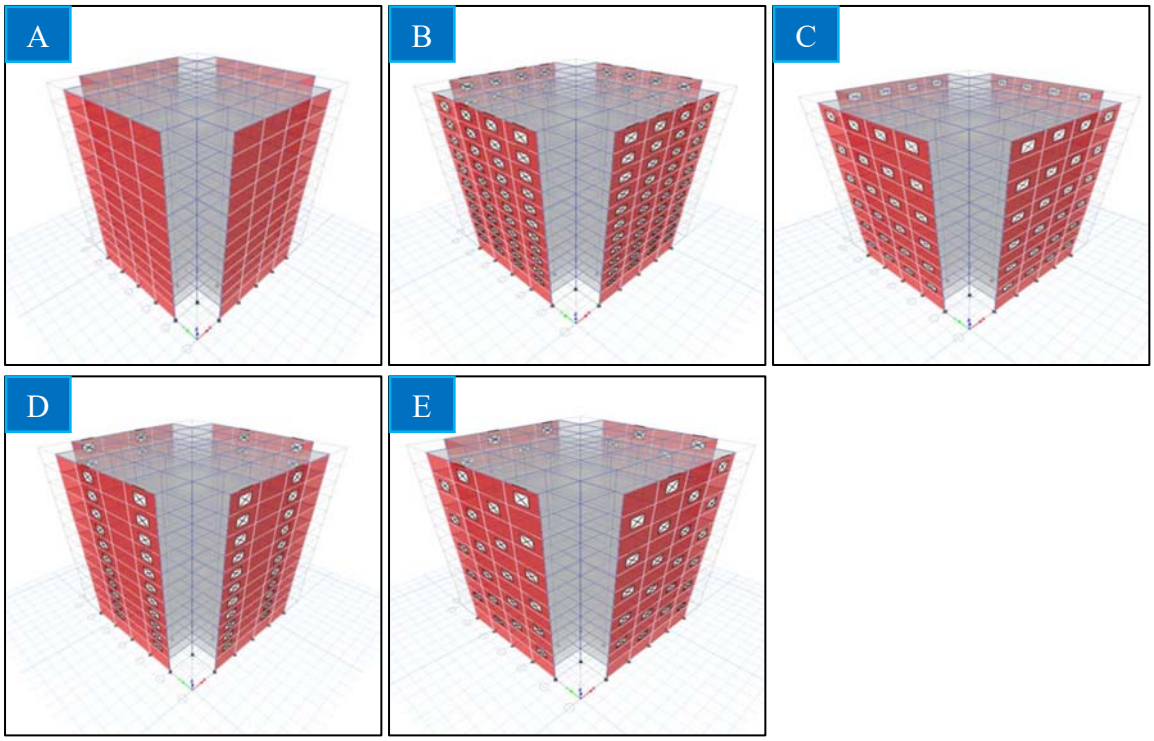

Figure 2.18 The five models studied (A) structure without opening, (B) structure with regular opening, (C) structure with horizontal opening, (D) structure with vertical opening, (E) Structure with Zig-zag opening.

In 2023, Hassan, H. et al., evaluated the performance of reinforced concrete shear walls that based on the size and placement of the opening. For RC walls, the study measures the percentage change in natural frequency, whether it increases or decreases. Finding the best places to satisfy the walls' dynamic needs more effectively and efficiently is the goal of the inquiry, which also tries to find openings that provide undesirable results. Based on the results, it can be concluded that different arrangements of openings can affect the natural frequency of the walls in both positive and negative ways. Because of this, the dynamic characteristic may vary by as much as 17% or 37%, contingent upon how the openings are arranged [48].

2.4 Concluding Remarks

The previous review demonstrates that the location, shape, and size of the openings significantly affect the strength and behavior of shear walls. Therefore, to assess the deformations, load capacities under various loading scenarios, and boundary conditions of shear walls with multiple opening configurations, further theoretical and experimental research is required. This study aims to address this gap by evaluating the impact of multiple openings and several factors, including the size and shape of openings, different reinforcement patterns, and variations in the strength and thickness of concrete shear walls.

CHAPTER THREE: EXPERIMENTAL INVESTIGATION

3.1 General

The primary objective of this experimental work is to conduct a comprehensive investigation for the structural behavior of reinforced concrete shear walls with a screen of openings, characterized by various sizes, shapes, thicknesses, concrete strengths, and reinforcement patterns around openings. Additionally, this chapter aims to provide a detailed description of the material properties, including cement, sand, gravel, superplasticizer, silica fume, and steel reinforcement. It also encompasses a comprehensive overview of the experimental models, from the fabrication of wooden molds and reinforcement placement to the casting and curing processes. Furthermore, the chapter outlines the instruments and equipment used to test these models. The experimental work was carried out in the Civil Engineering Laboratory of Engineering College in Misan University and Construction Materials Laboratory Engineering Materials of Technical Institute in Amarah-Misan province.

3.2 Material

In this study, all the basic materials needed for making mixes and constructing concrete shear wall models were easily available and commonly found on the market. These materials included cement, aggregates, water, superplasticizer, and silica fumes. To maintain their quality, the materials were carefully stored to prevent moisture exposure. Moreover, rigorous tests were conducted on all the materials to ensure they met the required standards and specifications for producing a top-notch mix. The reinforcement was also kept away from moisture to prevent corrosion, and tests were carried out within specified limits to guarantee its quality.

3.2.1 **Cement**

Ordinary Portland cement (OPC) Type- I was used in this study. Tables 3.1 and 3.2 provide the physical and chemical characteristics of the cement, which meets Iraqi Standard No. 5/1984 [49].

Table 3.1 Cement's physical characteristics.

Physical Characteristics	Test Result	Limits of IQS No.5/1984
Fineness using (Blaine method) (m^2/kg)	361	≥230
Vicat Method for Setting Time:		
Initial Setting Time (min)	85	≥45 min
Final Setting Time (min)	305	≤600 min
Compressive Strength for Cement Paste Cube(70.7mm) at:		
3 days (N/mm^2)	16.05	≥15
7 days (N/mm^2)	25.32	≥23

Table 3.2 Chemical composition of cement.

Compound Composite	%Weight	Limit of IQS No.5/1984
Limes (Cao)	62.3	.....
Silicas (Sio_2)	23.5	.....
Alumina's (Al_2O_3)	3.15	.....
Iron oxidizes (Fe_2O_3)	4.56	.....
Magnesians (MgO)	2.15	≤5%
Sulphates (SO_3)	2.27	≤2.8%
Loss on Ignitions (L.O.I.)	1.83	≤4%
Insoluble residuals (I.R.)	0.47	≤1.5%
Limes saturation issue (L.S.I.)	0.837	(0.66-1.02) %

3.2.2 **Aggregates**

3.2.2.1 **Fine Aggregate**

The fine aggregates used in this study consisted of natural sand sourced. This fine aggregate complies with ASTM C33/C33M-18 [50] and meets the specifications outlined in Iraqi Specification No. 45/2017 [51], as detailed in Table 3.3.

Table 3.3 Grading of the fine aggregates.

No.	Sieve size (mm)	% Passing percentages		
		Fines aggregates	Limits of IQS No.45/2017 zone II	ASTM C33/C 33M
1	9.5	100	100	100
2	4.75	95	90-100	95-100
3	2.36	86	75-100	80-100
4	1.18	73	55-90	50-85
5	0.60	55	35-59	25-60
6	0.30	24	8-30	5-30
7	0.15	5	0-10	0-10

- The fineness modulus (FM) of the fine aggregates is 2.62, within the range of 2.3 to 3.1.
- The sulfate content (SO_3) is 0.323%, within the permissible limit for concrete (≤0.5%).

3.2.2.2 **Coarse Aggregate**

Crushed gravel, shown in Figure 3.1, was used in all concrete mixes in this study. Laboratory test results in Table 3.4 indicate that the coarse aggregate complies with Iraqi Standard Specification No. 45/2017.[51].

Figure 3.1 The crushed gravel used in all concrete mixes.

Table 3.4 Grading of the coarse aggregates.

No.	Sieve size (mm)	% Passing by weight	
		Coarse aggregate	Limits according to IQS 45/2017
1	12.5	100	100
2	9.5	95	85-100
3	4.75	15	10-30
4	2.36	0.4	0-10
5	1.18	0	0-5

3.2.3 **Water**

Tap water was used in the production of all concrete mixtures used in this research.

3.2.4 **Superplasticizer**

All concrete mixes in this study used Flocrete SP90S from DCP. This is made of certain polymers that are intended to improve the performance of the concrete's water content. This impact can help maintain mixed qualities while enhancing workability, raising ultimate strengths, or making it easier to reduce the cement content. There is good workability and retention with flocrete SP90S. Additionally, depending on the dose employed, flocrete SP90S conforms to ASTM C494/C494, Types B, D, and G [52]. Table 3.5 illustrates the technical requirements for this type of superplasticizer according to the data sheet referred to in the Appendix.

Table 3.5 Properties of used superplasticizer (Flocrete SP90S).

Superplasticizer	Chloride content BS 5075	Specific gravity	Colors	Dosage
Flocrete SP90S	NIL	1.16 ± 0.02	Brown liquid	0.80 – 2.10 L/100 kg of cement weight

❖ Provided by the manufacture

3.2.5 **Silica Fume**

MegaAdd MS (D) is a ready-to-use mineral addition that provides exceptional performance in concrete. It is compatible with ASTM C1240-20a [53], enhances particle packing in concrete or mortar, and acts as a highly reactive pozzolan. MegaAdd MS (D) dissolves in water after one hour. Silica in solution forms an amorphous gel of silica fume particles and agglomerates that is high in silica but low in calcium. Table 3.6 illustrates typical properties.

Table 3.6 Silica fume's characteristics (Mega Add MS(D)).

Characteristic	Test Method	Value
State	Amorphous	Sub-micrometer particles
Appearance	-	Powder ranging from grey to medium grey
Specific Gravity	-	2.10 to 2.40
Moisture Content (H2O)	-	Minimum 3%
dosage ranges		5-8% of the cement weight

❖ Provided by the manufacture

3.2.6 **Steel Reinforcement**

Steel reinforcement bars with diameters of 8 mm and 6 mm were used in all shear wall models, as shown in Figure 3.2. Mechanical tests were conducted on three bars of each diameter according to BS 4449:1997 [54]. The test results are summarized in Table 3.7.

Figure 3.2 Steel bars used in the models (A) Ø 8mm, (B) Ø 6mm.

Table 3.7 Properties of reinforcing bar.

$D_{nominal}$ (mm)	$D_{measured}$ (mm)	Bar type	Test results		
			Yield strength *fy* (N/mm^2)	Ultimate strength *fu* (N/mm^2)	Elongation (%)
6	5.8	Deformed	439	612	11.79
8	8	Deformed	477.67	634	18

3.3 **Concrete Mix Proportions**

In this study, three experimental concrete mixes were prepared to achieve the target strength for reinforced concrete shear walls, with compressive strengths of 30, 45, and 60 N/mm² after 28 days. A small mixing truck was used for concrete production, and the coarse aggregate was washed with potable water to remove any dust or impurities, in order to achieve a saturated-dry surface. Sand was used as fine aggregate, and ordinary Portland cement was utilized in the mixes. Tap water was employed in all the concrete mixtures.

To enhance strength and ensure high performance, silica fume and specific additives were incorporated. Table 3.8 presents the mix proportions by weight, showing the quantities of materials required per cubic meter of concrete to achieve the desired strength.

Table 3.8 Material quantities per cubic meter ($1m^3$) for concrete mix designs.

Target concrete strength (MPa) in 28 days	Cement (kg/m^3)	Sand (kg/m^3)	Gravel (kg/m^3)	W/C	Super-plasticizer (kg/m^3)	Silica fume (kg/m^3)
30	400	656	1064	0.53	-----	-----
45	485	635	1082	0.37	4.80	-----
60	495	582	1110	0.32	4.87	3.68*

*W/B, Binder = Cement +Silica Fume

3.4 **Fresh and hardened Concrete Tests**

To verify the quality of the concrete used for pouring shear walls, a series of quality tests were conducted. These tests, aimed at ensuring the concrete met the required standards, included tensile tests, slump tests, and compressive strength tests.

3.4.1 **Workability Test**

All concrete mixes produced and utilized in this research were tested for workability using ASTM C-143 standards [55]. A slump cone was used as shown in Figure 3.3, and the results are given in Table 3.9.

Figure 3.3 Slump cone test for three concrete mixtures (A) 30 MPa, (B) 45 MPa, (C) 60 MPa.

Table 3.9 Results of the concrete slump test.

Mix No.	Target concrete strength (MPa) in 28 days	Slump value (mm)
1	30	175
2	45	200
3	60	210

3.4.2 Compressive Strength of Concrete (f_{cu})

For each concrete type, six cubes with dimensions of 150 mm × 150 mm × 150 mm were cast. The casting process was preceded by meticulous preparation, including mold cleaning and lubrication. Following casting, the specimens were demolded and placed in a container filled with tap water, where they were stored until testing, in compliance with ASTM C31/C31M-21a standards [56], as shown in Figure 3.4.

Figure 3.4 Casting and curing of concrete specimens.

The specimens were tested in accordance with BS 1881: Part 116 [57] at 7 and 28 days. A hydraulic machine with a capacity of 2000 kN was used for the tests, as illustrated in Figure 3.5. The results of these tests are presented in Table 3.10.

Figure 3.5 Compressive strength testing machine.

Table 3.10 Compressive strength results.

Target concrete strength (MPa) in 28 days	Cubes number	Density (kg/m^3)	f_{cu} (MPa)			
			7 days	Average at 7 Days	28 days	Average at 28 Days
30	1	2279.2	23.2	23.2	33.4	33.03
	2		23.8		32.0	
	3		22.6		33.7	
45	1	2412.4	41.3	40.2	45.7	45.70
	2		39.9		46.1	
	3		39.4		45.3	
60	1	2459.5	49.2	49.9	62.3	61.63
	2		51.8		59.6	
	3		48.8		63.0	

3.4.3 **Split Tensile Strength (f_t)**

The tensile strength is tested on cylinders with dimensions (height 300 mm, diameter 150 mm) at 7 and 28 days, as shown in Figure 3.6. According to ASTM C496-17 [58], the cylinders are cast and cured using the same processes utilized for the compressive strength test specimens. The cylindrical specimen is positioned horizontally between the compression testing machine's loading surfaces, and a load is progressively applied until the specimen fails. Table 3-11 presents the test results. Equation 3.1 is used to calculate the split tensile strength of the concrete.

$$f_t = \frac{2P}{\pi LD} \quad \text{.....(3.1)}$$

Where:

f_t= tensile strength (MPa)

P = the maximal force (N) applied to the specimen

L = the specimen's length (mm)

D = the specimen's diameter (mm)

π =3.14.

Figure 3.6 Splitting tensile strength test

Table 3.11 Results of splitting tensile strength.

Target concrete strength (MPa) in 28 days	Cylinder number	f_t (MPa)			
		7 days	Average of 7 days	28 days	Average of 28 days
30	1	2.1	2.13	2.4	2.40
	2	2.0		2.2	
	3	2.3		2.6	
45	1	2.6	2.44	2.9	2.86
	2	2.3		2.7	
	3	2.4		3.0	
60	1	3.0	3.26	3.7	3.63
	2	3.6		3.4	
	3	3.2		3.8	

3.5 **Preparation of Test Specimens**

3.5.1 **Mold**

Wooden molds were used to cast the shear wall specimens, with each mold consisting of a wooden base and four sides connected to the base with screws. The dimensions of the molds were (600×600×80 mm), (600×600×100 mm), and (600×600×120 mm). The openings were designed in square and circular shapes and

made from wood. Each model featured a screen of square openings that were equivalent in size to the circular openings in another model. The opening ratio was increased by enlarging their size while keeping the number of openings constant. Details of the shear wall openings are provided in Table 3.12, and Figure 3.7 illustrates the labelling scheme for shear wall configurations. Regarding reinforcement, a mesh with a diameter of 8 mm was carefully placed in all models, ensuring proper concrete cover on all sides. Additionally, 6 mm-diameter inclined bars were used around the openings in two of the models. The tested specimens and their reinforcement details are presented in Figures 3.8 to 3.12.

Table 3.12 Shear wall specimens' designation.

Item	Shear Wall Specimen coding	Shape of Openings	Thickness (cm)	Size of Openings (mm)			Opening Ratio (%)	Grade of Concrete (MPa)
				Width	Height	Diameter		
1	SW10S0	Solid	10	-	-	-	0.0	45
2	SW10S40	Square	10	40	40	-	7.1	45
3	SW10S50			50	50	-	11.1	
4	SW10S60			60	60	-	16.0	
5	SW10S70			70	70	-	21.8	
6	SW10C45	Circular	10	-	-	45	7.1	45
7	SW10C57			-	-	57	11.1	
8	SW10C68			-	-	68	16.0	
9	SW10C79			-	-	79	21.8	
10	SW08S60	Square	8	60	60	-	16.0	45
11	SW12S60		12	60	60	-		
12	SW08C68	Circular	8	-	-	68	16.0	45
13	SW12C68		12	-	-	68		
14	SW10S60#	Square	10	60	60	-	16.0	30
15	SW10S60##			60	60	-		60
16	SW10C68#	Circular	10	-	-	68	16.0	30
17	SW10C68##			-	-	68		60
18	SW10C45I	Circular	10	-	-	45	7.1	45
19	SW10C45II			-	-	45		

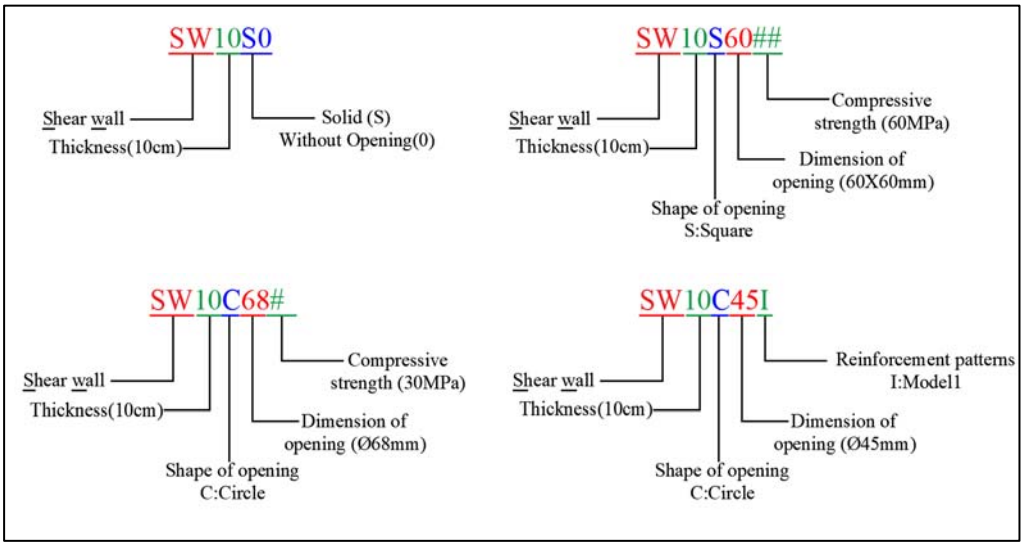

Figure 3.7 Shear wall specimens' designation.

Figure 3.8 Fabrication of reinforced concrete shear wall models.

Figure 3.9 Details of specimens for models SW10S0 to SW10C45.

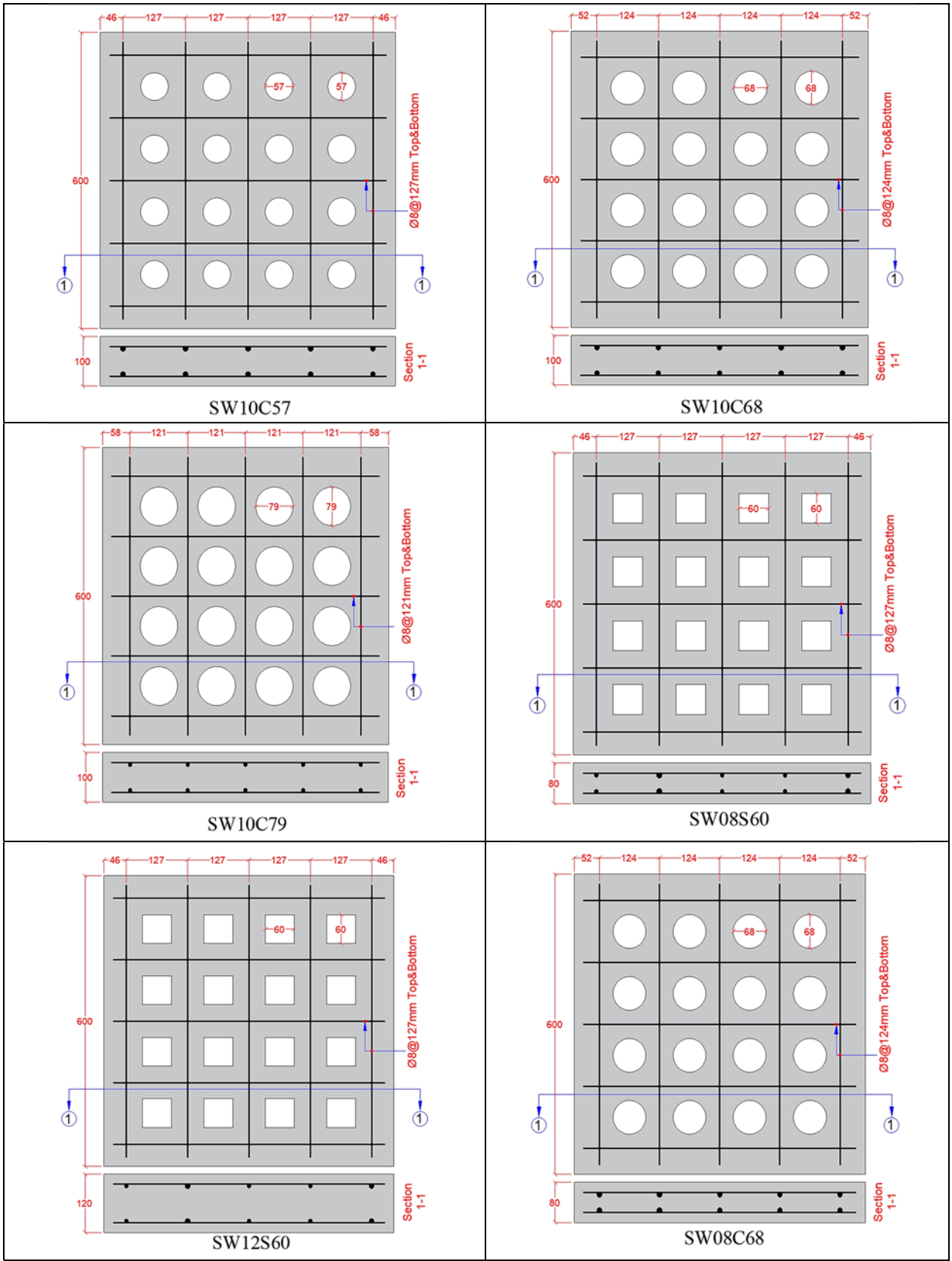

Figure 3.10 Details of specimens for models SW10C57 to SW08C68.

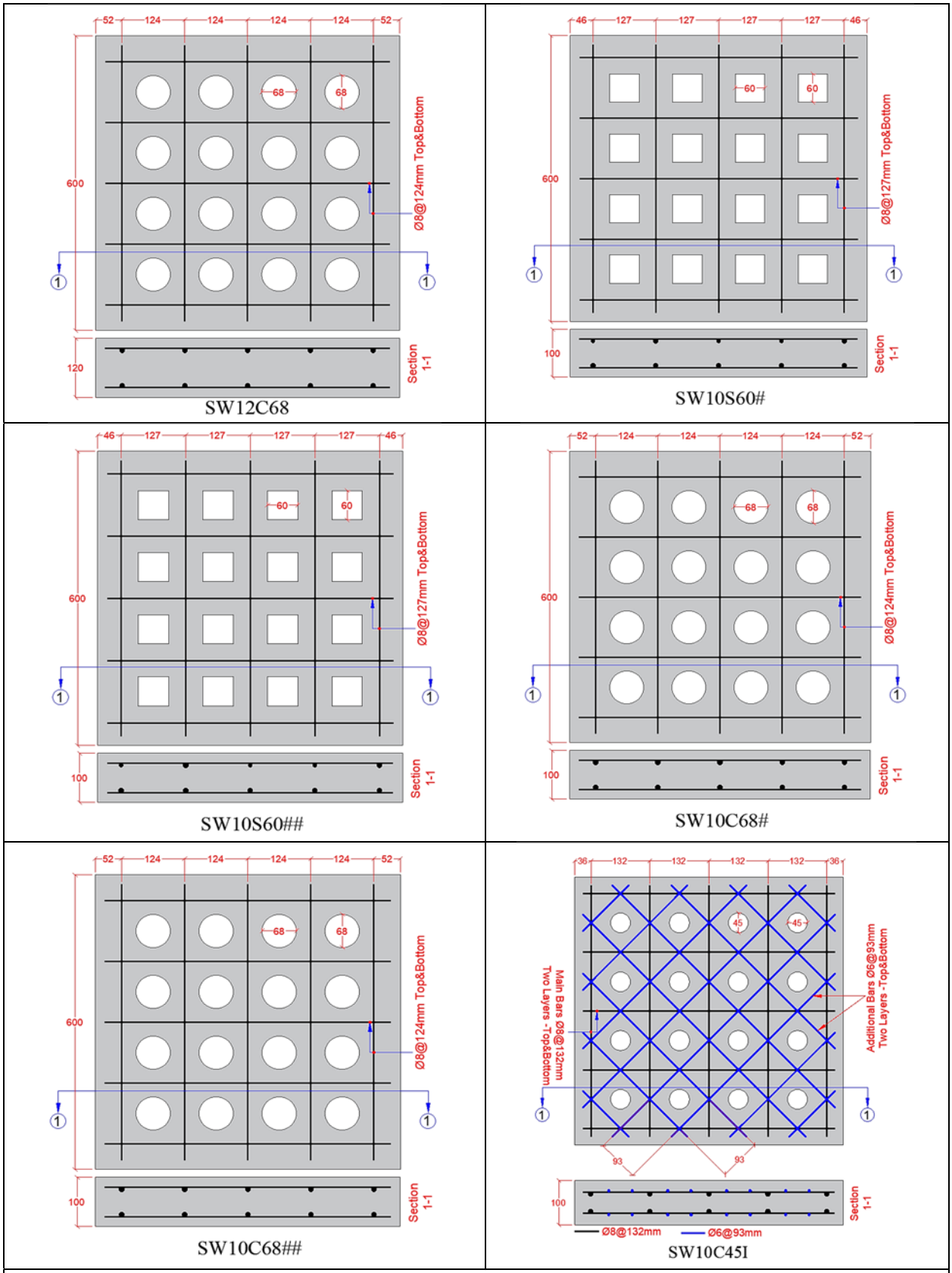

Figure 3.11 Details of specimens for models SW12C68 to SW10C45I.

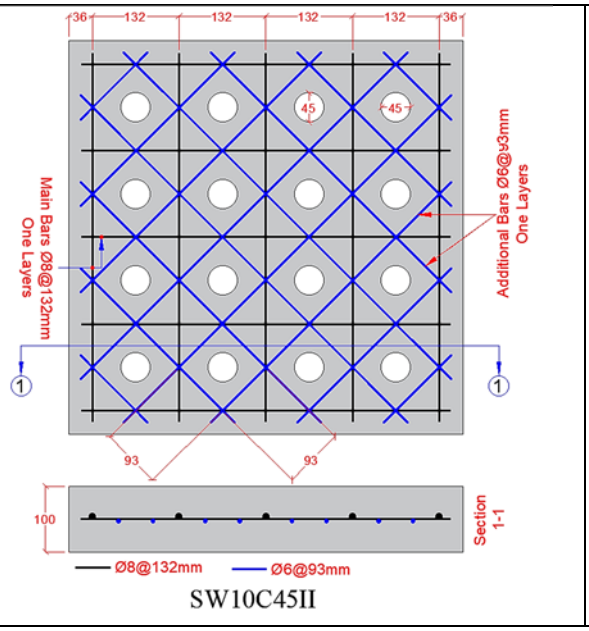

Figure 3.12 Details of model SW10C45II.

3.6 **Casting and Curing the Specimens.**

Nineteen reinforced concrete shear walls specimens with openings were cast following a precise engineering procedure. The process began with the preparation of raw materials, which were carefully weighed and packed before mixing. The concrete was mixed according to the requirements specified in ASTM C 94/C 94M -23[59], ensuring that the proportions and mixing procedures adhered to industry standards.

A 3-cubic-meter capacity mixing truck was used to mix the concrete. The molds were coated with oil to ensure easy removal after curing. The spacing between the reinforcement bars and concrete cover was verified. During casting, a "road vibrator" was used continuously to eliminate trapped air and prevent honeycombing.

After the casting was completed, the specimens were promptly covered with moistened burlap bags to retain moisture and prevent premature drying. The curing process was meticulously controlled by keeping the specimens wet for seven consecutive days, to ensuring that the concrete achieved its intended strength and

durability. Figure 3.13 provides a visual representation of the casting and curing steps, illustrating the detailed procedure followed.

Figure 3.13 Casting and curing procedure of the specimens (A) loading raw materials into the concrete mixer, (B) concrete mix after mixing, (C) pouring the specimens, (D) specimens after pouring, (E), curing of specimens.

3.7 **Instrumentation and Equipment of the Test**

3.7.1 **Test Machine**

All shear wall specimens were tested with the ALFA Testing Machine, which has a 5000 kN compressive capacity, as shown in Figure 3.14. This device automatically sets the load rate, includes an auto-stop function, and offers both automatic and manual modes for adjusting the load rate and test duration. It provides real-time graphs and stress data and can be operated via computer using ALFA's software, which supports saving, recalling, and reporting the test results.

Figure 3.14 Universal testing machine.

3.7.2 **Data Logger**

The data acquisition system consists of a personal computer and the GEODATALOG 30-WF6016 data logger, which collects input from multiple strain gauges on the shear wall. With 16 channels, it allows simultaneous measurement of multiple sensors. It operates on a 110-240 V, 50-60 Hz single-phase power supply. The system includes DATACOMM software for efficient data collection, monitoring, and analysis, as shown in Figure 3.15.

Figure 3.15 Data logger.

3.7.3 **Concrete Strain Gauges**

Two Tokyo concrete strain gauges, type PFL-30-11-3LJC-F, with a length of 30 mm, were affixed to the face of the reinforced concrete shear walls. Figure 3.16 illustrates the strain gauges and the adhesive used for their fixation.

Figure 3.16 Electrical strain gauges.

3.7.4 **Displacement measurement**

Displacements in both the horizontal (lengthening) and vertical (shortening) directions for each shear wall were measured using linear variable differential transformers (LVDT). To ensure accuracy and consistency, data recording was automated. Figure 3.17 shows the measurement setup.

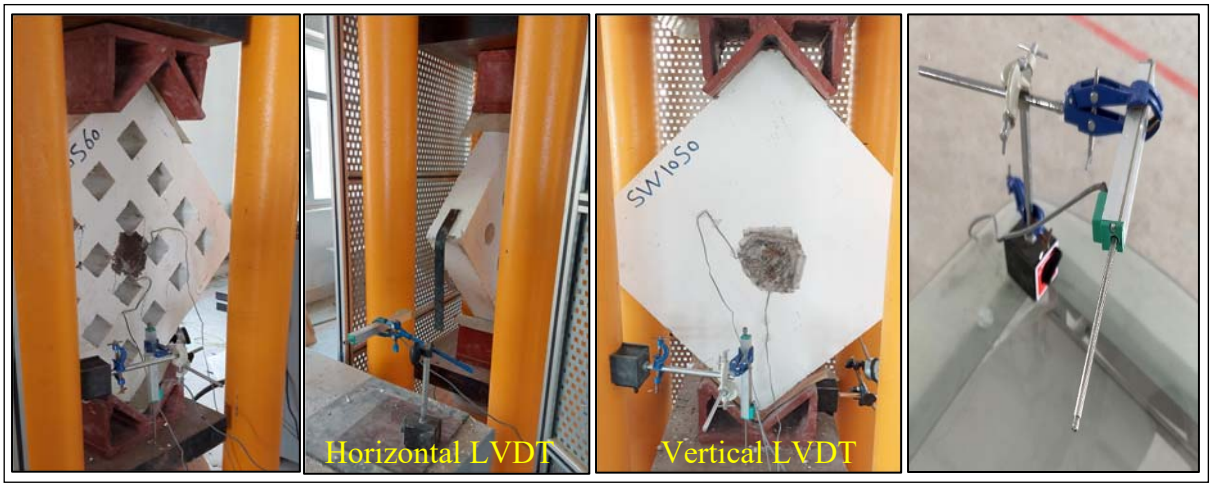

Figure 3.17 Setup of LVDT.

3.8 **Test Procedure**

After 28 days of cast the reinforced concrete shear wall tested specimens, the specimens were prepared for testing. To enhance the visibility of cracks during the test, the tested specimens were painted with white color, as illustrated in Figure 3.18.

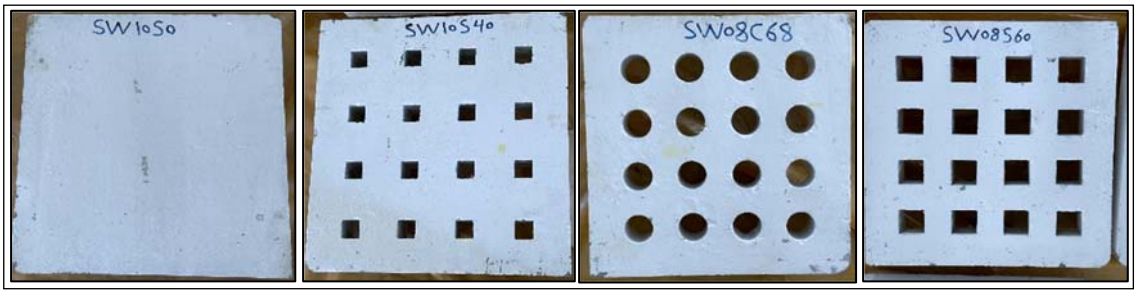

Figure 3.18 Shear wall specimens after being painted white.

Electrical strain gauges were fixed to the surfaces of the tested reinforced concrete specimens after these surfaces were smoothed to ensure proper adhesion. In the center of the tested concrete shear wall, two electrical strain gauges were installed. Each gauge is aligned with one of the diagonal lines of the wall, intersecting at the center. One gauge is fixed to measure the tensile strains, while the another is fixed to measure the compressive strains. After the strain gauges were attached, their functionality was calibrated using a voltmeter, as shown in Figure 3.19.

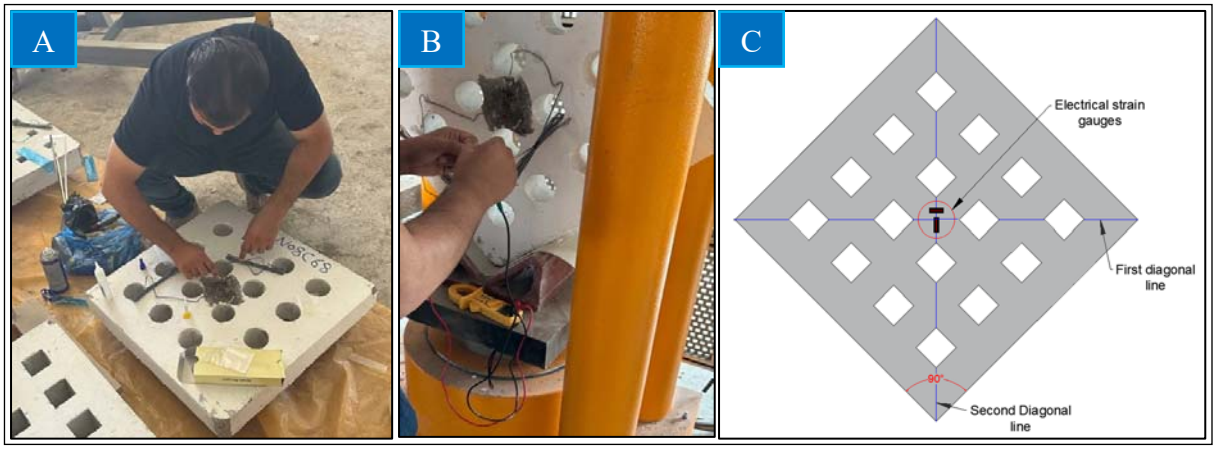

Figure 3.19 Set up of electrical strain gauges (A) installing strain gauges, (B) calibration of strain gauges using a voltmeter, (C) strain gauge's locations.

The tested shear walls were subjected to monotonic loading conditions with an automatic loading rate of 1 kN/sec to provide optimal testing conditions and prevent initial failure or concrete crushing due to large loading steps. The diagonal compression method was used to measure shear (or diagonal tensile) strength. Specimens were positioned with their diagonal axes aligned vertically in the direction of compression.

The testing followed the requirements of ASTM E519/E519M [60], with two steel supports placed at the top and bottom of the specimen as shown in Figure 3.20. A spirit level was used to ensure the specimens remained level and to guarantee diagonal loading on the shear wall specimens. Figure 3.21 shows the specimens prepared inside the testing machine.

The mechanism used in testing shear walls relies on the diagonal compression test, a fundamental method for analyzing the behavior of walls under different loads. In this test, a diagonal load is applied at the corners of the specimen. This angled load is decomposed into two main components: a vertical component that compresses the specimen along the vertical axis and a horizontal component that causes lateral expansion along the horizontal axis. Through the interaction of these two forces, a complex stress distribution is generated within the specimen.

The stresses generated inside the shear walls include diagonal compressive stresses that develop along the axis where the load is applied. These stresses compress the material along this axis, increasing the density of the wall. Simultaneously, diagonal tensile stresses form in the direction perpendicular to the diagonal axis, causing the specimen to expand in this direction.

In addition to compressive and tensile stresses, shear forces play a crucial role in the testing mechanism. Shear forces arise from the interaction between the vertical and horizontal components of the load, leading to the generation of shear stresses within the specimen. As shown in Figure 3.22, these stresses are particularly high in

areas near the corners or the middle of the specimen. When these stresses exceed the material's capacity, failure begins to occur, typically manifesting as cracks that propagate diagonally across the specimen.

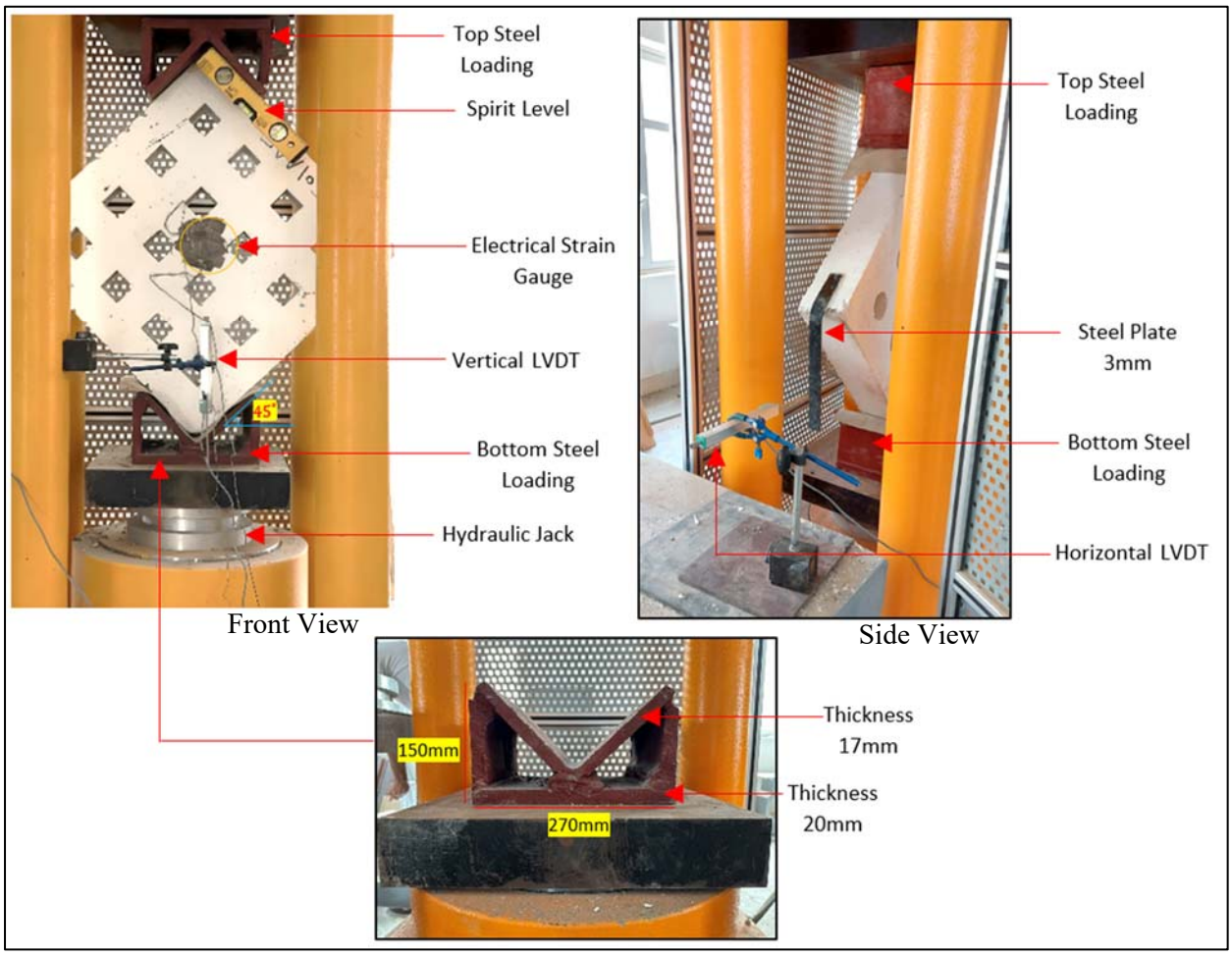

Figure 3.20 Testing setup for the tested shear wall specimens.

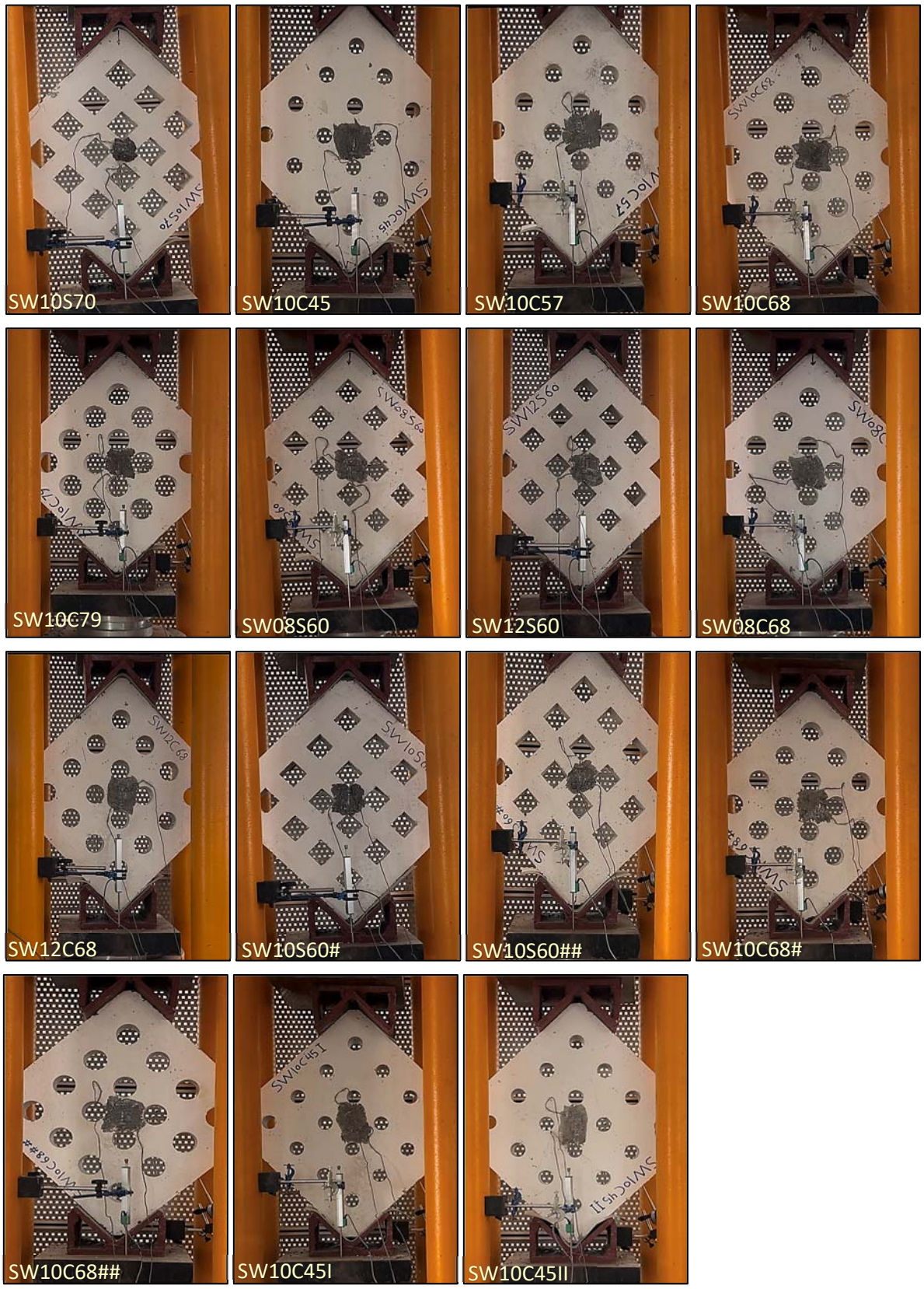

Figure 3.21 Shear wall specimens during testing.

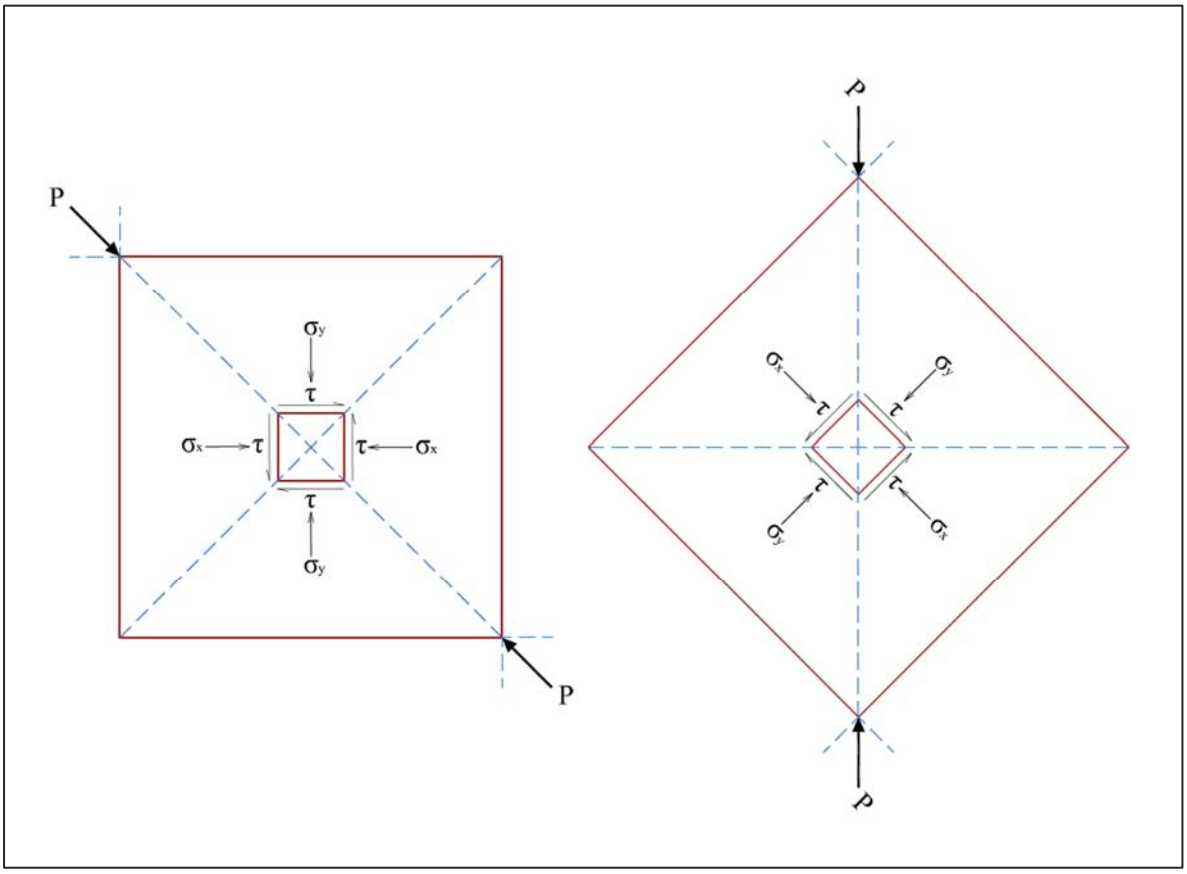

Figure 3.22 Internal stresses on the specimens.

CHAPTER FOUR: RESULTS & DISCUSSION

4.1 General

This chapter presents the experimental results for nineteen concrete shear wall specimens, including those with and without screen openings. The primary variables studied were the size, shape, and thickness of the openings, along with the concrete strength and reinforcement patterns around the openings. The concrete specimens were categorized based on compressive strengths of 30, 45, and 60 MPa, and thicknesses of 80, 100, and 120 mm were considered. All specimens were reinforced with 8 mm diameter meshes, while two specific specimens had additional 6 mm diameter bars placed around the openings. Each specimen was tested to failure, with key parameters assessed, including ultimate load, first crack load, crack patterns, displacement, shear stiffness, ductility, energy absorption, and strain.

4.2 General Behavior of Tested Shear Walls

Through shear wall specimen testing, many variables were taken into consideration. These variables included the shape and size of the openings, as well as thickness, strength, and reinforcement patterns around the openings, so that the specimens were categorized into four groups. The first group comprised a solid specimen and eight specimens with square and circular openings to investigate the impact of the shape and size of the openings on the structural behavior of concrete shear walls. The second group included six specimens to investigate the effect of thickness on the structural behavior of concrete shear walls. The third group, also comprising six specimens, aimed to examine the impact of strength on shear wall behavior. The fourth group included three specimens to investigate the effects of

various reinforcement patterns on shear wall openings. Figure 4.1 depicts the classification of shear wall models based on variables.

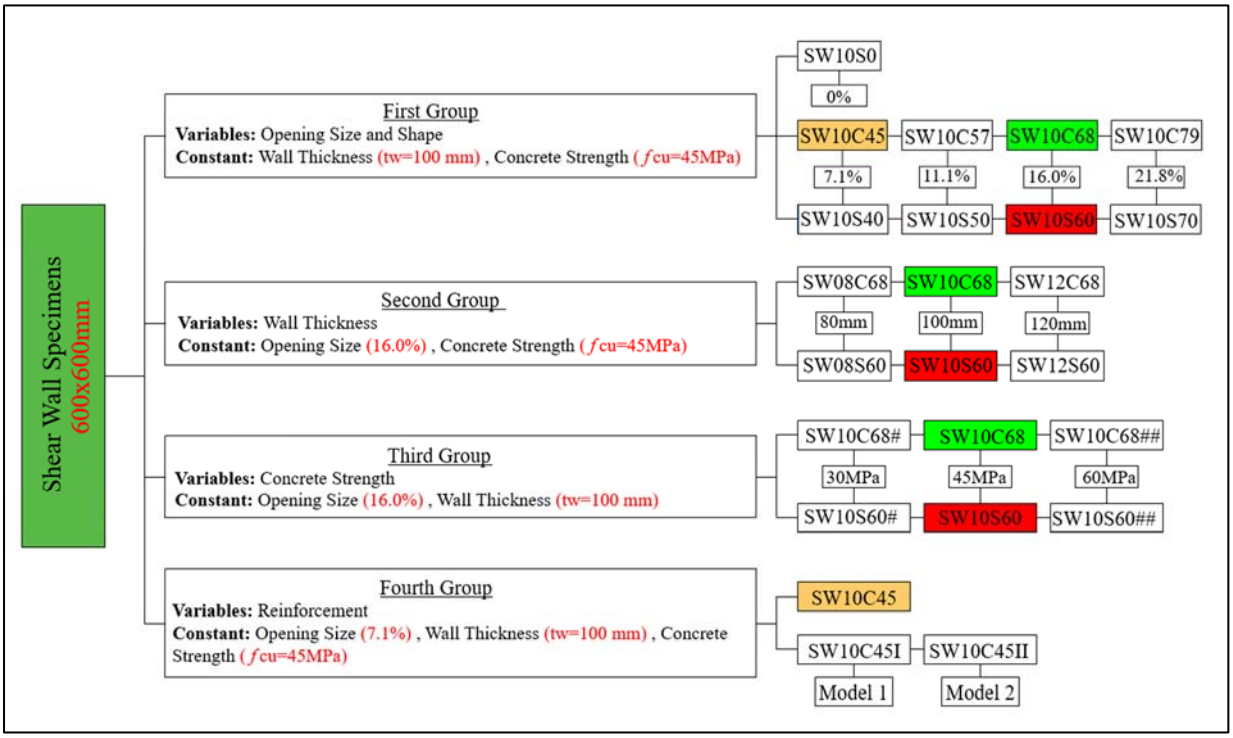

Figure 4.1 Categorization of shear wall models based on variables.

4.2.1 **Ultimate Load**

The ultimate load values recorded during testing reflect each specimen's structural performance under maximum loading conditions, providing key insights into how factors like opening size and shape, wall thickness, concrete strength, and reinforcement patterns affect shear wall behavior.

It is worth noting that the creating openings in shear walls reduces the wall's self-weight, leading to economic benefits such as lower material usage and costs. However, these openings can negatively impact the wall's load-bearing capacity. Therefore, the ultimate strength-to-weight ratio is considered one of the indicators used to evaluate the wall's efficiency in load resistance while accounting for the reduced weight.

The impact of these factors on the structural performance of the shear walls will be analyzed based on the results presented in Table 4.1.

Table 4.1 The ultimate loads of tested specimens.

Group No.	Specimens (ID)	Opening Ratio%	Ultimate Load (kN)	Weight (kg)	Ultimate Strength / Weight
1	SW10S0	0.0	827	86.85	9.52
	SW10S40	7.1	541	80.67	6.71
	SW10S50	11.1	328	77.20	4.25
	SW10S60	16.0	210	72.95	2.88
	SW10S70	21.8	160	67.93	2.36
	SW10C45	7.1	620	80.67	7.69
	SW10C57	11.1	460	77.20	5.96
	SW10C68	16.0	343	72.95	4.70
	SW10C79	21.8	197	67.93	2.90
2	SW08S60	16.0	176	58.36	3.02
	SW10S60	16.0	210	72.95	2.88
	SW12S60	16.0	244	87.54	2.79
	SW08C68	16.0	258	58.36	4.42
	SW10C68	16.0	343	72.95	4.70
	SW12C68	16.0	407	87.54	4.65
3	SW10S60#	16.0	189	68.92	2.74
	SW10S60	16.0	210	72.95	2.88
	SW10S60##	16.0	251	74.38	3.37
	SW10C68#	16.0	309	68.92	4.48
	SW10C68	16.0	343	72.95	4.70
	SW10C68##	16.0	362	74.38	4.87
4	SW10C45	7.1	620	80.67	7.69
	SW10C45I	7.1	742	82.99	8.94
	SW10C45II	7.1	630	79.95	7.88

4.2.1.1 **Effect of Opening Size on the Ultimate Load**

The effect of opening size is a primary focus of this study. In the first group, four tested specimens with square openings and four tested specimens with circular openings of the same size were assessed. The opening ratios on the shear wall

surfaces were 7.1%, 11.1%, 16.0%, and 21.8%. The increasing of opening size was achieved by enlarging the openings while keeping the number of openings constant. Figure 4.2 illustrates the impact of the size and shape of openings on the ultimate load. Comparison with the reference model, which has no openings and thus represents the maximum ultimate load, revealed significant insights. For square openings with a 7.1% opening ratio, a notable reduction in ultimate load by 35% was observed. As the ratio increased to 11.1%, 16.0%, and 21.8%, the ultimate load decreased by 60%, 75%, and 81%, respectively. Similarly, for circular openings, a parallel trend was noted. At a 7.1% opening ratio, a reduction in ultimate load by 25% was recorded. Increasing the ratio to 11.1%, 16.0%, and 21.8% resulted in corresponding reductions in ultimate load of 44%, 59%, and 76%, respectively.

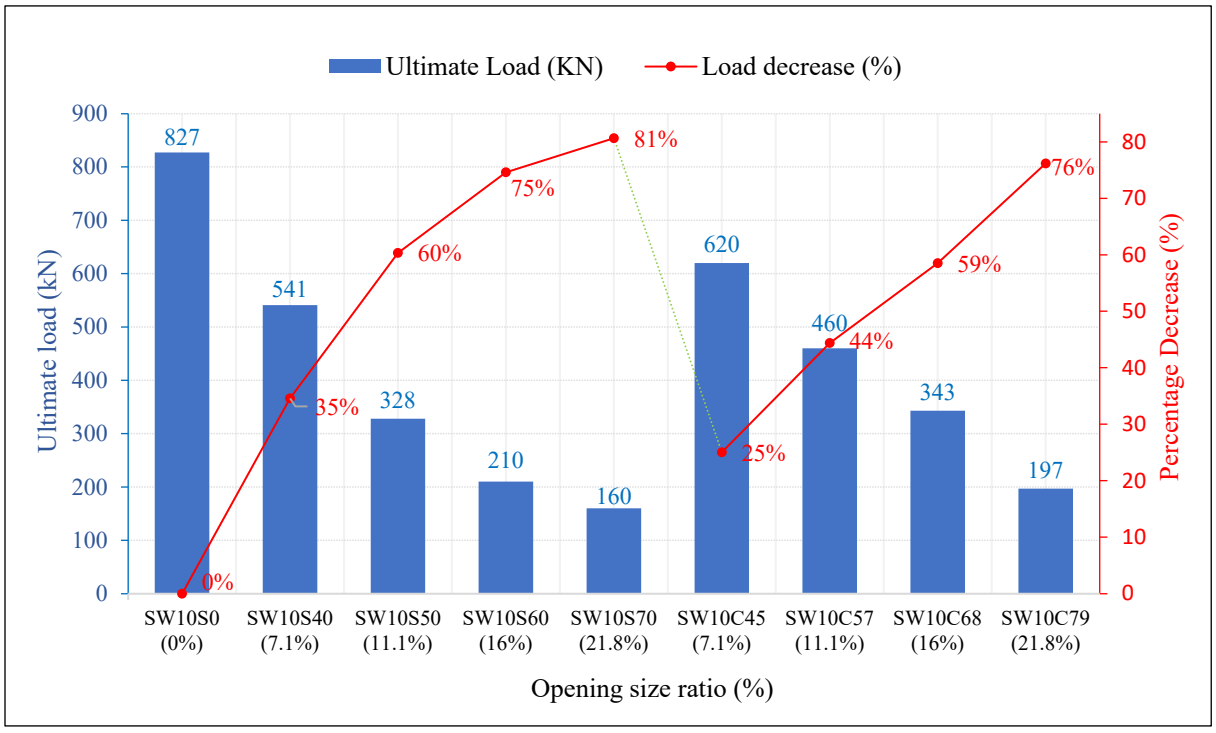

Figure 4.2 Effect of opening size and shape on the ultimate load.

The results indicate that increasing the size of square or circular openings reduces the ultimate load capacity of shear walls due to a decrease in shear stiffness caused by the removal of concrete parts. Larger openings decrease the effective

resisting area, leading to greater deformation and a higher likelihood of collapse under loads. Additionally, the reduction in shear stiffness limits the wall's ability to absorb and resist energy, further contributing to a decrease in its load capacity.

The solid wall without openings demonstrates the highest ultimate strength-to-weight ratio, indicating superior structural efficiency. As the opening ratio increases from 7.1% to 21.8%, a significant reduction in the ultimate strength-to-weight ratio is observed. For square openings, the reductions are 30%, 55%, 70%, and 75% for opening ratios of 7.1%, 11.1%, 16.0%, and 21.8%, respectively. Similarly, for circular openings, the reductions are 19%, 37%, 51%, and 70% at the same opening ratios as shown in Table 4.1.

4.2.1.2 **Effect of Opening Shape on the Ultimate Load**

In this study, two types of openings were used, as mentioned previously. The circular and square openings, showed that the impact of varying the shape of the openings should not be ignored. According to Figure 4.2, it is evident that circular openings exert a relatively lesser effect on the ultimate load compared to square openings of the same opening size ratio. Furthermore, as illustrated in Figure 4.3, when comparing circular openings to square openings with the same size ratios, it is evident that square openings result in a more significant decrease in ultimate load compared to circular openings, where at a 7.1% opening ratio, circular openings enhanced the wall's ultimate load capacity by 15% compared to square openings. At an 11.1% opening ratio, this improvement escalated to 40%, and at 16.0%, it increased further to 63%. Finally, at a 21.8% opening ratio, circular openings exhibited a 23% increase in the wall's ultimate load capacity relative to square openings. This difference is due to the fact that circular openings distribute loads more evenly, reducing the negative impact on the wall’s ultimate load capacity compared to square openings with sharp corners.

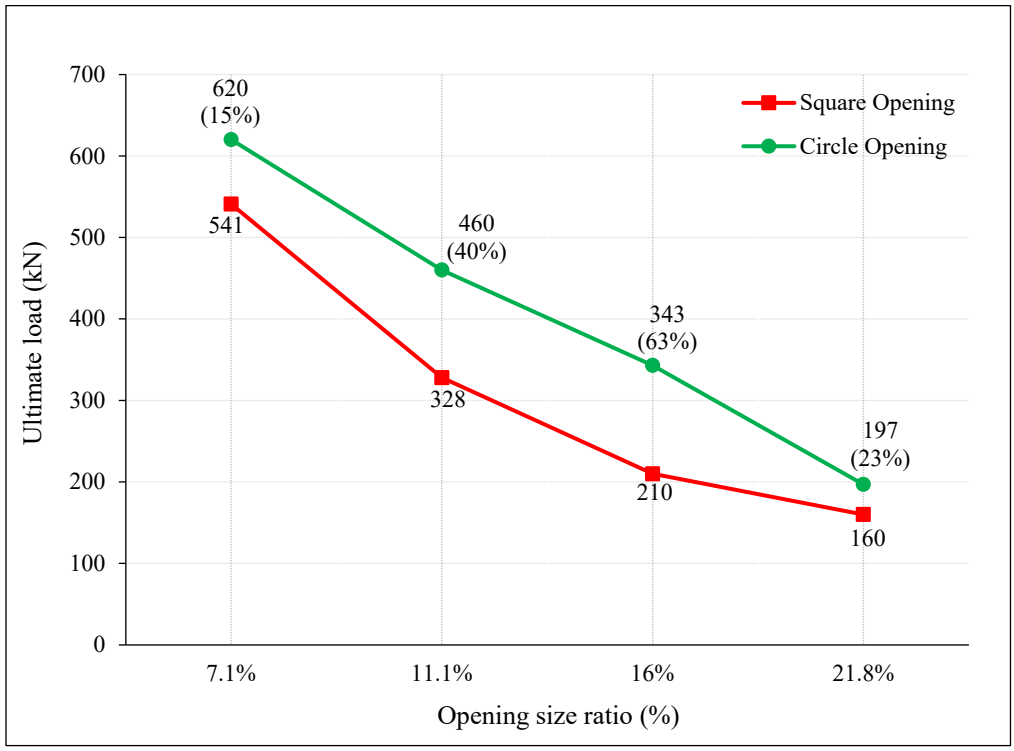

Figure 4.3 Effect of openings shape on the ultimate load.

4.2.1.3 **Effect of Thickness on Ultimate Load**

In the second group, three different shear wall thicknesses were used in this study 80, 100, and 120 mm, with an opening ratio of 16.0%. All results for the shear walls at this opening ratio showed an increase in ultimate load value for both square and circular openings. For specimens with square openings, increasing the wall thickness from 80 to 100 mm results in a 19% increase in ultimate load. Similarly, increasing the wall thickness from 100 to 120 mm leads to a 16.0% increase in ultimate load. For specimens with circular openings, the ultimate load increases by 33% when the wall thickness increases from 80 to 100 mm. Similarly, increasing the wall thickness from 100 to 120 mm results in a 19% increase in ultimate load. Figure 4.4 clearly shows that, regardless of the opening shape, increasing wall thickness increases the ultimate load for shear walls. On the other hand, compared to square openings at the same thickness, circular openings benefit more from increases in thickness.

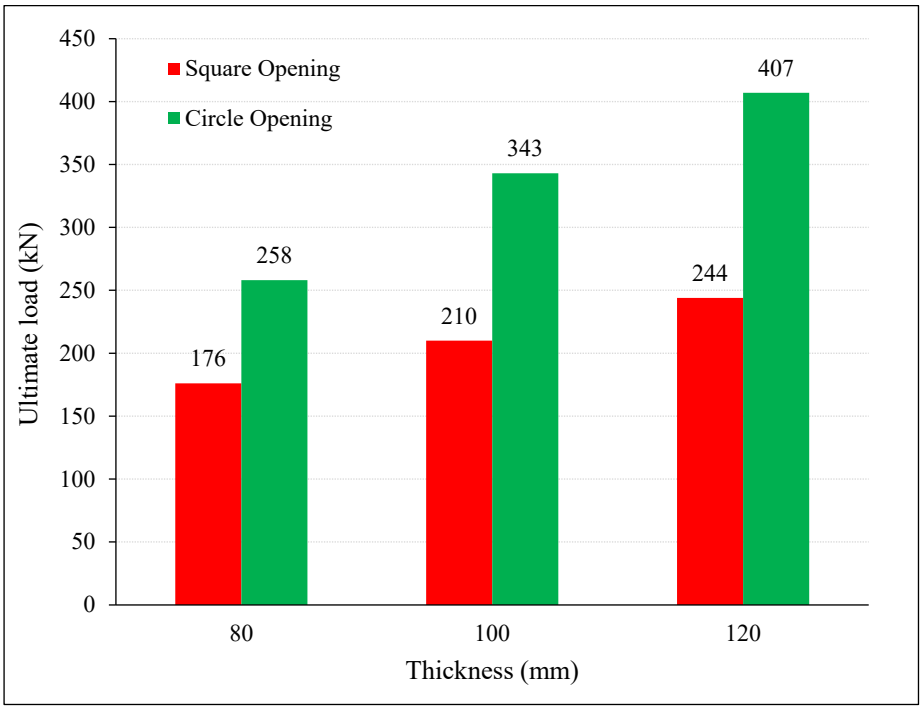

Figure 4.4 Effect of thickness on ultimate load.

The increase in ultimate load with increased thickness can be attributed to the increase in the cross-sectional area of the wall. As the thickness increases, the cross-sectional area also increases, and the effective depth further enhances this increase, improving the wall's ability to resist shear forces induced by loads and increasing its capacity to withstand the ultimate load.

In the wall without openings, the ultimate strength-to-weight ratio was 9.52. When comparing other walls, it is evident that square openings lead to a greater reduction in this ratio compared to circular openings. In 80 mm thick walls, the wall with a square opening shows a reduction of 68%, while the wall with a circular opening decrease by 54%. In 100 mm thick walls, the square opening wall decreases by 70%, while the circular opening wall decreases by 51%. In 120 mm thick walls, the square opening wall decreases by 71%, while the circular opening wall decreases by 51%. Overall, circular openings retain higher resistance compared to square openings.

4.2.1.4 **Effect of Strength on Ultimate Load**

In the third group, three different concrete strengths were used in shear walls 30, 45, and 60 MPa. At an opening ratio of 16.0%, all results showed a clear increase in ultimate load with increasing concrete strength for both square and circular openings. For specimens with square openings, increased concrete strength from 30 to 45 MPa resulted in an 11% increase in the ultimate load. and by 20% when it was increased from 45 to 60 MPa. Similarly, for specimens with circular openings, there was an 11% increase in ultimate load when concrete strength increased from 30 to 45 MPa and a 6% increase when strength increased from 45 to 60 MPa. As illustrated in Figure 4.5. The results indicate that shear walls with square openings benefit more from increased concrete strength, while circular openings show a higher ultimate load.

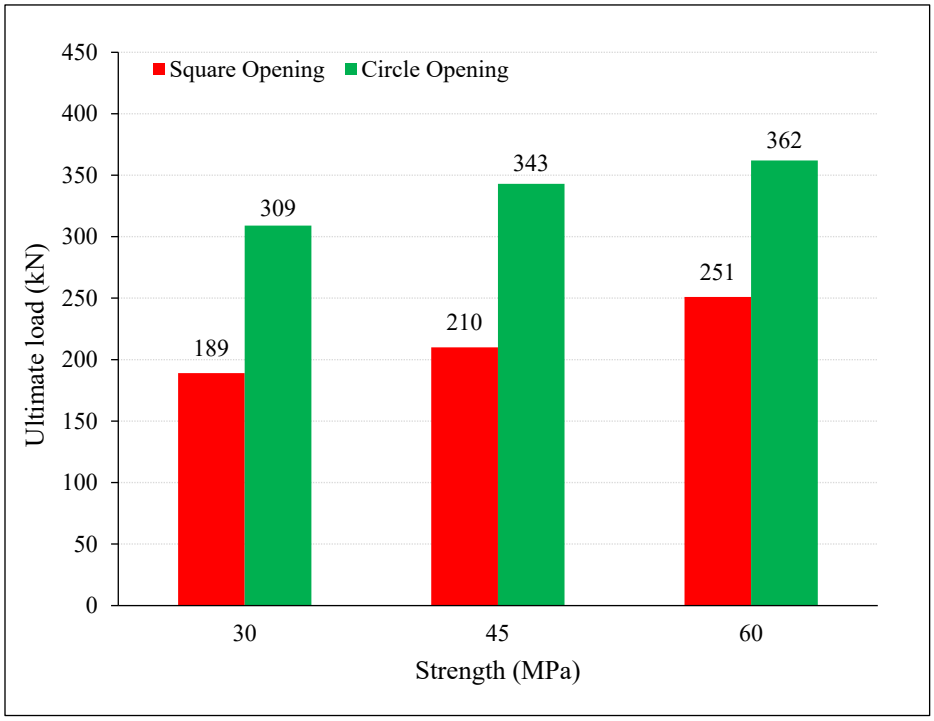

Figure 4.5 Effect of strength on ultimate load.

The increase in ultimate load with higher concrete strength can be scientifically attributed to the relationship expressed in the equation $V_c = \frac{1}{6}\sqrt{f'_c}$ b_w d [61]. This

equation indicates that the nominal shear strength provided by concrete, V_c is directly proportional to the square root of the compressive strength f'_c . As a result, an increase in f'_c enhances the shear resistance V_c, thereby improving the ultimate load-bearing capacity of the shear wall. This correlation reflects the fundamental influence of concrete compressive strength on the structural performance under shear forces.

4.2.1.5 **Effect of Reinforcement Patterns on Ultimate Load**

In the fourth group, the effect of two reinforcement patterns around circular openings with a fixed opening ratio of 7.1% was studied and compared to the reference model (SW10C45) with conventional reinforcement. Model 1, which has two reinforcement layers and additional diagonal reinforcement, showed a 20% increase in ultimate load compared to the reference model. In contrast, Model 2, with one reinforcement layer and an additional diagonal layer, showed only a slight 2% increase in ultimate load.

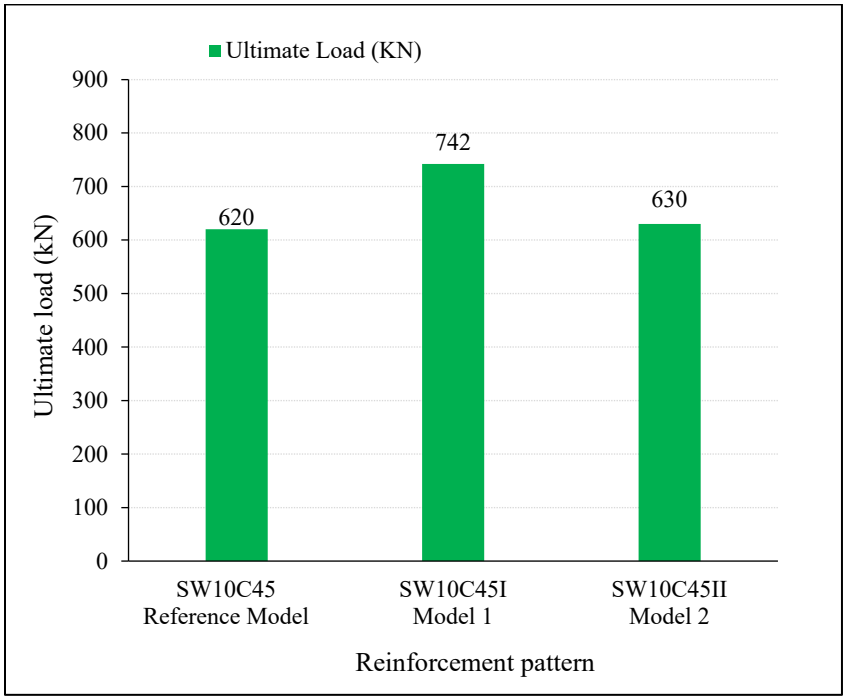

Figure 4.6 Effect of reinforcement patterns on ultimate load.

The increase in ultimate load in Model 1 is due to the second layer of reinforcement, which improves stress distribution and enhances the wall's shear resistance, thereby increasing load-bearing capacity. In Model 2, the slight increase in ultimate load is attributed to the single layer of reinforcement, which does not provide sufficient stress distribution, reducing the effectiveness of the additional diagonal reinforcement in improving structural performance.

4.2.2 **Load-Displacement Relationship**

During the testing process, a vertically mounted LVDT device is used to measure displacement at each load increment. Figures 4.7 to 4.10 show the load-displacement curves for the four groups, showing that all specimens initially experienced an initial setting region, followed by a linear elastic phase as loading increased. As loading continued, the specimens entered the plastic phase, where deformation and cracking increased until reaching the peak load, representing the ultimate strength. Beyond this point, the specimens transitioned into the progressive failure phase.

The curves are an effective tool for understanding the behavior of the shear walls under the influence of various factors, including the shape of openings (square and circle), opening size ratio (7.1%, 11.1%, 16.0%, and 21.8%), wall thickness (80, 100, 120 mm), concrete strength (30, 45, 60 MPa), and the distribution of reinforcement around the openings (diagonal reinforcement). Key indicators such as ductility, shear stiffness, and energy absorption were calculated in this study to assess how these factors impact the performance of the tested shear walls. This evaluation helps in understanding the effects of openings and reinforcement on load-carrying capacity and overall stiffness, providing critical insights for improving the design of these structural elements.

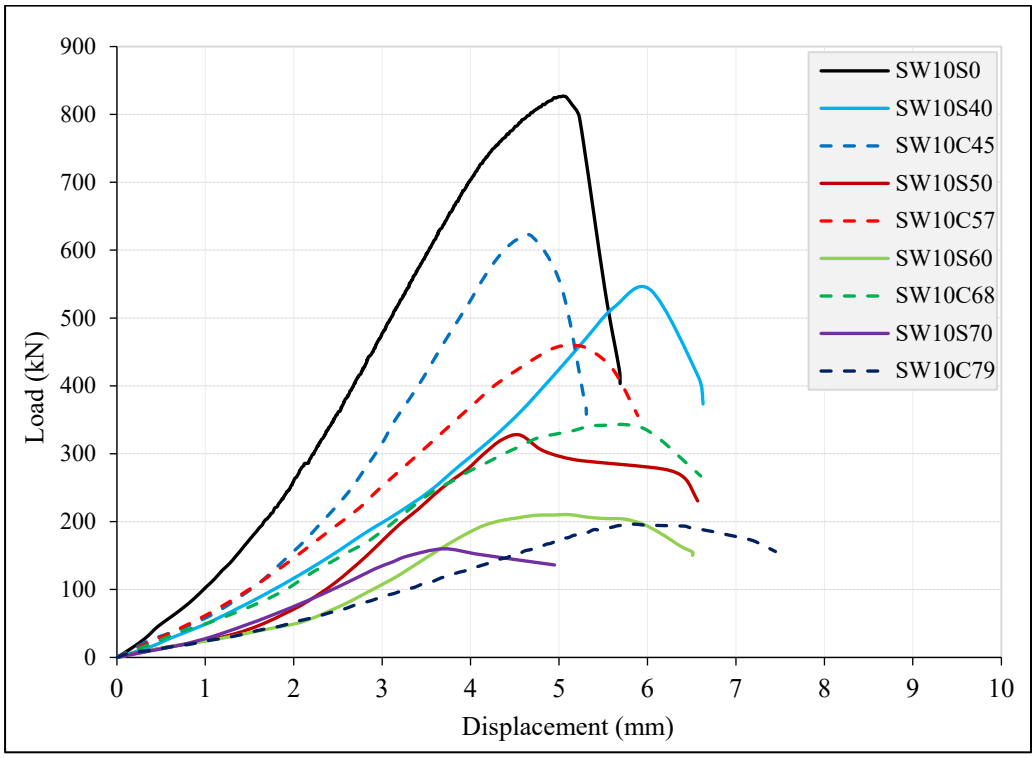

Figure 4.7 Load-displacement curve of specimens in the first group.

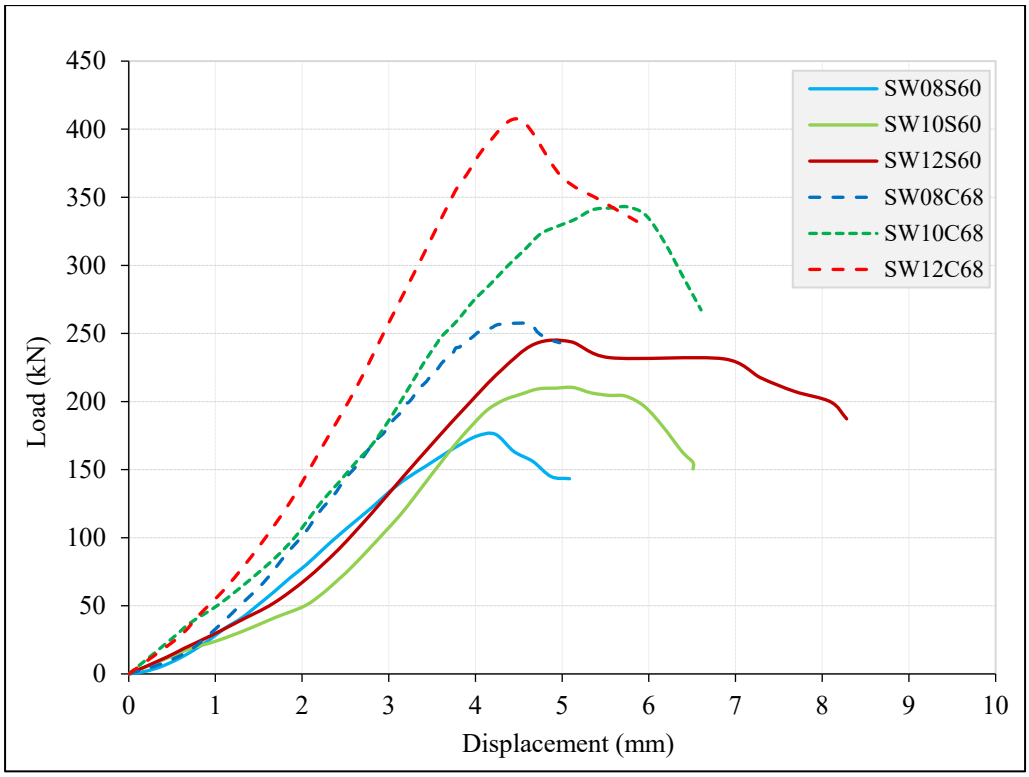

Figure 4.8 Load-displacement curve of specimens in the second group.

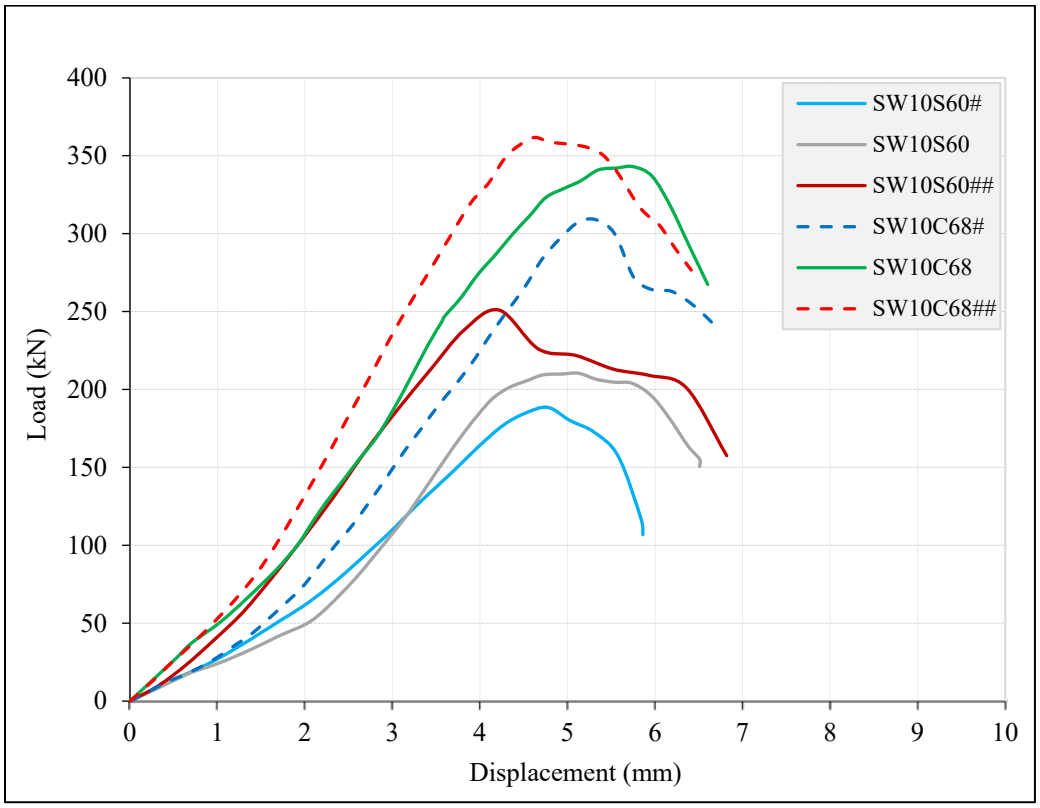

Figure 4.9 Load-displacement curve of specimens in the third group.

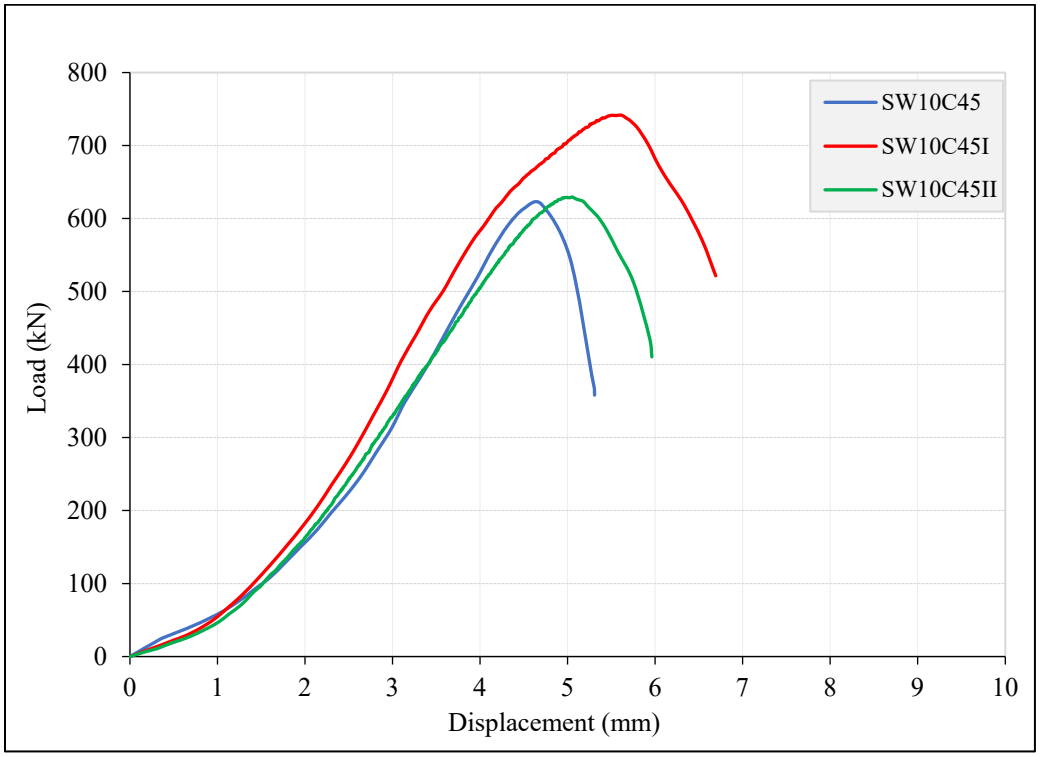

Figure 4.10 Load-displacement curve of specimens in the fourth group.

4.2.3 **Ductility Index**

Ductility index measures a structure's ability to keep carrying loads while deforming past its yield point. Could be determine using Equation 4.1

$$\text{Ductility Index} = \frac{\Delta_u}{\Delta_y} \quad \ldots\ldots\ldots\ldots\ldots\ldots \quad 4.1$$

Where $\Delta_u$the ultimate displacement is Δ_y is the yield displacement. Various methods exist to define these two limit states, which can lead to different ductility index coefficients. Park (1989) [62] found that multiple definitions can accurately estimate the ductility index coefficient based on extensive laboratory test data. In this study, the yield displacement is established by the intersection of a horizontal line at the maximum force with a line drawn from the origin to the point on the envelope curve corresponding to 75% of the maximum force. The ultimate state is defined as the point on the declining portion of the envelope curve where the force has reduced by 15%. These concepts are illustrated in Figure 4.11, and the ductility index values for the four groups are detailed in Table 4.2 [63, 64].

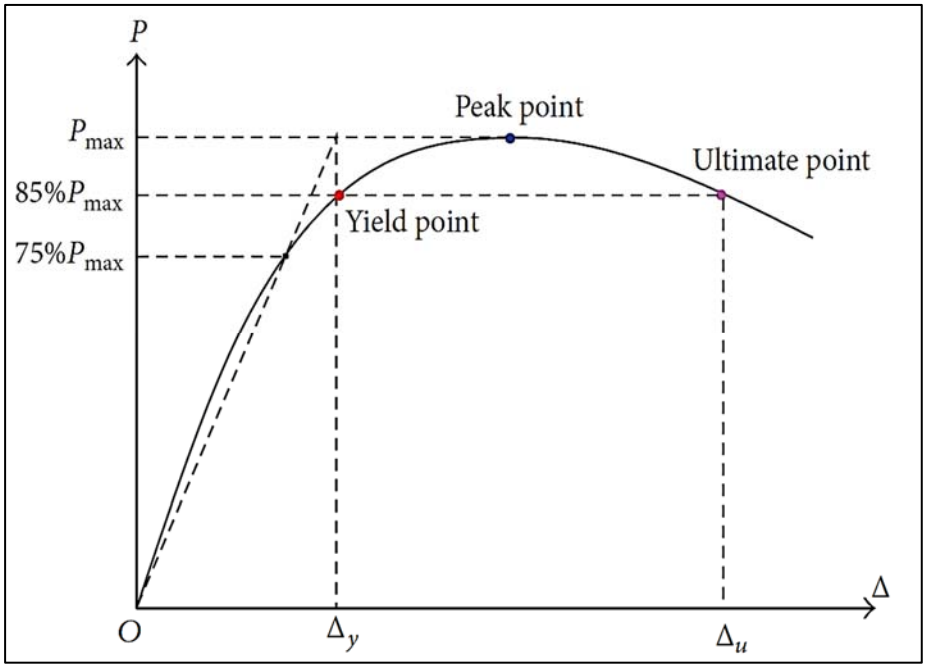

Figure 4.11 Definition of yielding and ultimate state of the shear wall.

Table 4.2 Ductility index values for the four groups.

Group No.1				Group No.2			
Specimens	Δu (mm)	Δy (mm)	Ductility index	Specimens	Δu (mm)	Δy (mm)	Ductility index
SW10S0	5.34	4.51	1.184	SW08S60	4.78	3.80	1.258
SW10S40	6.38	5.84	1.092	SW10S60	6.20	4.33	1.430
SW10S50	6.12	4.35	1.407	SW12S60	7.69	4.55	1.689
SW10S60	6.20	4.33	1.430	SW08C68	4.97	3.94	1.262
SW10S70	4.95	3.40	1.456	SW10C68	6.39	5.03	1.271
SW10C45	5.06	4.45	1.136	SW12C68	5.49	4.20	1.308
SW10C57	5.75	4.75	1.210	-	-	-	-
SW10C68	6.39	5.03	1.271	-	-	-	-
SW10C79	7.27	5.60	1.298	-	-	-	-
Group No.3				Group No.4			
Specimens	Δu (mm)	Δy (mm)	Ductility index	Specimens	Δu (mm)	Δy (mm)	Ductility index
SW10S60#	5.52	4.35	1.269	SW10C45	5.06	4.45	1.136
SW10S60	6.20	4.33	1.430	SW10C45I	6.26	4.94	1.269
SW10S60##	5.50	3.90	1.409	SW10C45II	5.66	4.71	1.202
SW10C68#	6.18	5.10	1.213	-	-	-	-
SW10C68	6.39	5.03	1.271	-	-	-	-
SW10C68##	6.01	4.15	1.448	-	-	-	-

4.2.3.1 **Effect of Opening Size and Shape on the Ductility Index**

In the first group, which aimed to study the effect of opening size and shape on ductility index, as shown in Figure 4.12, the specimens with square openings exhibited an 8% decrease in ductility index at an opening ratio of 7.1%. Conversely, at opening ratios of 11.1%, 16.0%, and 21.8%, increases in ductility index of 19%, 21%, and 23% were observed, respectively. These results indicate that square openings significantly improve ductility index at higher opening ratios. For specimens with circular openings, a 4% decrease in ductility index was noted at an opening ratio of 7.1%. However, the results showed an increase in ductility index with higher opening ratios, with ductility index increasing by 2%, 7%, and 10% at

opening ratios of 11.1%, 16.0%, and 21.8%, respectively. Although there was a noticeable increase in ductility index with circular openings, the improvement was less pronounced compared to square openings. Regarding the effect of opening shape on ductility index, the results clearly demonstrated that square openings achieved a greater increase in ductility index compared to circular openings.

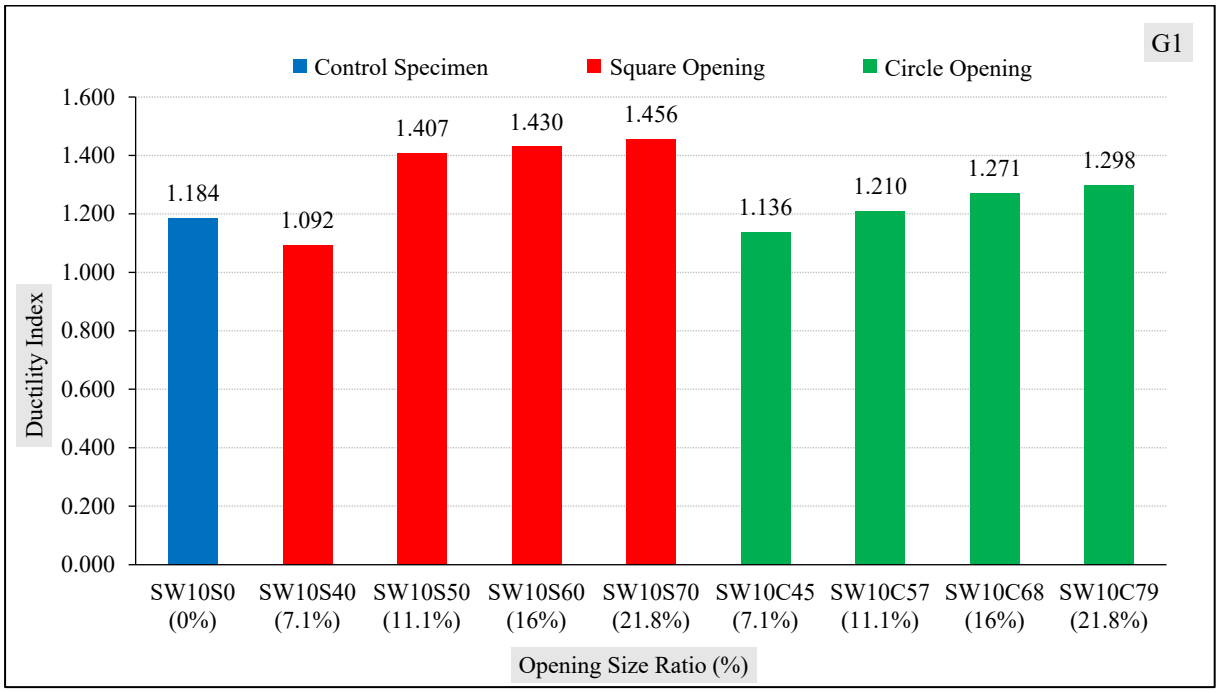

Figure 4.12 Ductility index of shear wall specimens for the first group.

Ductility index largely depends on the material's ability to withstand plastic deformation before failure. In the case of walls with openings, ductility index increases when the remaining material around the openings allows for the development of larger plastic deformation zones. Larger openings provide more area for the distribution of deformations, enhancing the wall's capacity to withstand increased deformations without sudden fracture.

4.2.3.2 **Effect of Thickness on the Ductility Index**

In the second group, which aimed to study the effect of increasing thickness at a constant opening ratio of 16.0% on ductility index, as shown in Figure 4.13, the

results revealed that specimens with square openings experienced a significant improvement in ductility index. When the thickness increased from 80 to 100 mm, ductility index increased by 14%. When the thickness was further increased from 100 to 120 mm, ductility index increased by 18%. This substantial increase in ductility index highlights the effectiveness of increased thickness in enhancing the structural performance of specimens with square openings. In contrast, specimens with circular openings showed only a slight increase in ductility index, with increases of 1% and 3% for the same thickness changes. This suggests that the effect of thickness on improving ductility index is less pronounced for specimens with circular openings compared to those with square openings.

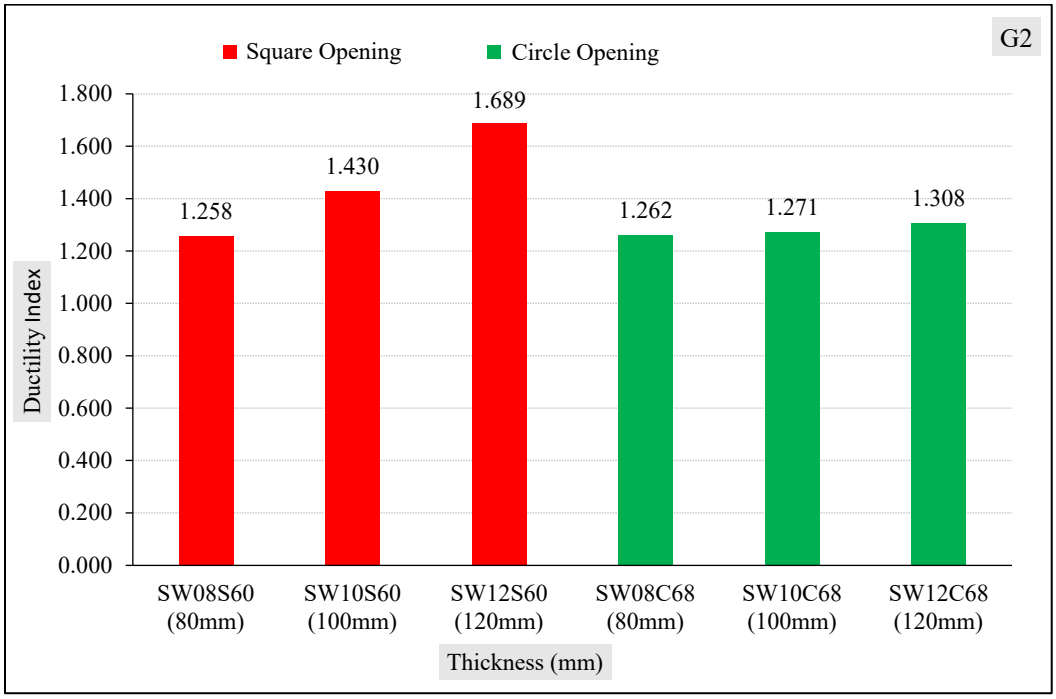

Figure 4.13 Ductility index of shear wall specimens for the second group.

4.2.3.3 **Effect of Strength on the Ductility Index**

In the third group, which aimed to study the effect of increasing strength at a constant opening ratio of 16.0% on ductility index, as shown in Figure 4.14, the results indicated that specimens with square openings experienced a 13% increase

in ductility index when the strength increased from 30 to 45 MPa. However, when the strength increased from 45 to 60 MPa, ductility index decreased by 1%. This suggests that while initial increases in strength positively impact ductility index for square openings, further increases may lead to diminishing returns in terms of ductility index. In contrast, specimens with circular openings showed a consistent increase in ductility index. Specifically, ductility index increased by 5% when the strength increased from 30 to 45 MPa, and by 14% when the strength increased from 45 to 60 MPa. This consistent improvement indicates that circular openings benefit continuously from increases in strength, leading to more effective enhancements in ductility index across different strength.

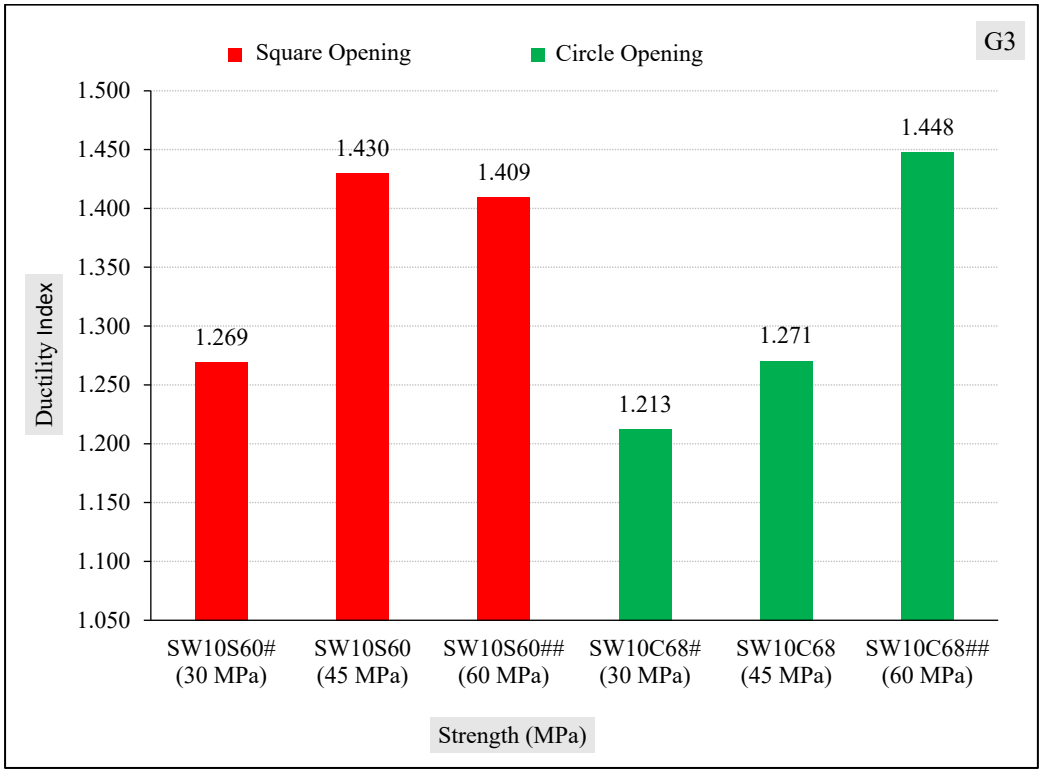

Figure 4.14 Ductility index of shear wall specimens for the third group.

4.2.3.4 **Effect of Reinforcement Patterns on the Ductility Index**

In the fourth group, which examined the effect of two reinforcement patterns around circular openings with a constant opening ratio of 7.1% on the ductility

index, as shown in Figure 4.15, results were compared with a traditional reference model (SW10C45). Model 1, with two additional layers of diagonal reinforcement, achieved a 12% increase in ductility index compared to the reference model. Model 2, which had one layer of conventional and one layer of diagonal reinforcement, showed a 6% improvement. Although diagonal reinforcement contributed to increased ductility, its effect was less significant in Model 2 than in Model 1.

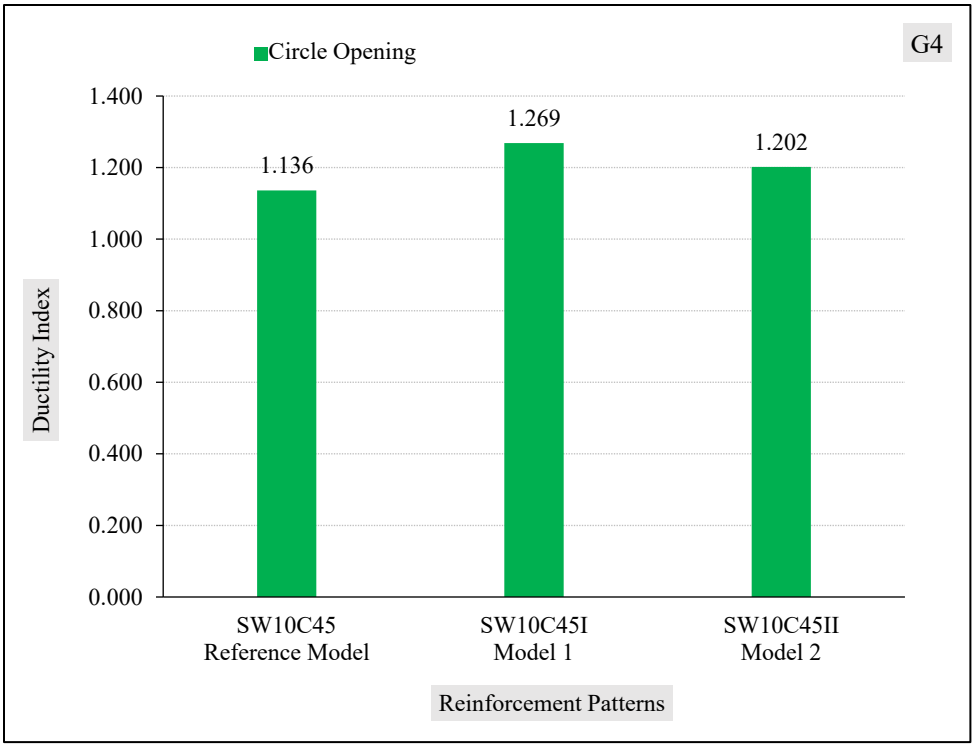

Figure 4.15 Ductility index of shear wall specimens for the fourth group.

4.2.4 **Shear Stiffness**

Shear stiffness in shear walls refers to the wall's capacity to resist lateral displacement when subjected to loads, serving as an indicator of its strength in withstanding external forces without undergoing substantial deformation. This property is crucial in ensuring the stability and integrity of structures, especially during seismic or wind events. Shear stiffness is typically calculated as the slope of

the linear portion of the load-displacement curve, as represented in Equation 4.2 [65]:

$$\text{Shear stiffness} = \frac{P_y}{\Delta_y} \quad \ldots\ldots\ldots\ldots\ldots\ldots (4.2)$$

Where:

Py**:** The yield load (kN).

Δy: The yield displacement (mm).

Table 4.3 presents the shear stiffness measurements for all four groups, offering a detailed comparison of the structural performance across different configurations.

Table 4.3 Shear stiffness values for the four groups.

Group No.1				Group No.2			
Specimens	Py (kN)	Δy (mm)	Stiffness (kN/mm)	Specimens	Py (kN)	Δy (mm)	Stiffness (kN/mm)
SW10S0	782.48	4.51	174	SW08S60	167.68	3.80	44
SW10S40	529.47	5.84	91	SW10S60	201.28	4.33	46
SW10S50	320.68	4.35	74	SW12S60	235.74	4.55	52
SW10S60	201.28	4.33	46	SW08C68	246.37	3.94	62
SW10S70	152.32	3.40	45	SW10C68	330.85	5.03	66
SW10C45	607.26	4.45	136	SW12C68	392.16	4.20	93
SW10C57	441.28	4.75	93	-	-	-	-
SW10C68	330.85	5.03	66	-	-	-	-
SW10C79	192.03	5.60	34	-	-	-	-
Group No.3				Group No.4			
Specimens	Py (kN)	Δy (mm)	Stiffness (kN/mm)	Specimens	Py (kN)	Δy (mm)	Stiffness (kN/mm)
SW10S60#	179.70	4.35	41	SW10C45	607.26	4.45	136
SW10S60	201.28	4.33	46	SW10C45I	698.25	4.94	141
SW10S60##	240.78	3.90	62	SW10C45II	608.29	4.71	129
SW10C68#	306.31	5.10	60	-	-	-	-
SW10C68	330.85	5.03	66	-	-	-	-
SW10C68##	337.05	4.15	81	-	-	-	-

4.2.4.1 **Effect of Opening Size and Shape on the Shear Stiffness**

The results of the first group, illustrated in Figure 4.16, which include shear walls with circular and square openings compared to the control model (SW10S0), indicate a substantial reduction in shear stiffness due to the increased opening ratio. For square openings, at opening ratios of 7.1%, 11.1%, 16.0%, and 21.8%, the shear wall stiffness decreased by 48%, 57%, 74%, and 74%, respectively, compared to the control model. Similarly, for circular openings with the same opening ratios, the shear stiffness decreased by 22%, 47%, 62%, and 80%, respectively, in comparison to the control model. The results also showed that walls with circular openings exhibit better shear stiffness at lower opening ratios, with a smaller reduction in shear stiffness compared to walls with square openings. However, at the largest opening ratio of 21.8%, the reduction in shear stiffness for walls with circular openings becomes greater than that for walls with square openings.

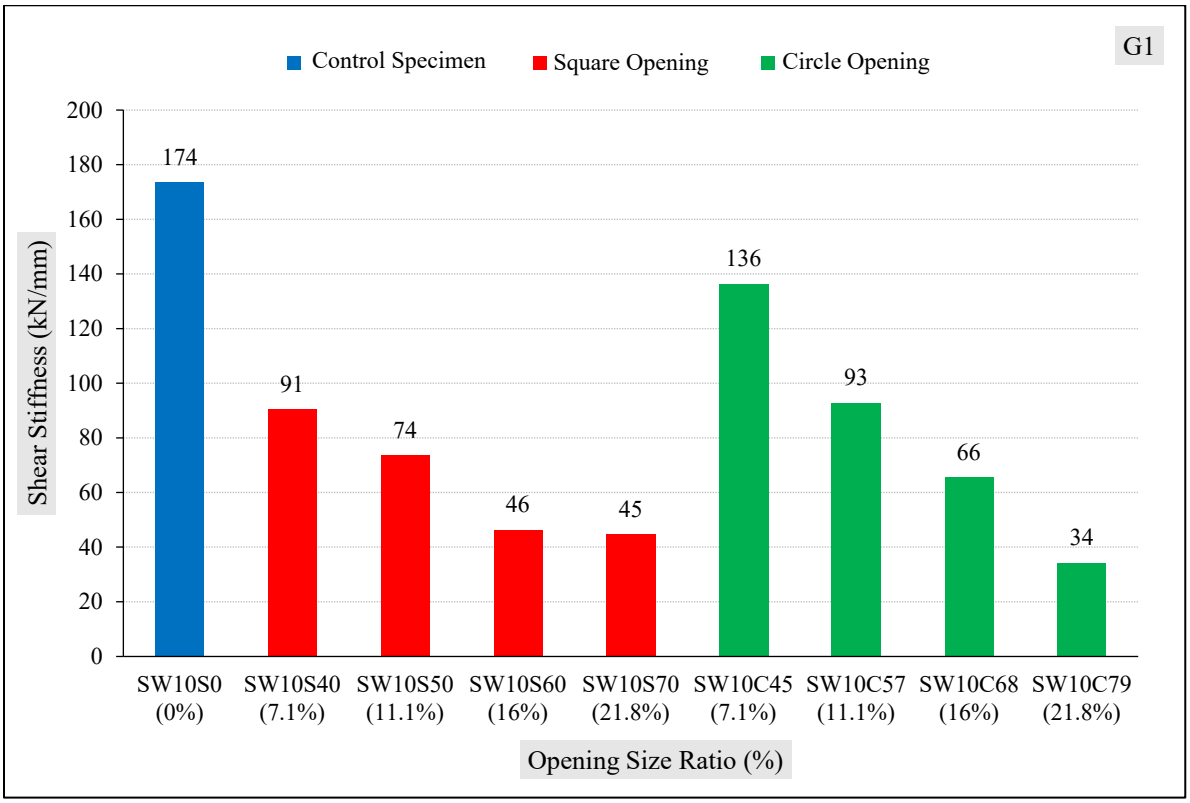

Figure 4.16 Shear stiffness of the first group specimens.

4.2.4.2 **Effect of Thickness on the Shear Stiffness**

In the second group, which aimed to study the effect of increasing thickness at a constant opening ratio of 16.0% on shear stiffness, as shown in Figure 4.17, The concrete shear walls with square and circular openings showed a significant improvement in shear stiffness, according to the results. For square openings, increasing the wall thickness from 80 to 100 mm resulted in an increase of 5% in shear stiffness, and a 13% increase when the thickness was increased from 100 to 120 mm. In contrast, circular openings exhibited a 6% increase in shear stiffness when the thickness was increased from 80 to 100 mm, and a substantial 41% increase when the thickness was increased from 100 to 120 mm, highlighting the greater impact of thickness on the shear stiffness of walls with circular openings.

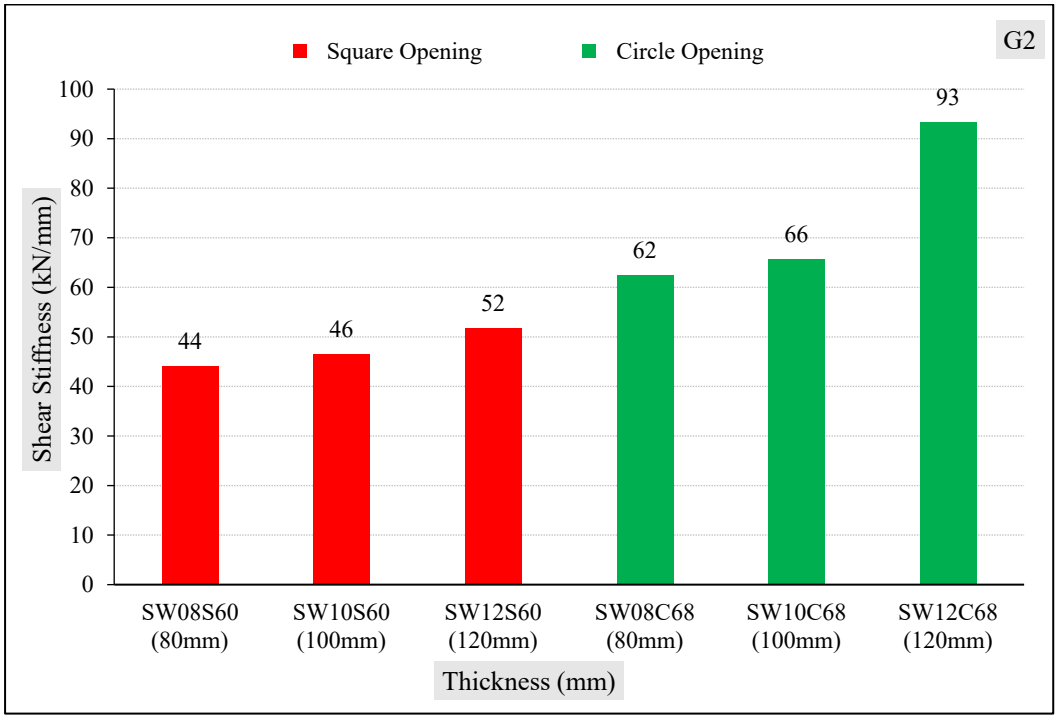

Figure 4.17 Shear stiffness of the second group specimens.

4.2.4.3 **Effect of Strength on the Shear Stiffness**

For the third group, which aimed to study the effect of increasing strength at a constant opening ratio of 16.0% on shear stiffness, as shown in Figure 4.18, the

results demonstrated an increase in shear stiffness for concrete shear walls with both square and circular openings. Square openings showed a 12% increase in shear stiffness when increasing the strength from 30 to 45 MPa, and a 35% increase when the strength was increased from 45 to 60 MPa. In contrast, circular openings exhibited a 10% increase in shear stiffness with the same strength increase from 30 to 45 MPa, and a 23% increase from 45 to 60 MPa. These findings suggest that increasing strength significantly enhances shear stiffness, particularly for walls with square openings. This highlights the effectiveness of higher strength in improving structural performance.

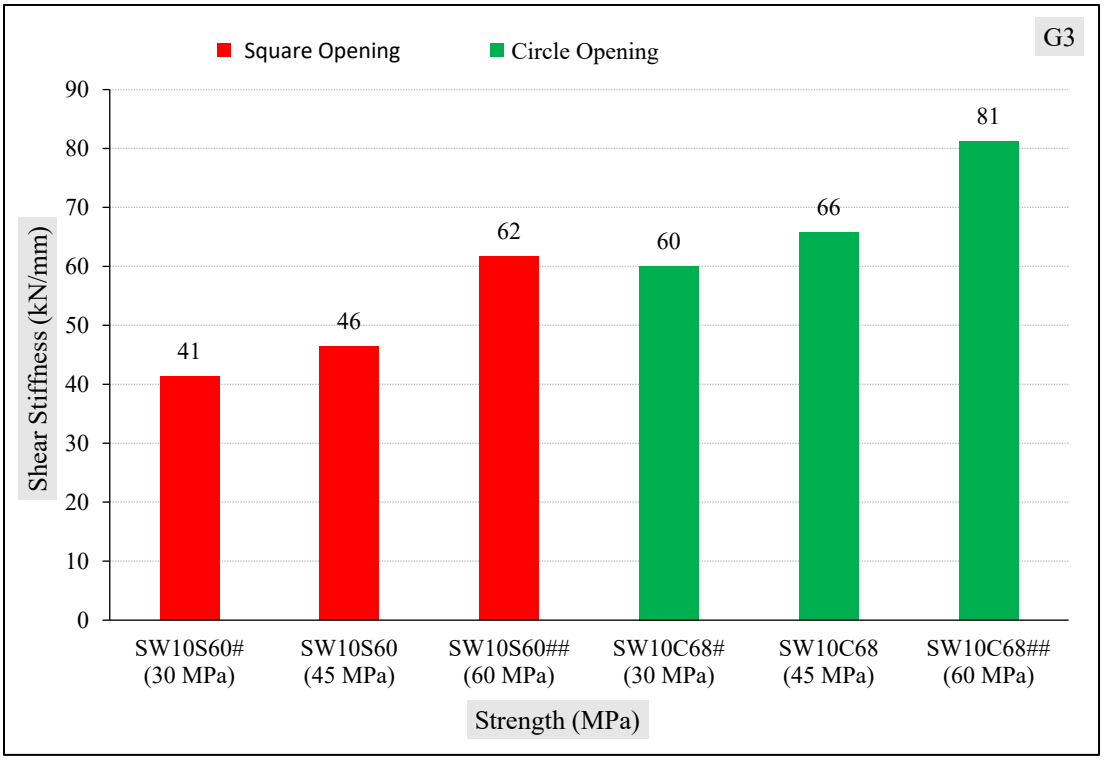

Figure 4.18 Shear stiffness of the third group specimens.

4.2.4.4 **Effect of Reinforcement Patterns on the Shear Stiffness**

In the fourth group, which examined the effect of two reinforcement patterns around circular openings with a constant opening ratio of 7.1% %, as shown in Figure 4.19, the results were compared to the reference model (SW10C45) with

conventional reinforcement. Model 1, with the addition of diagonal reinforcement, showed a slight 4% increase in shear stiffness compared to the reference model. In contrast, Model 2, with one layer of conventional reinforcement and an additional diagonal layer, exhibited a 5% decrease in shear stiffness compared to the reference model.

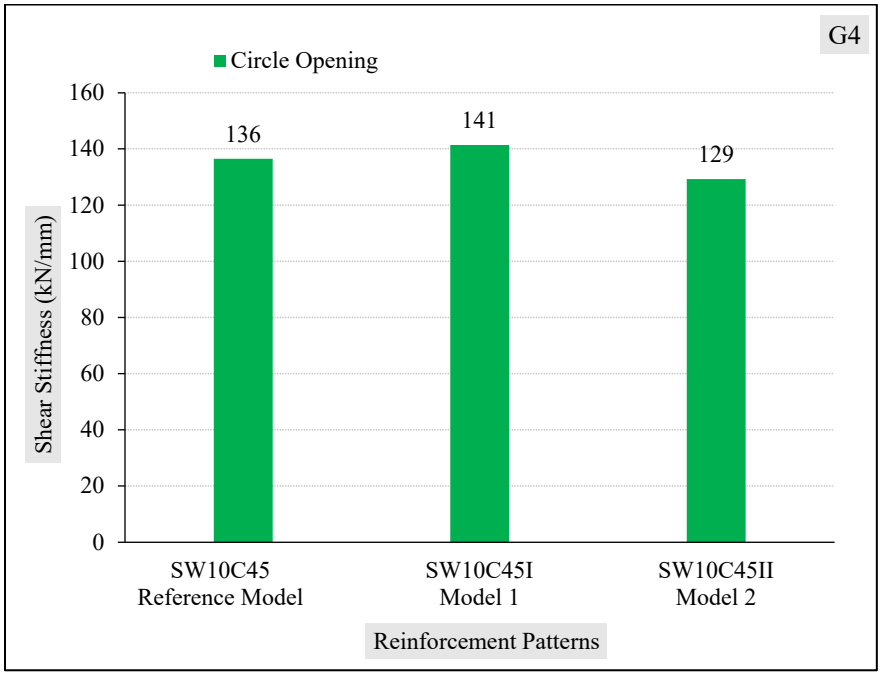

Figure 4.19 Shear stiffness of the fourth group specimens.

4.2.5 **Energy Absorption**

The energy absorption capacity of a structure, determined by the area under the load-displacement curve, reflects its ability to dissipate energy. Higher capacity indicates better performance, especially for shear walls tested under diagonal compression.

In this study, the energy absorption capacity of the shear walls was calculated using the trapezoidal rule method in an Excel sheet, as outlined in Equation 4.3 4.3[66].

$$E=\frac{1}{2}\sum_{i=1}^{n}(P_i + P_{i+1}).\Delta x_i \quad \ldots\ldots\ldots\ldots\ldots\ldots (4.3)$$

Where:

E: Energy absorption (joules or kN.mm)

P_i and P_{i+1}: Loads (kN) at points *i* and *i+1*, respectively

Δx_i: Displacement (mm) between points *i* and *i+1*, respectively

All four groups' energy absorption measurements are shown in Table 4.4, offering a detailed comparison of the structural performance across different configurations.

Table 4.4 Energy absorption values for the four groups.

Group No.1			Group No.2
Specimens	Energy Absorption (kN.mm)	Specimens	Energy Absorption (kN.mm)
SW10S0	2419	SW08S60	498
SW10S40	1652	SW10S60	768
SW10S50	1151	SW12S60	1294
SW10S60	768	SW08C68	686
SW10S70	457	SW10C68	1310
SW10C45	1513	SW12C68	1397
SW10C57	1441	-	-
SW10C68	1310	-	-
SW10C79	834	-	-
Group No.3			Group No.4
Specimens	Energy Absorption (kN.mm)	Specimens	Energy Absorption (kN.mm)
SW10S60#	598	SW10C45	1513
SW10S60	768	SW10C45I	2719
SW10S60##	1058	SW10C45II	1902
SW10C68#	1108	-	-
SW10C68	1310	-	-
SW10C68##	1424	-	-

4.2.5.1 **Effect of Opening Size and Shape on the Energy Absorption**

The first group, as shown in Figure 4.20, studied the impact of the size and shape of openings on absorbed energy compared to the reference specimen. For square openings, the specimen with a 7.1% opening size experienced a 32% decrease in

absorbed energy. For opening sizes of 11.1%, 16.0%, and 21.8%, absorbed energy decreased by 52%, 68%, and 81%, respectively. Similarly, when comparing specimens with circular openings, the specimen with a 7.1% opening size saw a 37% reduction in absorbed energy. For opening sizes of 11.1%, 16.0%, and 21.8%, absorption decreased by 40%, 46%, and 66%, respectively. The results also show that specimens with square openings exhibit a greater reduction in absorbed energy compared to specimens with circular openings at the same opening size ratio, highlighting the importance of the shape and size of the opening on energy absorption capacity.

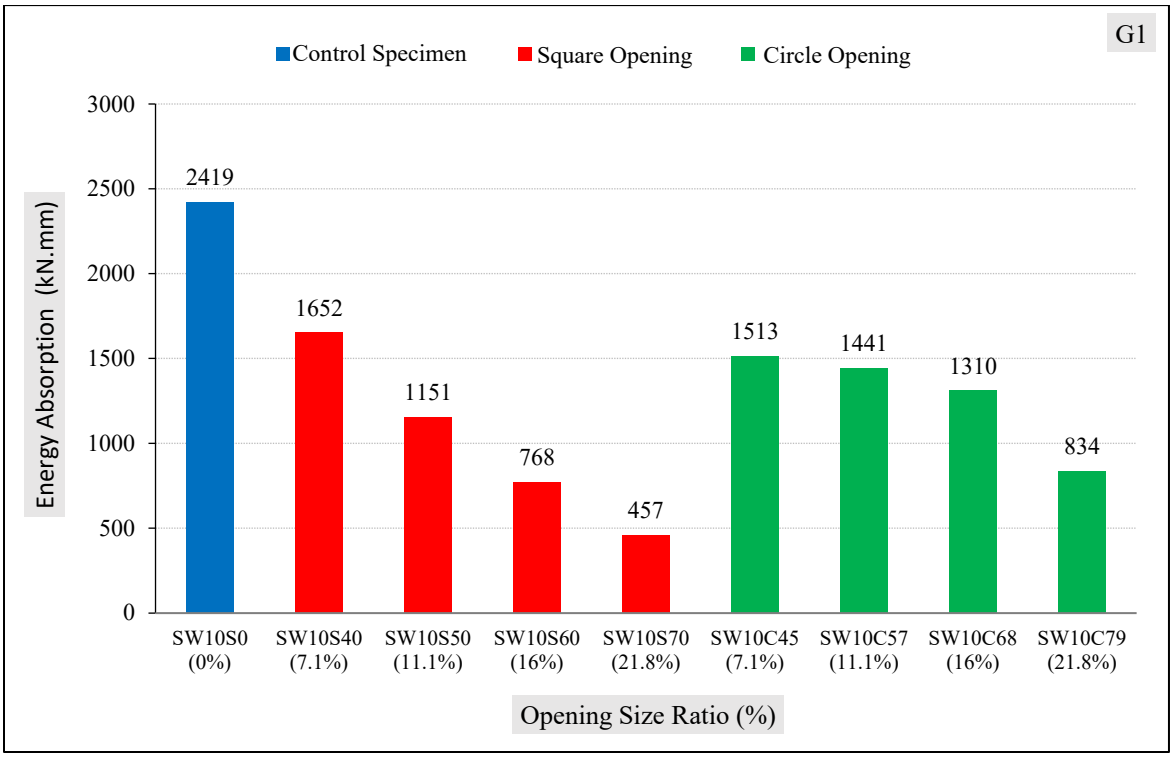

Figure 4.20 Energy absorption of first group shear wall specimens.

The presence of openings in walls reduces their stiffness and increases their ductility, which decreases their ability to resist large deformations. Openings reduce the area available to carry loads, weakening the wall's capacity to withstand applied forces. Furthermore, square openings have a more significant impact on the wall's stiffness compared to circular openings due to the sharp corners where stresses are

concentrated, increasing the likelihood of cracking and reducing the wall's energy absorption capacity.

4.2.5.2 **Effect of Thickness on the Energy Absorption**

For the second group, which aimed to study the impact of increasing thickness at a constant opening ratio of 16.0% on energy absorption, as shown in Figure 4.21, significant increases in energy absorption capacity were observed. For square openings, the capacity increased by approximately 54% when the thickness was raised from 80 to 100 mm and by 68% when increased from 100 to 120 mm. In contrast, for circular openings, a substantial increase of about 91% was noted when the thickness increased from 80 to 100 mm. However, when the thickness was further increased from 100 to 120 mm, the energy absorption capacity increased slightly by around 7%.

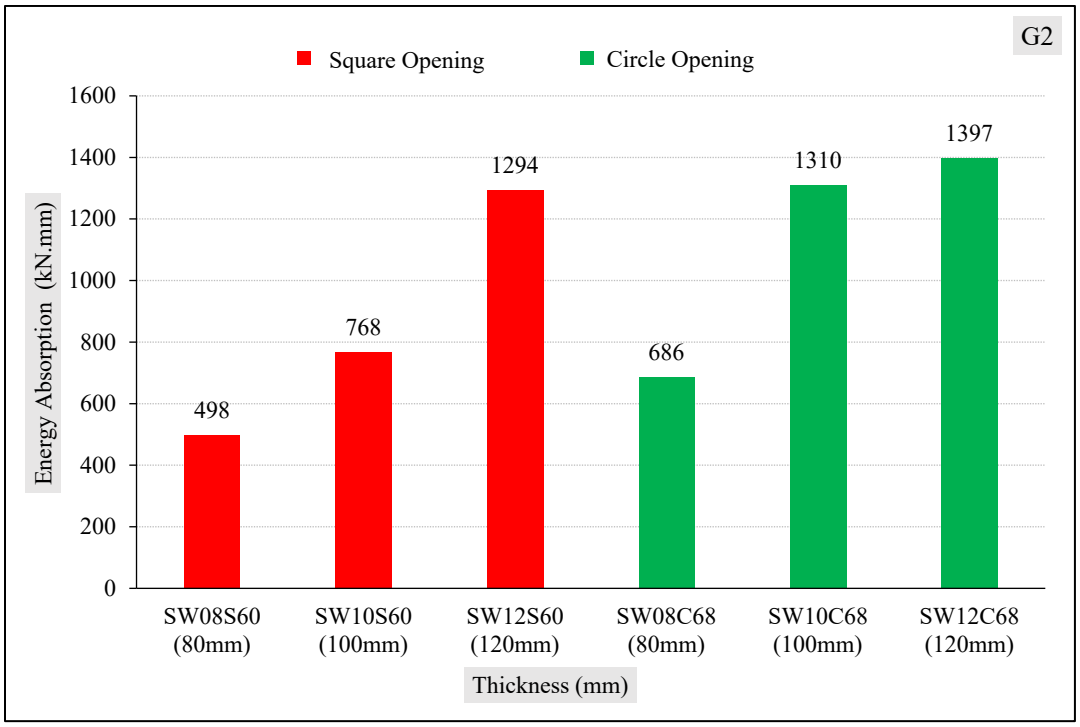

Figure 4.21 Energy absorption of second group shear wall specimens.

4.2.5.3 **Effect of Strength on the Energy Absorption**

In the third group, which studied the effect of increasing strength at a constant opening ratio of 16.0%, results showed a significant increase in energy absorption for square openings, as shown in Figure 4.22. Energy absorption increased by 28% when strength rose from 30 to 45 MPa and by 38% from 45 to 60 MPa. For circular openings, energy absorption increased by 18% from 30 to 45 MPa and by 9% from 45 to 60 MPa, demonstrating the positive impact of increased strength on energy absorption.

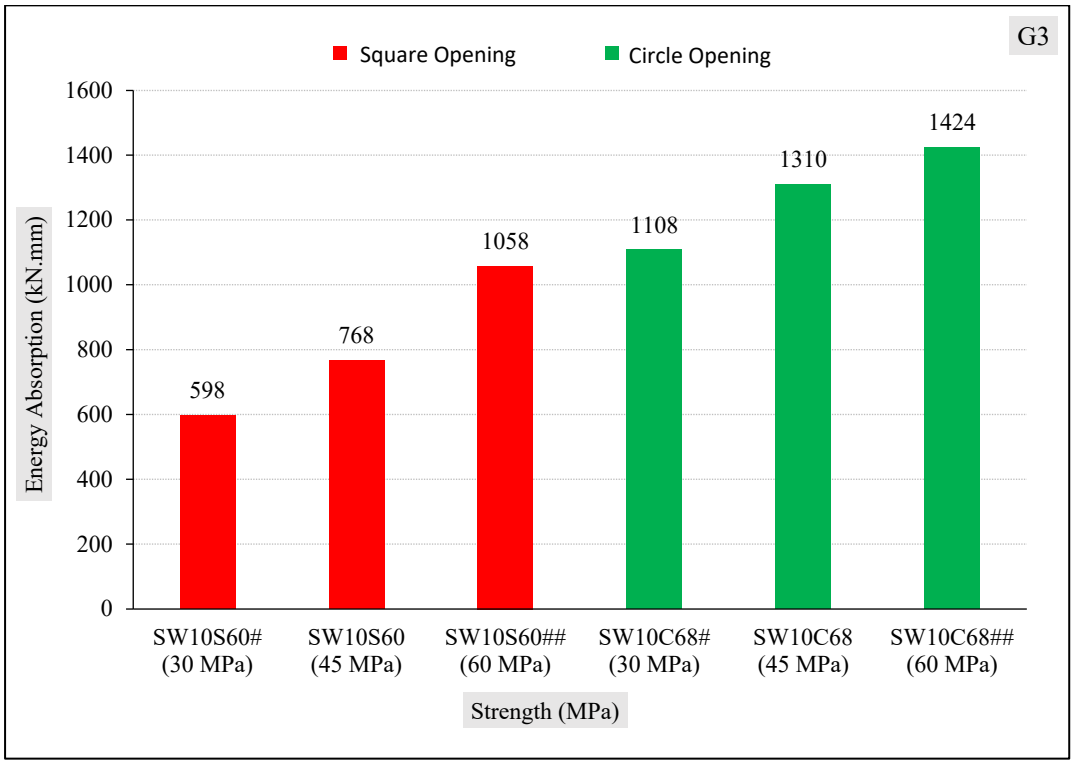

Figure 4.22 Energy absorption of third group shear wall specimens.

4.2.5.4 **Effect of Reinforcement Patterns on the Energy Absorption**

The fourth group examined the effect of two reinforcement patterns around circular openings with a fixed opening ratio of 7.1%, as shown in Figure 4.23. Model 1, featuring two layers of reinforcement with additional diagonal reinforcement, showed an 80% increase in energy absorption compared to the reference model

(SW10C45). In contrast, Model 2, with one layer of reinforcement and an additional diagonal reinforcement layer, showed a 26% increase in energy absorption.

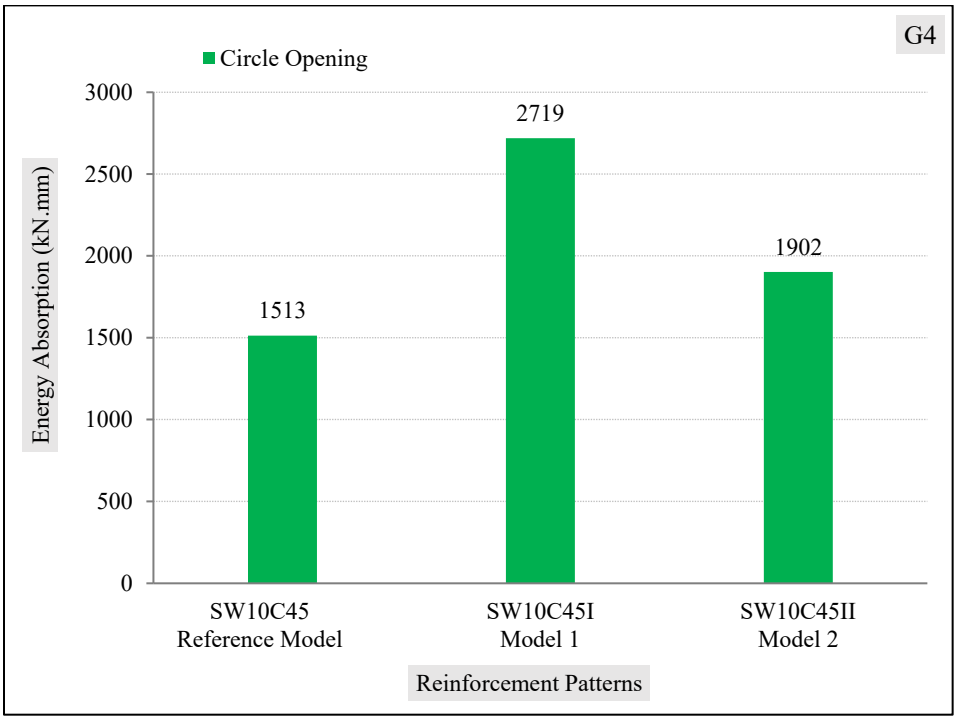

Figure 4.23 Energy absorption of fourth group shear wall specimens.

4.2.6 **Concrete Surface Strain**

Two electrical strain gauges were used, with each gauge placed at the center of the specimen. One gauge was oriented parallel to the loading direction to measure compressive strains (i.e., in the vertical direction), while the another was positioned perpendicular to the loading direction to measure tensile strains (i.e., in the horizontal direction). All readings were meticulously recorded. Figures 4.24 to 4.27 illustrate the load versus compressive and tensile strain curves for all tested specimens.

The strain responses varied across different groups, with shear walls containing square openings generally exhibiting higher strain values compared to those with circular openings. Additionally, Figures 4.28 to 4.31 show the relationship between the maximum compressive and tensile strains.

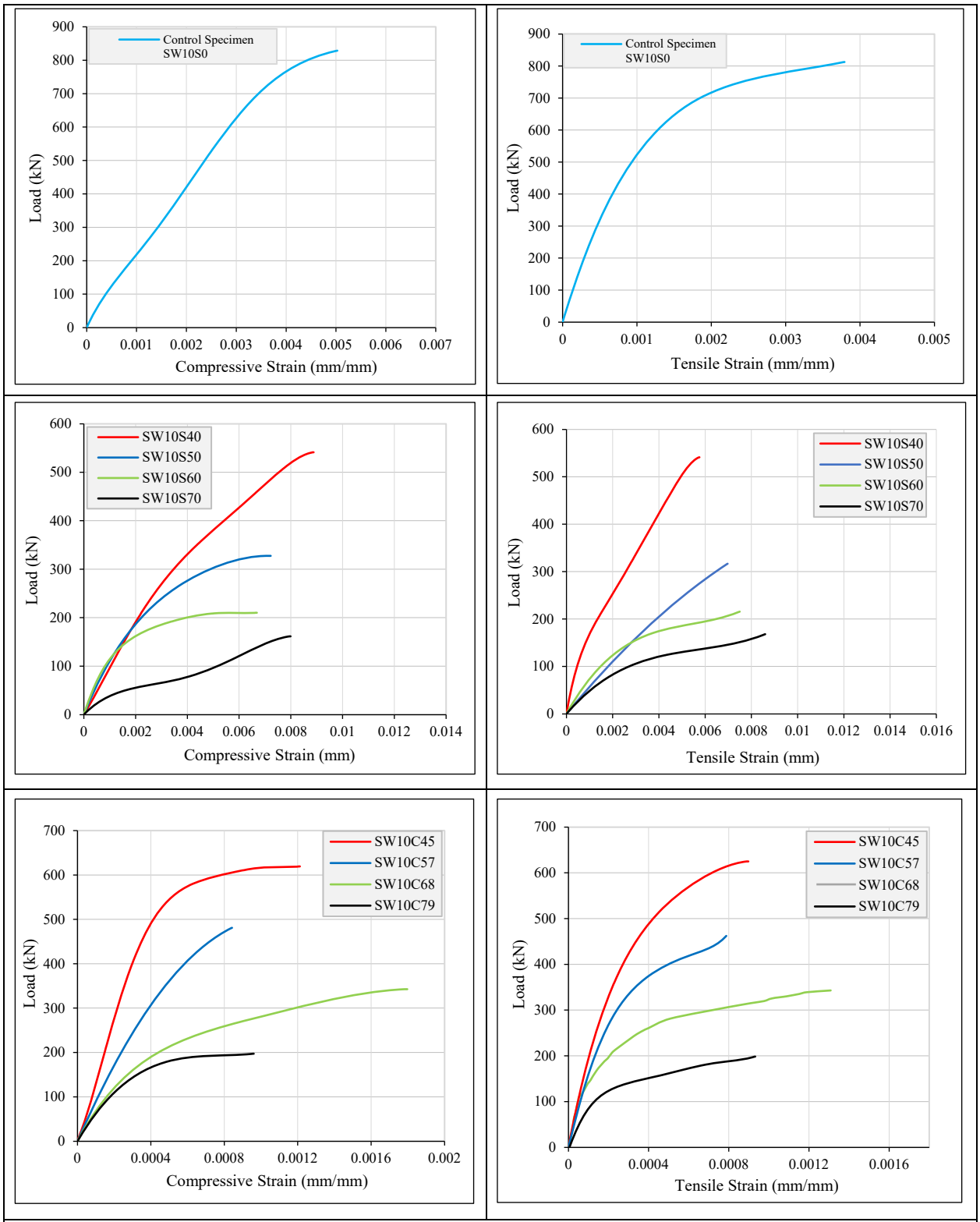

Figure 4.24 Load-strain curves for compressive and tensile first group.

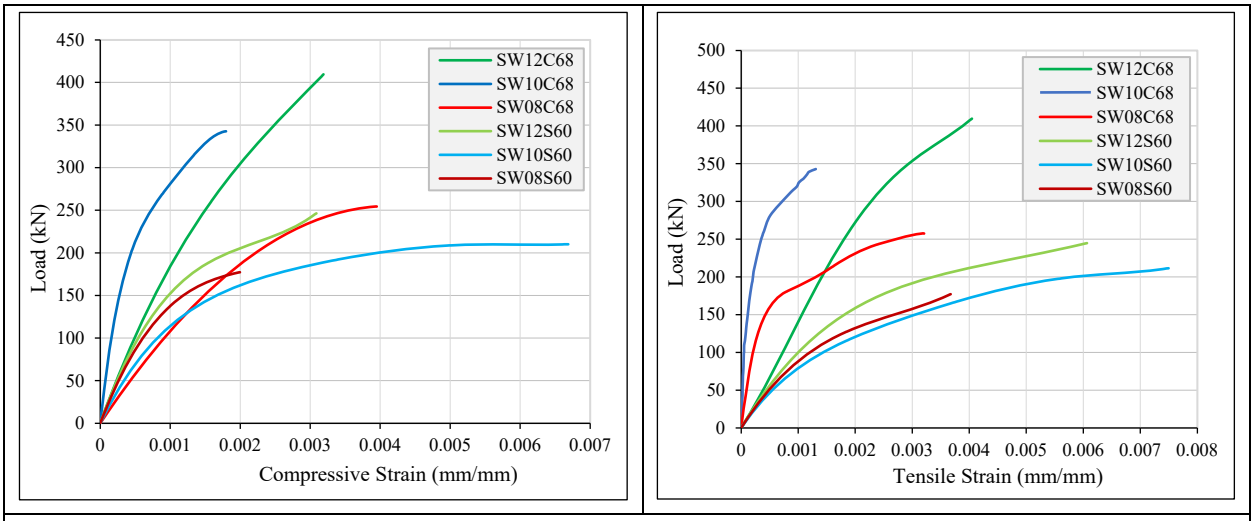

Figure 4.25 Load-strain curves for compressive and tensile second group.

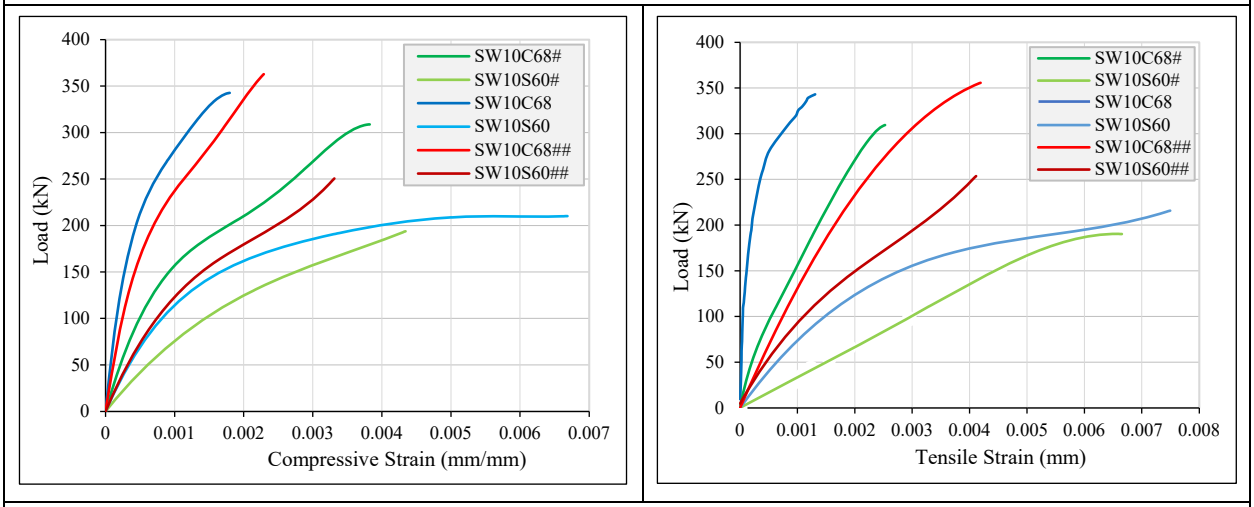

Figure 4.26 Load-strain curves for compressive and tensile third group.

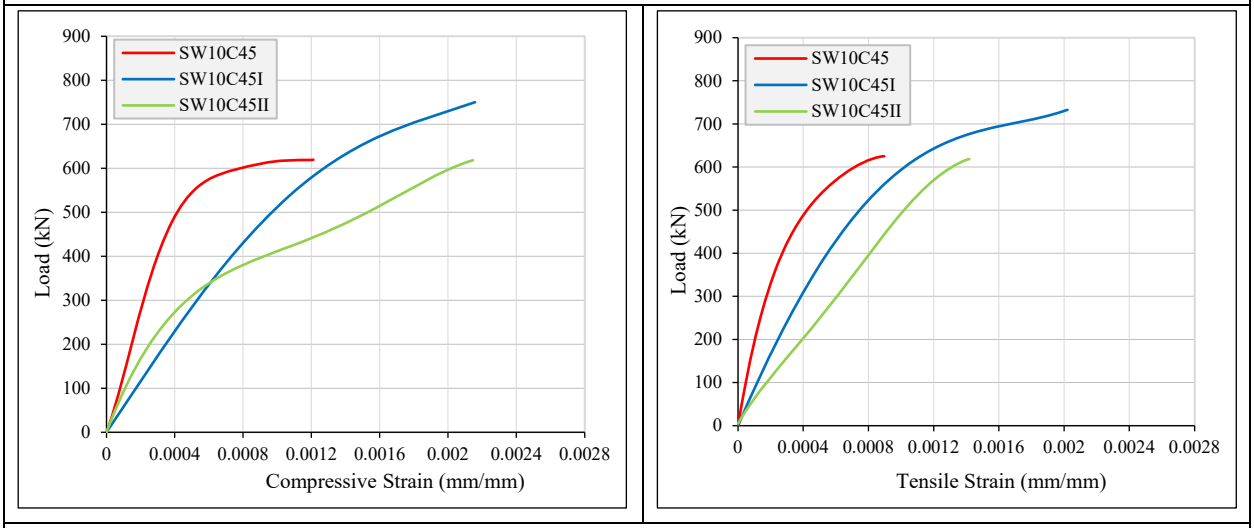

Figure 4.27 Load-strain curves for compressive and tensile fourth group.

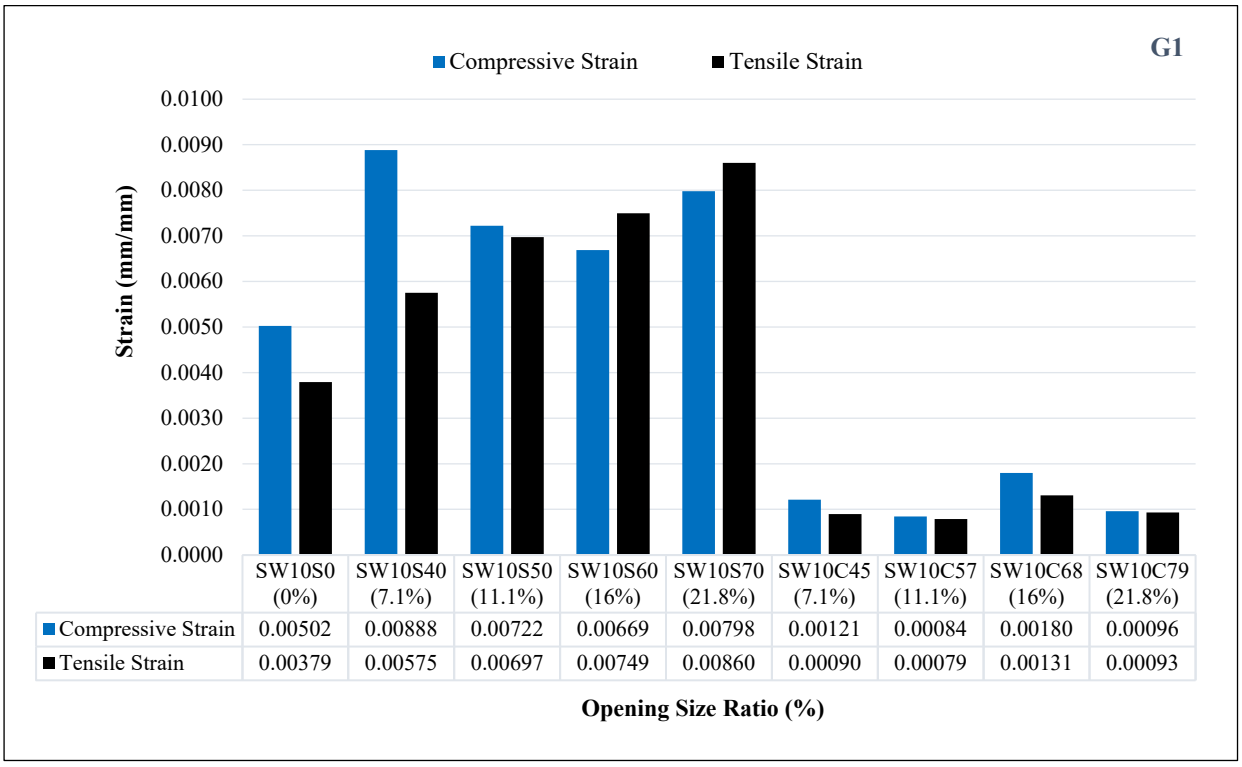

	SW10S0 (0%)	SW10S40 (7.1%)	SW10S50 (11.1%)	SW10S60 (16%)	SW10S70 (21.8%)	SW10C45 (7.1%)	SW10C57 (11.1%)	SW10C68 (16%)	SW10C79 (21.8%)
Compressive Strain	0.00502	0.00888	0.00722	0.00669	0.00798	0.00121	0.00084	0.00180	0.00096
Tensile Strain	0.00379	0.00575	0.00697	0.00749	0.00860	0.00090	0.00079	0.00131	0.00093

Figure 4.28 Maximum tensile and compressive concrete strains for first group.

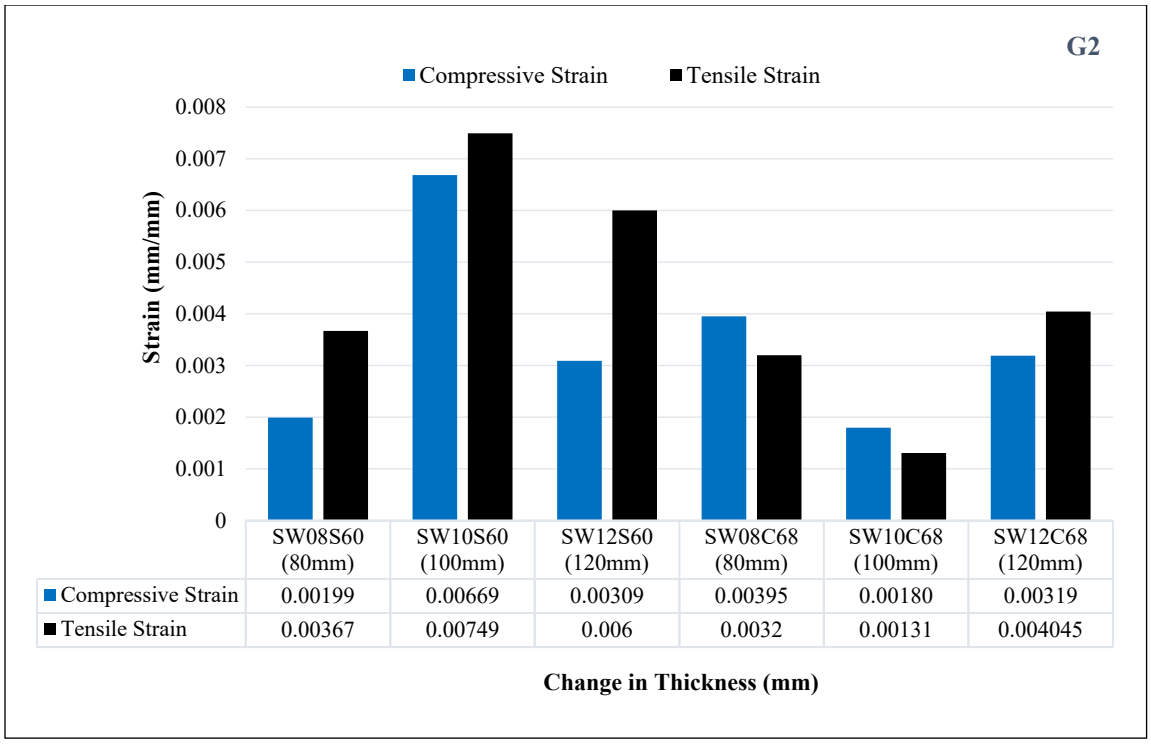

	SW08S60 (80mm)	SW10S60 (100mm)	SW12S60 (120mm)	SW08C68 (80mm)	SW10C68 (100mm)	SW12C68 (120mm)
Compressive Strain	0.00199	0.00669	0.00309	0.00395	0.00180	0.00319
Tensile Strain	0.00367	0.00749	0.006	0.0032	0.00131	0.004045

Figure 4.29 Maximum tensile and compressive concrete strains for second group.

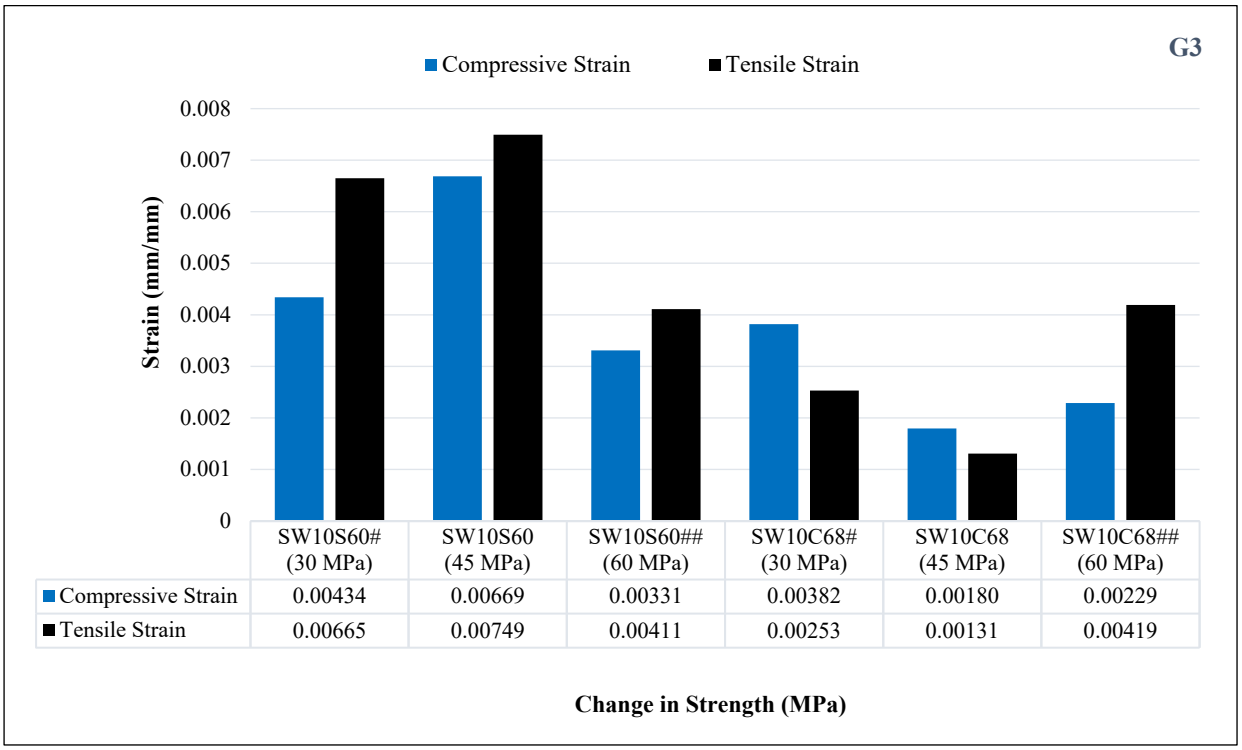

Figure 4.30 Maximum tensile and compressive concrete strains for third group.

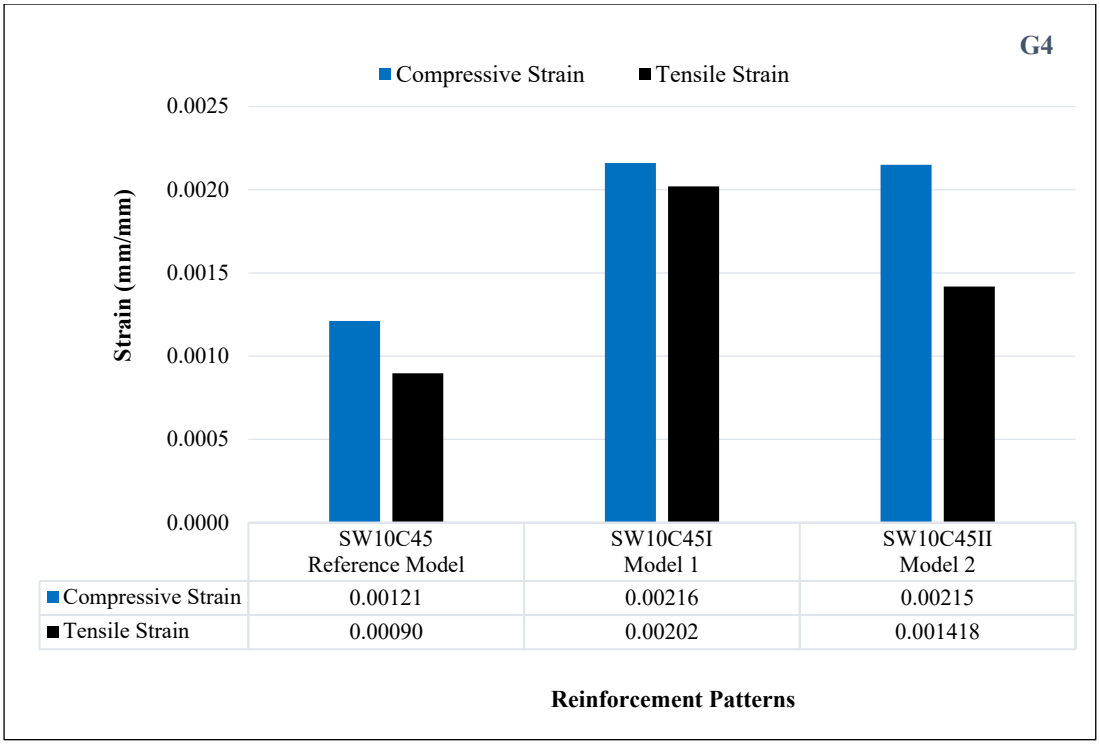

Figure 4.31 Maximum tensile and compressive concrete strains for fourth group.

4.2.7 **General Behavior, Mode of Failure and Cracks Pattern**

As the load on the shear walls increased, numerous cracks began to appear. The load at the first crack and the ultimate load that led to the failure of the walls were recorded. To make the cracks more visible, all of them were marked in blue. Table 4.5 shows the load at the first crack, the ultimate load, and the ratio between them.

Table 4.5 Ultimate and cracking loads of tested specimens.

Group No.	Specimens	Opening Ratio (%)	First Crack Load* Pcr (kN)	Ultimate Load Pu (kN)	Pcr / Pu (%)
1	SW10S0	0	324	827	39.18
	SW10S40	7.1	321	541	59.33
	SW10S50	11.1	129	328	39.33
	SW10S60	16.0	116	210	55.24
	SW10S70	21.8	64	160	40.00
	SW10C45	7.1	109	620	17.58
	SW10C57	11.1	220	460	47.83
	SW10C68	16.0	243	343	70.85
	SW10C79	21.8	77	197	39.09
2	SW08S60	16.0	80	176	45.45
	SW10S60	16.0	116	210	55.24
	SW12S60	16.0	91	244	37.30
	SW08C68	16.0	88	258	34.11
	SW10C68	16.0	243	343	70.85
	SW12C68	16.0	211	407	51.84
3	SW10S60#	16.0	97	189	51.32
	SW10S60	16.0	116	210	55.24
	SW10S60##	16.0	160	251	63.75
	SW10C68#	16.0	113	309	36.57
	SW10C68	16.0	243	343	70.85
	SW10C68##	16.0	183	362	50.55
4	SW10C45	7.1	109	620	17.58
	SW10C45I	7.1	295	742	39.76
	SW10C45II	7.1	267	630	42.38

*Longitudinal Crack

In the first group, as shown in Figure 4.32, for the control solid specimen, the diagonal cracks initiated at the central part and propagated to both upward and downward at approximately 324 kN. As the load increased, the cracks grew larger and concentrated in the center of the wall, moving closer to the support areas. New cracks appeared, and some portions of the wall experienced crushing at failure.

For specimens with square openings (7.1%, 11.1%, 16.0%, 21.8%), sudden diagonal cracks appeared from the corners of the openings at loads of 321, 129, 116, and 64 kN, respectively. The cracks increased in size and number with the load, with larger openings showing more cracks.

For specimens with circular openings (7.1%, 11.1%, 16.0%, and 21.8%), diagonal cracks began to appear around the edges of the circles at loads of 109, 220, 243, and 77 kN, respectively. These cracks were narrower compared to those in square openings. Across all specimens, shear failure was observed with cracks inclined at angles between 30° and 45°. Figure 4.33 shows the cracking pattern of the tested specimens.

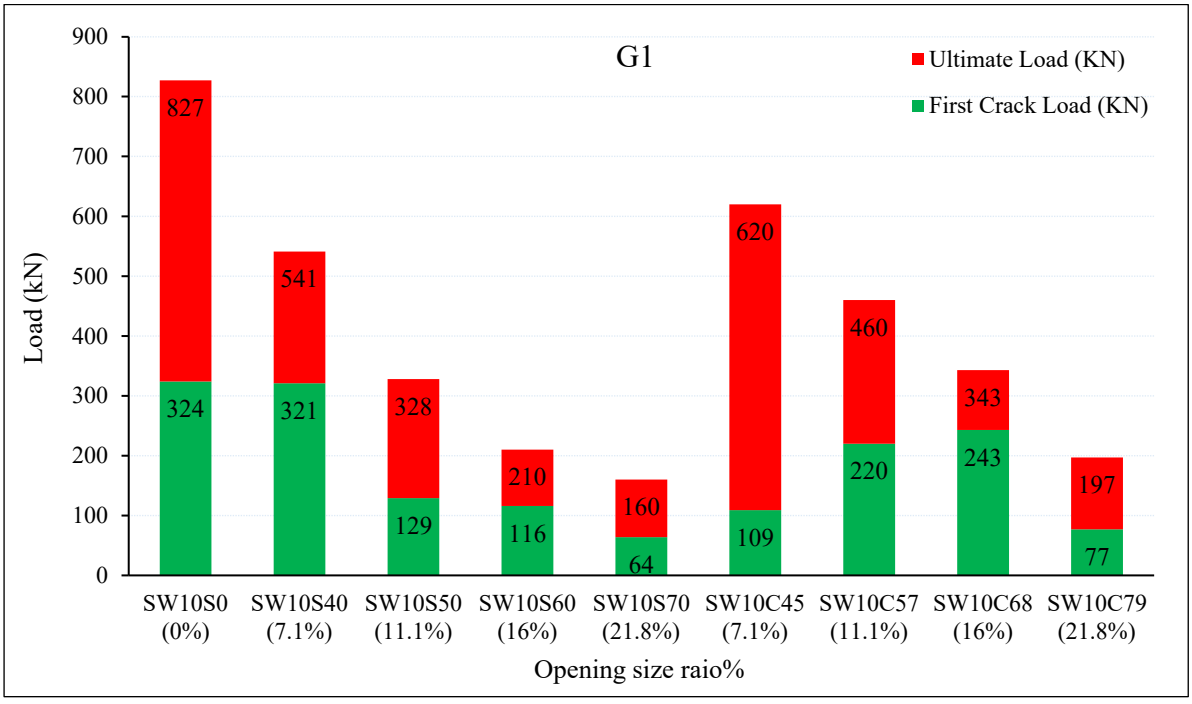

Figure 4.32 First crack load and ultimate load of first group.

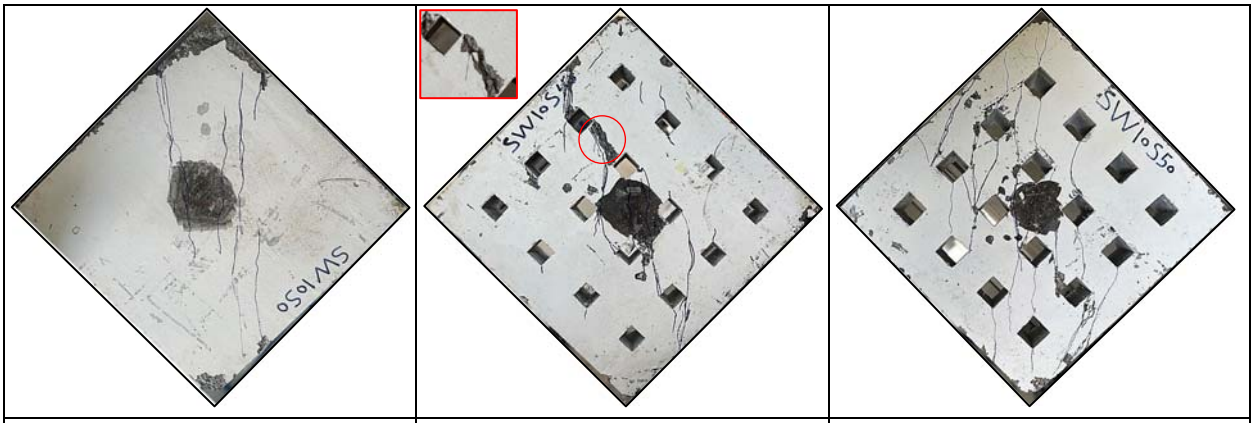

SW10S0
0%

SW10S40
7.1%

SW10S50
11.1%

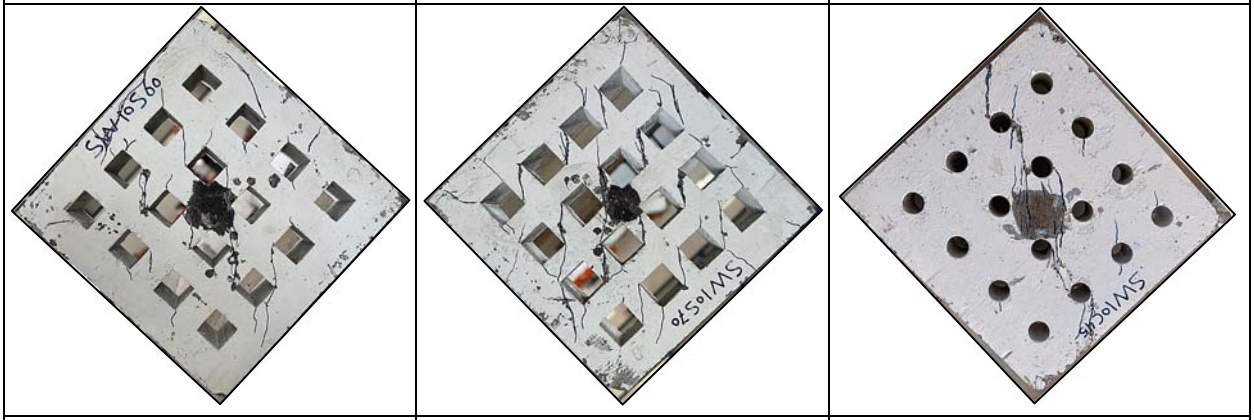

SW10S60
16.0%

SW10S70
21.8%

SW10C45
7.1%

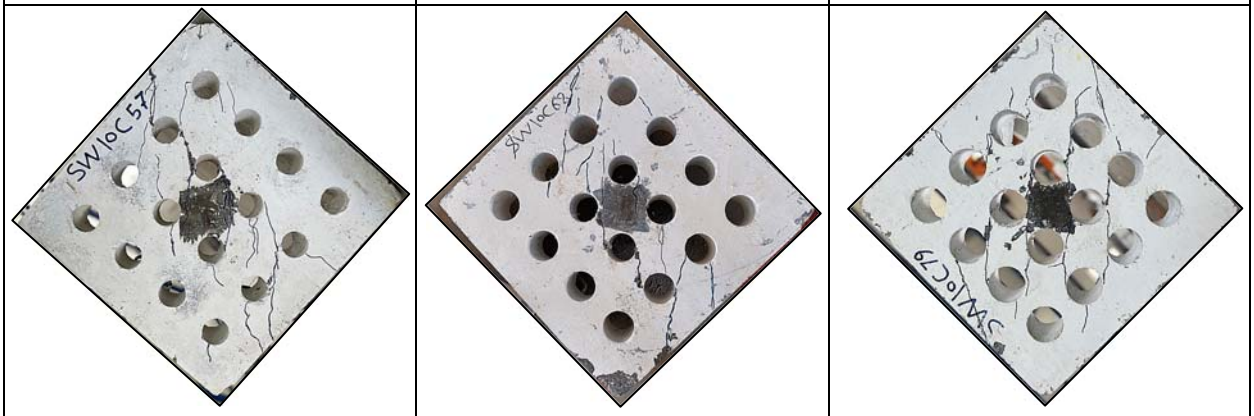

SW10C57
11.1%

SW10C68
16.0%

SW10C79
21.8%

Figure 4.33 Failure mechanism of the first group.

In the second group of specimens, depicted in Figure 4.34, diagonal cracks with inclinations between 30° and 45° appeared suddenly at specific load levels: 80 kN for specimens with square openings and 80 mm thickness, 116 kN for 100 mm

thickness, and 91 kN for 120 mm thickness. For the tested specimens with circular openings, these cracks were observed at 88 kN for 80 mm thickness, 243 kN for 100 mm thickness, and 211 kN for 120 mm thickness. As the applied load increased, these cracks propagated and expanded toward the loading and support regions, eventually leading to crushing in the loading area, as illustrated in Figure 4.35. Figure 4.36 presents the cracking patterns observed in this group of specimens.

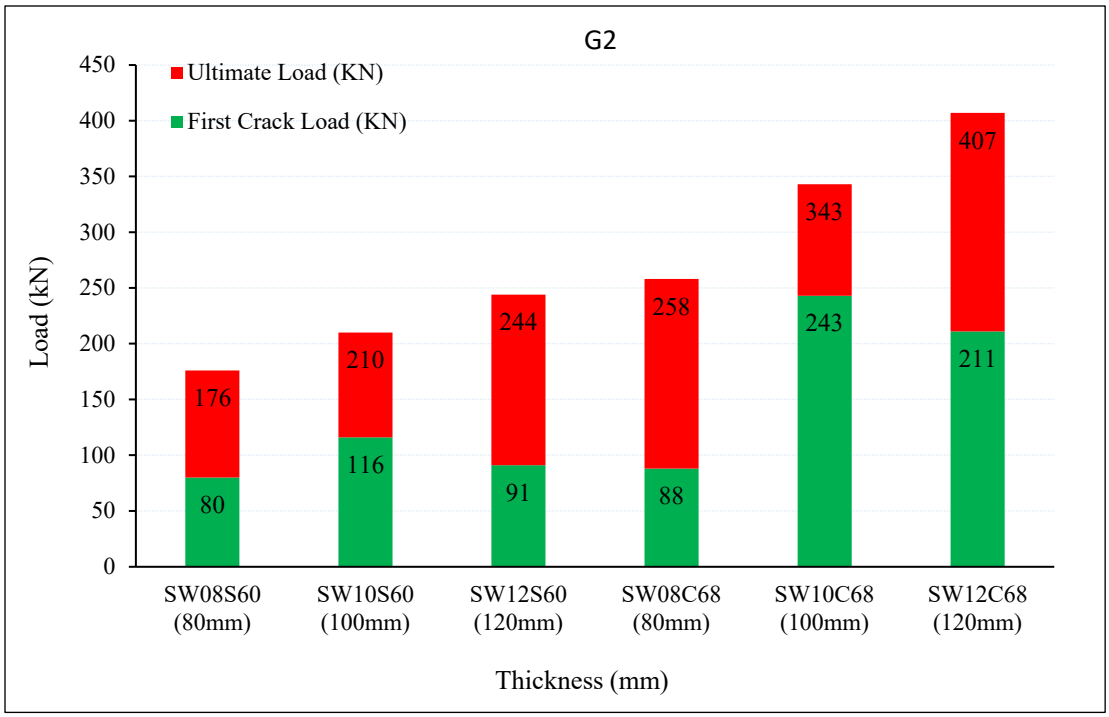

Figure 4.34 First crack load and ultimate load of second group.

Figure 4.35 Crushed Concrete at loading area.

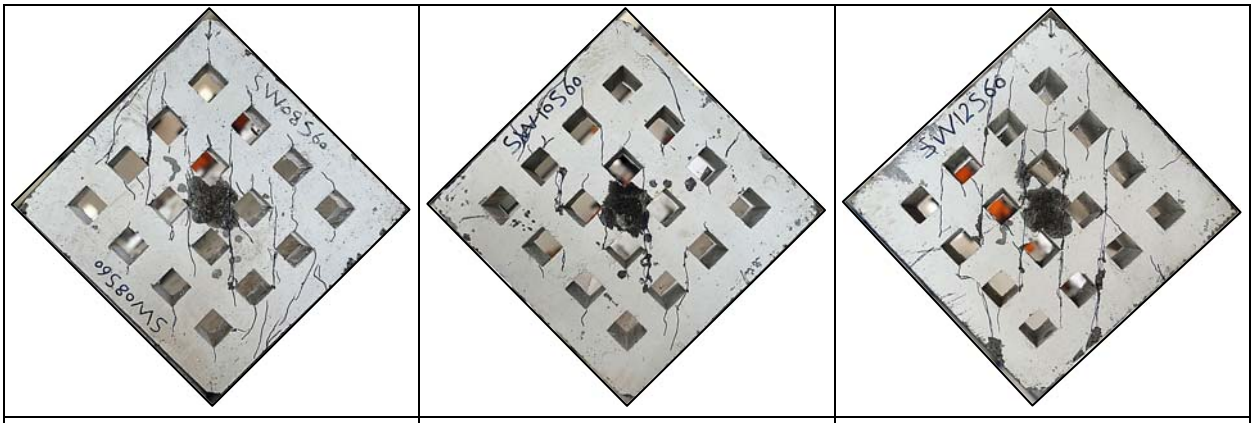

SW08S60 80mm	SW10S60 100mm	SW12S60 120mm

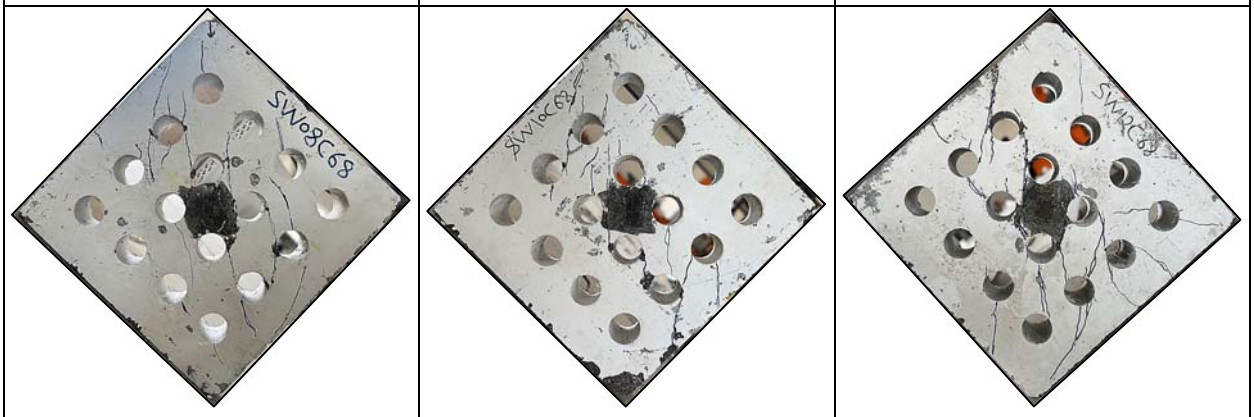

SW08C68 80mm	SW10C68 100mm	SW12C68 120mm

Figure 4.36 Failure mechanism of the second group.

In the third group of specimens, cracks were observed in both square and circular openings at specific loads for each concrete strength. For the square openings, at a strength of 30 MPa, cracks appeared at a load of 97 kN. At a strength of 45 MPa, cracks were recorded at 116 kN, and at a strength of 60 MPa, cracks occurred at a load of 160 kN. Regarding the circular openings, cracks were observed at a strength of 30 MPa at a load of 113 kN. At a strength of 45 MPa, cracks were recorded at 243 kN, while at a strength of 60 MPa, cracks appeared at a load of 183 kN, as shown in Figure 4.37. With increasing loads in both cases, the cracks worsened and began to propagate towards the loading and support areas. Figure 4.38 presents the cracking patterns observed in this group of specimens.

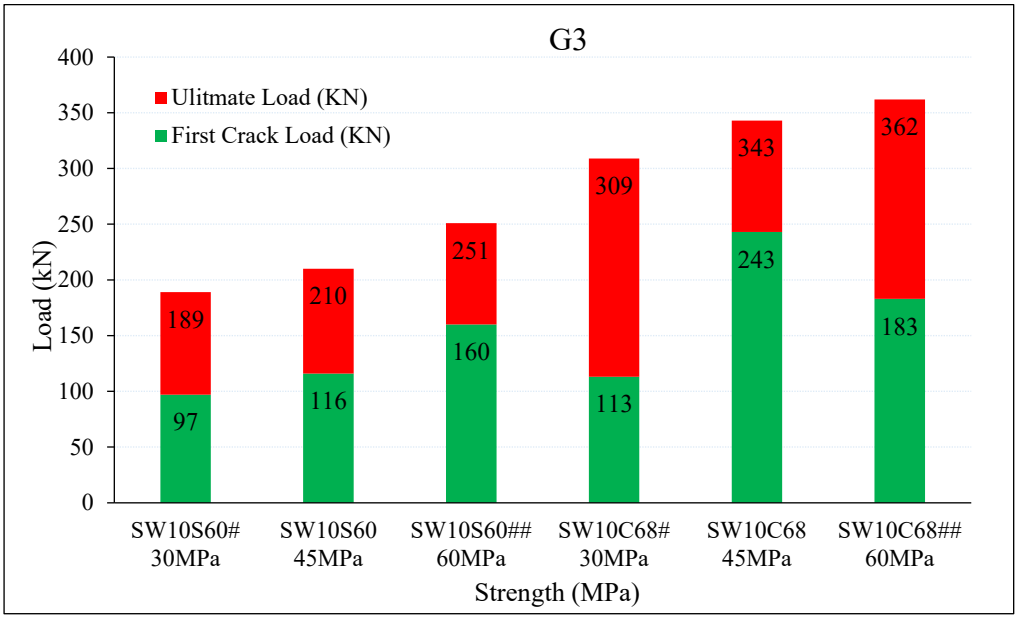

Figure 4.37 First crack load and ultimate load of third group.

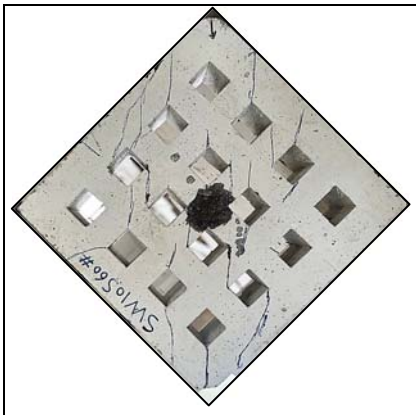	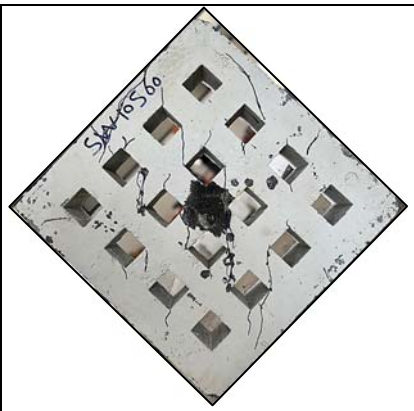	
SW10S60# 30MPa	SW10S60 45MPa	SW10S60## 60MPa
		
SW10C68# 30MPa	SW10C68 45MPa	SW10C68## 60MPa

Figure 4.38 Failure mechanism of the third group.

In the fourth group of specimens (SW10C45, SW10C45I, and SW10C45II), as shown in Figure 39, diagonal cracks appear around the edges of the circular openings at loads of 109, 295, and 267 kN, respectively. As the load increases, the cracks enlarge and move towards the support and loading areas, with crushing also occurring in the loading areas. The width of some cracks increases as the failure load approaches. Figure 4.40 illustrates the crack patterns observed in this group.

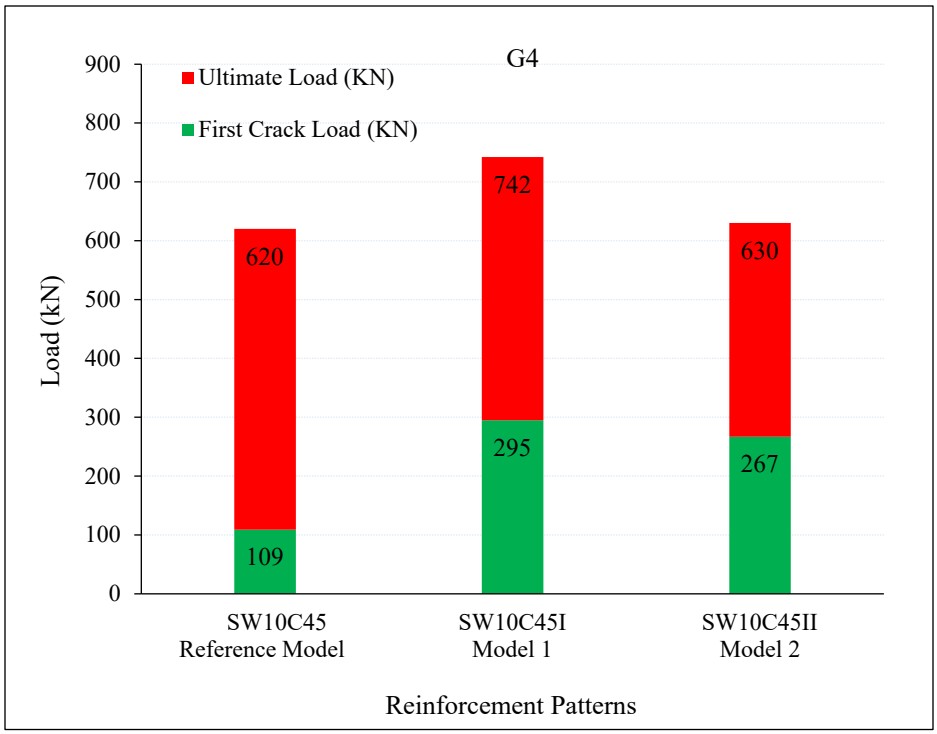

Figure 4.39 First crack load and ultimate load of fourth group.

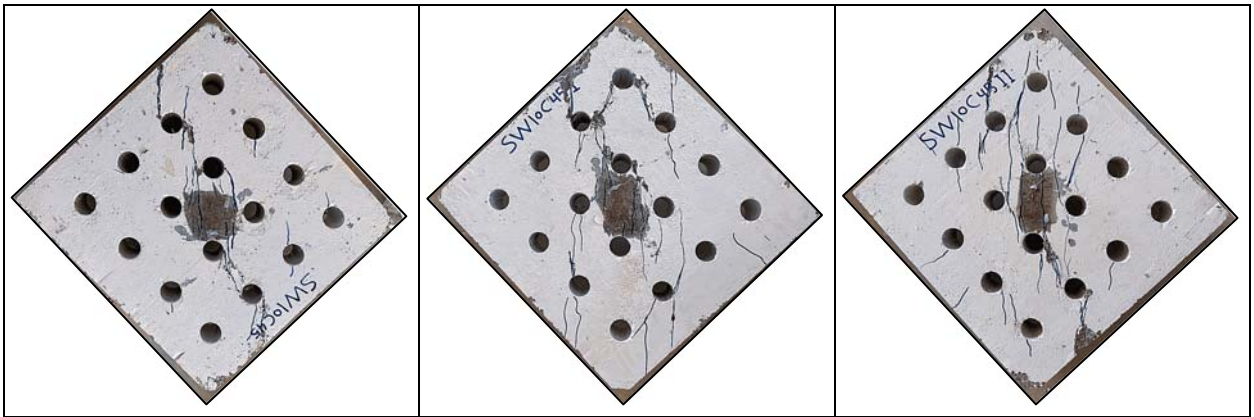

SW10C45	SW10C45I	SW10C45II

Figure 4.40 Failure mechanism of the fourth group.

CHAPTER FIVE: CONCLUSION & RECOMMENDATION

5.1 **Conclusions**

This study provided qualitative assessments of the structural behavior of reinforced concrete shear walls with various configurations of openings. Through extensive experimental investigations of nineteen shear wall specimens with different sizes, shapes, thicknesses, and strengths, as well as reinforcement patterns around the openings, several key findings were revealed.

1) The Openings in shear walls significantly affect the structural performance, as increasing their size that leads to a reduction in ultimate load. For the square openings, the load was decreased by 35% at a 7.1% opening ratio and decreased by up to 81% at a 21.8% ratio. In the case of circular openings, a reduction of 25% is observed at a 7.1% ratio, with a maximum decrease of 76% at a 21.8% ratio.

2) The shape of openings in shear walls affects the ultimate load and cannot be ignored. The circular openings exhibit better performance than the square openings, as they contribute to maintaining the ultimate load more effectively when using the same opening ratio.

3) Increasing the thickness of the shear walls at a 16.0% opening ratio led to increasing the ultimate load of shear walls. The load was increased by 39% for the tested walls with square openings and by 58% for the circular openings when the thickness is increased from 80 to 120 mm. The circular openings benefit more from the increased thickness compared to the square openings.

4) Increasing the concrete strength at a 16.0% opening ratio led to increasing the ultimate load of shear walls. The ultimate load for the square openings was

increases by 33% when the strength is increased from 30 to 60 MPa, while it increases by 17% for the circular openings over the same range. The square openings benefit more from increased strength, while the circular openings show a higher ultimate load across various concrete strengths.

5) At a 7.1% opening ratio, the diagonal reinforcement around the circular openings increases the ultimate load. For model-1(with two layers of mesh and diagonal reinforcement), the ultimate load increased by 20%. In contrast, for model-2 (with one layer of mesh and diagonal reinforcement), the results show a 2% increase compared to traditional reinforcement.

6) For the tested shear walls, the size and shape of openings affect both ductility index and energy absorption. For the square openings, ductility index increases by 23% at a 21.8% opening ratio, while the energy absorption is reduced by 81% at the same ratio. In contrast, for the circular openings the result shows a 10% increase in ductility index at a 21.8% opening ratio and a reduction in energy absorption of 66% at the same ratio. Overall, the square openings increase the ductility index and reduce energy absorption more than circular openings.

7) Increasing the thickness of concrete shear walls with both square and circular openings, at a constant opening ratio of 16.0%, lead to increases both ductility index and energy absorption capacity. Also, the increasing of wall thickness from 80 to 120 mm led to increase the ductility index by 34% for the walls with square openings, while the increase in ductility for walls with circular openings was 4%. Regarding energy absorption capacity, the same thickness increase led to a substantial 160% increase for walls with square openings and a 104% increase for walls with circular openings. Overall, the square openings increase both ductility and energy absorption more than the circular openings.

8) The increasing the strength of concrete shear walls strength with square and circular openings at a constant opening ratio of 16.0% lead to increase both ductility and energy absorption capability. Also, the increasing of strength from 30 to 60 MPa increased ductility by 11% for walls with square openings and 19% for walls with circular openings. The tested walls with square openings had a 77% increase in energy absorption capacity, whereas the circular openings had a 29% increase.

9) Diagonal reinforcement around circular openings at a 7.1% opening ratio increases ductility and energy absorption. Model 1, which has two layers of mesh and diagonal reinforcement, shows a 12% increase in ductility. In contrast, Model 2, with one layer of mesh and diagonal reinforcement, results in a 6% increase compared to traditional reinforcement. In terms of energy absorption, Model 1 shows a significant increase of 80%, whereas Model 2 shows a 26% increase compared to traditional reinforcement.

10) The shear stiffness of concrete shear walls decreases with increasing opening size. At an opening ratio of 21.8%, the shear stiffness of walls with square openings decreased by 74%, while the shear stiffness of walls with circular openings decreased by 80%. However, the shear stiffness of walls with circular openings remains higher than that of walls with square openings at smaller opening ratios.

11) Increasing the thickness of the shear walls with a 16.0% opening ratio resulted in an increase in shear stiffness. For shear walls with square openings, the shear stiffness increased by 18% when the thickness was increased from 80 to 120 mm. In contrast, shear walls with circular openings experienced a 50% increase in shear stiffness for the same thickness increase.

12) Increasing the compressive strength of concrete in tested shear walls with a 16.0% opening ratio led to increase the shear stiffness. When the strength was increased from 30 to 60 MPa, the shear stiffness of walls with square openings increased by 51%. In contrast, the shear stiffness of walls with circular openings increased by 35% for the same increase in strength.

13) The diagonal reinforcement around the circular openings at a 7.1% opening ratio has a clear effect on shear stiffness. Model 1, which has two layers of mesh and diagonal reinforcement, shows slightly increases in shear stiffness by 4%. In contrast, Model 2, with one layer of mesh and diagonal reinforcement, the tested results show 5% decreasing in shear stiffness compared to traditional reinforcement.

14) Reducing weight alone is not sufficient to achieve good results if it comes at the expense of structural strength. Openings cause a weakening of the walls, leading to a reduction in the ultimate strength-to-weight ratio. To improve efficiency, a balance must be found between reducing weight and maintaining the strength of the wall.

15) Cracks in walls with square openings typically start at the corners, spreading and extending into the support and loading areas. In contrast, the cracks in walls with circular openings begin at the top and bottom edges and follow a similar propagation pattern. All tested walls, regardless of the shape of the openings, exhibited a shear failure mode.

5.2 **Recommendation for Future Works**

The following is a list of problems on which further studies are recommended:

1) Utilize advanced materials like carbon fiber reinforced polymer (CFRP) to strengthen the shear walls with openings to improving load-bearing capacity.

2) Conduct additional analysis using software like ANSYS or Abaqus to study the effects of different opening sizes and shapes, comparing results with experimental data. Focus on the stresses around the openings and determine the stress concentration factor for each shape to better understand the structural behavior of the shear walls.
3) Extend testing to consider the dynamic conditions to assess real-world performance and natural frequency effects.
4) Fire Resistance: Assess the influence of fire protection strategies on the structural integrity of the shear walls with multiple openings under high temperature conditions.

APPENDICES

Appendix A

Longitudinal and Transverse Steel Ratios for Shear Walls

Specimen ID	W	T_w	A_{total}	$A_{openings}$	A_{net}	$A_{total\ steel}$	ρ_l& ρ_t	BS 8110-1:1997		ACI 318-19 11.6.2b
								ρ_{min}	ρ_{max}	$\rho_{l\&t}$(min)
SW10S0	600	100	60000	0	60000	502.4	0.0084	0.004	0.04	0.0025
SW10S40	600	100	60000	16000	44000	502.4	0.0114	0.004	0.04	0.0025
SW10S50	600	100	60000	20000	40000	502.4	0.0126	0.004	0.04	0.0025
SW10S60	600	100	60000	24000	36000	502.4	0.0140	0.004	0.04	0.0025
SW10S70	600	100	60000	28000	32000	502.4	0.0157	0.004	0.04	0.0025
SW10C45	600	100	60000	16000	44000	502.4	0.0114	0.004	0.04	0.0025
SW10C57	600	100	60000	20000	40000	502.4	0.0126	0.004	0.04	0.0025
SW10C68	600	100	60000	24000	36000	502.4	0.0140	0.004	0.04	0.0025
SW10C79	600	100	60000	28000	32000	502.4	0.0157	0.004	0.04	0.0025
SW08S60	600	80	48000	19200	28800	502.4	0.0174	0.004	0.04	0.0025
SW12S60	600	120	72000	28800	43200	502.4	0.0116	0.004	0.04	0.0025
SW08C68	600	80	48000	19200	28800	502.4	0.0174	0.004	0.04	0.0025
SW12C68	600	120	72000	28800	43200	502.4	0.0116	0.004	0.04	0.0025
SW10S60#	600	100	60000	24000	36000	502.4	0.0140	0.004	0.04	0.0025
SW10S60##	600	100	60000	24000	36000	502.4	0.0140	0.004	0.04	0.0025
SW10C68#	600	100	60000	24000	36000	502.4	0.0140	0.004	0.04	0.0025
SW10C68##	600	100	60000	24000	36000	502.4	0.0140	0.004	0.04	0.0025
SW10C45I	600	100	60000	16000	44000	954.6	0.0217	0.004	0.04	0.0025
SW10C45II	600	100	60000	16000	44000	477.3	0.0108	0.004	0.04	0.0025

Total cross-sectional area: A_{total}= 600 mm×100 mm = 60000 mm^2

Openings area: $\mathbf{A_{openings}}$= 4 × (70 mm×100 mm) = 28000 mm^2

Net cross-sectional area: A_{net}= 60000 mm^2 − 28000 mm^2 = 32000 mm^2

Reinforcement area (top & bottom layers):

$A_{bar} = \frac{\pi}{4} \times (8\ \text{mm})^2 = 50.24\ \text{mm}^2$

$A_{steel\ per\ layer} = 5 \times 50.24 = 251.2\ \text{mm}^2$

$A_{total\ steel} = 2 \times 251.35 = 502.4\ \text{mm}^2$

Reinforcement ratio: $\rho_{l\ \&\ t} = \frac{A_{total\ steel}}{A_{net}} = \frac{502.4}{32000} = 0.0157$

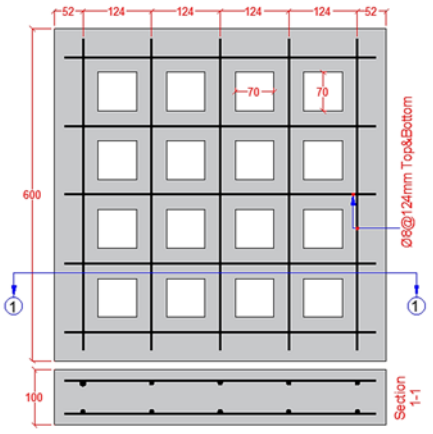

SW10S70

Appendix B

Flocrete SP90S

High range water reducing admixture with workability retention properties

Description

Flocrete SP90S is formulated from selected polymers specially designed to enable the water content of the concrete to perform more effectively. This effect can be used to improve workability, to increase ultimate strengths or to facilitate a reduction in the cement content while sustaining mix properties.

Flocrete SP90S has strong workability retention which helps in long distance and hot weather concrete deliveries, and is particularly suitable for ready-mix concrete.

Applications

- Long distance and hot weather concrete deliveries.
- Where high workability retention and retardation are of prime importance.
- To produce high quality concrete of improved durability and water tightness.

Advantages

- Higher strength with same cement content.
- Minimising segregation problems by improving cohesion.
- Excellent slump retention properties.
- Improved workability reduces placing and compaction problems.
- Cold joints can be avoided by extending initial and final concrete setting time.
- Saving cement without affecting strength specifications.
- More durable concrete by considerable reduction in permeability.

Compatibility

Flocrete SP90S is suitable for use with all types of Portland cement and cement replacement materials. Flocrete SP90S is compatible with other DCP's admixtures used in the same concrete mix.

If more than one type of admixture will be used in the concrete mix, they must be dispensed into the mix separately.

Technical Properties @ 25°C:	
Colour:	Brown liquid
Freezing point:	≈ -2°C
Specific gravity:	1.16 ± 0.02
Chloride content: BS 5075	Nil
Air entrainment:	Typically less than 2% additional air is entrained above control mix at normal dosages

Standards

Flocrete SP90S complies with ASTM C494, Type B, D and G, depending on dosage used.

Method of Use

Flocrete SP90S should be added to the concrete with the mixing water to achieve optimum performance.

An automatic dispenser should be used to dispense the correct quantity of Flocrete SP90S to the concrete mix.

Dosage

The recommended dosage is between 0.80 - 2.10 litre per 100 kg of cementitious materials in the mix, including GGBFS, PFA or microsilica.

Effects of Over Dosage

Flocrete SP90S overdosage will cause the following:

- Significant increase in retardation.
- Increase in workability.

Ultimate concrete strength will not be adversely affected and will generally be increased provided that proper concrete curing is maintained.

Flocrete SP90S

Setting Time

Although the setting time is dependent on the dosage of Flocrete SP90S, the following factors should be considered:

i. Retardation is increased with a lower level of tri-calcium in the cement.
ii. Lower temperatures will delay the setting time.
iii. SRC cement gives higher retardation level than ordinary cement.
iv. Using more than one type of admixture in the same concrete mix could affect the sitting time.
v. Retardation level is increased when cement replacement materials are used in the concrete mix.

Cleaning

Flocrete SP90S can be washed immediately by cold water.

Packaging

Flocrete SP90S is available in 25 litre pails, 210 litre drums and 1000 litre bulks supply.

Storage

Flocrete SP90S has a shelf life of 12 months from date of manufacture if stored at temperatures between 2°C and 50°C.

If these conditions are exceeded, DCP Technical Department should be contacted for advice.

Cautions

Health and Safety

Flocrete SP90S is not classified as a hazardous material. Flocrete SP90S should not come into contact with skin and eyes.
In case of contact with eyes, immediately flush with plenty of water and seek medical attention.

For further information, refer to the Material Safety Data Sheet.

More from Don Construction Products

A wide range of construction chemical products are manufactured by DCP which include:

- Concrete admixtures.
- Surface treatments
- Grouts and anchors.
- Concrete repair.
- Flooring systems.
- Protective coatings.
- Sealants.
- Waterproofing.
- Adhesives.
- Tile adhesives and grouts.
- Building products.
- Structural strengthening.

Silica Fume

MegaAdd MS(D)

Densified Microsilica

DESCRIPTION

MegaAdd MS(D) is a very fine pozzolanic, ready to use high performance mineral additive for use in concrete. It acts physically to optimize particle packing of the concrete or mortar mixture and chemically as a highly reactive pozzolan.

MegaAdd MS(D) in contact with water, goes into solution within an hour. The silica in solution forms an amorphous silica rich, calcium poor gel on the surface of the silica fume particles and agglomerates. After time the silica rich calcium poor coating dissolves and the agglomerates of silica fume react with free lime ($CaOH_2$) to form calcium silicate hydrates (CSH). This is the pozzolanic reaction in cementitious system.

STANDARDS

ASTMC1240

USES

MegaAdd MS(D) can be used in a variety of applications such as concrete, grouts, mortars, fibre cement products, refractory, oil/gas well cements, ceramics, elastomer, polymer applications and all cement related products.

ADVANTAGES

- High to ultra high strength
- High resistance to chlorides and sulfates
- Protection against corrosion
- Increased durability, longer service life for structures
- Enhanced rheology, control of mixture segregation and bleed
- Greater resistance to chemicals

TYPICAL PROPERTIES at 25°C

PROPERTY	TEST METHOD	VALUE
State	Amorphous	Sub-micron powder
Colour	-	Grey to medium grey powder
Specific Gravity	-	2.10 to 2.40
Bulk Density	-	500 to 700 kg/m^3
Chemical Requirements		
Silicon Dioxide (SiO_2)	-	Minimum 85%
Moisture Content (H_2O)	-	Maximum 3%
Loss on Ignition (LOI)	-	Maximum 6%
Physical Requirements		
Specifi Surface Area	-	Minimum 15 m^2/g
Pozzolanic Activity Index, 7 days	-	Maximum 105% of control
Over size particles retained on 45 micron sieve	-	Maximum 10%

COMPATIBILITY

MegaAdd MS(D) is suitable for use with all types of cement and cementitious materials.

With Admixtures :

MegaAdd MS(D) is compatible to use with all types of water reducing plasticisers / superplasticisers and poly carboxylate based superplasticiser.

DOSAGE

The normal dosage of **MegaAdd MS(D)** is 5 - 8% by weight of cement, but it can be used up to 10%. Site trials should be carried out to establish the optimum dosage for the mix to be used as the dosage varies depending on application.

MegaAdd MS(D)

BATCHING	Batch **MegaAdd MS(D)** into the concrete mixer and mix thoroughly with the other mixture ingredients, adopting a procedure that ensures full dispersion of the product.	
PACK SIZE	600 Kgs and 1200 Kgs Jumbo bags	
GENERAL INFORMATION	**Shelf Life**	12 months from date of manufacture when stored under warehouse conditions in original unopened packing. Extreme temperature / humidity may reduce shelf life.
	Cleaning	Clean all equipments and tools with water immediately after use.
HEALTH and SAFETY	**PPE's**	Gloves, goggles and suitable mask must be worn.
	Precautions	Contact with skin, eyes, etc. must be avoided.
	Hazard	Regarded as non-hazardous for transportation.
	Disposal	Do not reuse bags. To be disposed off as per local rules and regulations.
	Additional Information	Refer MSDS. (Available on request.)
TECHNICAL SERVICE	**CONMIX Technical Services** are available on request for onsite support to assist in the correct use of its products.	

MSASA
Construction Solutions for Africa

CAPE TOWN
Tel: +27 (0)87 231 0253
Unit 5 | M5 Freeway Park
Upper Camp Rd | Maitland | 7405
Cape Town | South Africa

JOHANNESBURG
Tel: +27 (0)82 785 8529
64 Maple Street | Pomona
Kempton Park | Johannesburg | 1619
South Africa

Email: info@msasa.co.za | www.msasa.co.za

Manufacturer:
CONMIX LTD.
P.O. Box 5936, Sharjah
United Arab Emirates
Tel: +971 6 5314155
Fax: +971 6 5314332
Email: conmix@conmix.com

Sales Office:
Tel: +971 6 5682422
Fax: +971 6 5681442
www.conmix.com

ISO9001

REFERENCE

[1] R. Sharma and J. A. Amin, "Effects of opening in shear walls of 30-storey building," *Journal of Materials Engineering Structures «JMES»,* vol. 2, no. 1, pp. 44-55, 2015.

[2] B. S. Taranath, *Reinforced concrete design of tall buildings*. CRC press, 2009.

[3] K. Shukla and K. Nallasivam, "Dynamic response of high-rise buildings with shear walls due to seismic forces," *Asian Journal of Civil Engineering,* vol. 24, no. 7, pp. 2645-2657, 2023.

[4] N. E. Nasr, M. Fayed, G. Hussien, and A. EL-Makhlasawi, "Evaluation of Response Modification Factor for Shear Wall with Openings in Multi-Storey Buildings," *Faculity of engineering, Ain Shams University,* vol. 43, no. 3, 2021.

[5] S. F. Mousavi and B. Barmayevar, "Comparative investigation of methods for determining the lateral stiffness of coupled RC shears walls," *Journal of Fundamental Applied Sciences,* vol. 9, no. 1S, pp. 789-807, 2017.

[6] A. Farzampour, J. A. Laman, and M. Mofid, "Behavior prediction of corrugated steel plate shear walls with openings," *Journal of Constructional Steel Research,* vol. 114, pp. 258-268, 2015.

[7] A. Syamsir, A. Allah, S. Naganathan, M. Zainoodin, N. Nor, and S. Beddu, "Effect of various type of shear walls on behavior of tall building due to seismic force," in *AIP Conference Proceedings*, 2021, vol. 2339, no. 1: AIP Publishing.

[8] H.-S. Kim and D.-G. Lee, "Analysis of shear wall with openings using super elements," *Engineering Structures,* vol. 25, no. 8, pp. 981-991, 2003.

[9] A. Syamsir, I. Iskandar, A. R. Malekzadah, and A. Alhayek, "Optimization of Rhombus Opening Area of Shear Walls On Tall Buildings," *International Journal of Integrated Engineering,* vol. 15, no. 1, pp. 367-376, 2023.

[10] M. Marius, "Seismic behaviour of reinforced concrete shear walls with regular and staggered openings after the strong earthquakes between 2009 and 2011," *Engineering Failure Analysis,* vol. 34, pp. 537-565, 2013.

[11] K. J. Al-Koiy, "Evaluation of Stiffness of Reinforced Concrete Shear Walls with Different Sizes of Opening Against Lateral Loading," Near East University, 2018.

[12] T. Shobha and S. A. Rao, "Design and Construction of Shear Walls," *International Journal of Advanced Technology Innovative Research,* vol. 8, no. 8, pp. 1549-1558, 2016.

[13] T. Paulay and M. N. Priestley, *Seismic design of reinforced concrete and masonry buildings*. Wiley New York, 1992.

[14] C. V. R. Murty, "Learning earthquake design and construction," *Resonance,* vol. 9, pp. 79-83, 2004.

[15] S. S. Sivaraja, S. Sengolmurugan, and Development, "Seismic Behavior of Structures with Moment Resisting Frame (MRF) and Shear Wall (SW)," *International Journal of Trend in Research,* vol. 4, no. 1, 2017.

[16] V. R. Harne, "Comparative study of strength of RC shear wall at different location on Multi-storied residential building," *International Journal of Civil Engineering Research,* vol. 5, no. 4, pp. 391-400, 2014.

[17] N. Meshram and G. M. Munde, "Seismic Analysis of Shear Wall at Different Location on Multi-storey RCC Building," *International Journal of Interdisciplinary Innovative Research & Development (IJIIRD), ISSN,* 2018.

[18] S. A. Ahamad and K. Pratap, "Dynamic analysis of G+ 20 multi storied building by using shear walls in various locations for different seismic zones by using Etabs," *Materials Today: Proceedings,* vol. 43, pp. 1043-1048, 2021.

[19] V. Lakshmi and B. R. Madhuri, "Analysis of a Steel Framed Building With and Without Shear Walls and Different Configurations of Bracings," *GE-International Journal of Engineering Research,* vol. 4, no. 12, Impact Factor-5.613 2016.

[20] C. Lin and C. Kuo, "Behavior of shear wall with Opening," in *Proceedings of Ninth world Conference on Earthquake Engineering. Tokyo-Kyoto, Japan, IV*, 1988, pp. 535-540.

[21] S. Fragomeni, J.-H. Doh, and D.-J. Lee, "Behavior of axially loaded concrete wall panels with openings: An Experimental Study," *Advances in structural engineering,* vol. 15, no. 8, pp. 1345-1358, 2012.

[22] J. Wang, M. Sakashita, S. Kono, and H. Tanaka, "Shear behaviour of reinforced concrete structural walls with eccentric openings under cyclic loading: experimental study," *The Structural Design of Tall Special Buildings,* vol. 21, no. 9, pp. 669-681, 2012.

[23] A. K. Marsono and S. Hatami, "Evaluation of Coupling Beams Behavior Concrete Shear Wall with Rectangular and Octagonal Openings," *Applied Mechanics Materials,* vol. 735, pp. 104-108, 2015.

[24] B. Li, Z. Pan, and Y. Zhao, "Seismic behaviour of lightly reinforced concrete structural walls with openings," *Magazine of Concrete Research,* vol. 67, no. 15, pp. 843-854, 2015.

[25] C. Popescu, G. Sas, C. Sabău, and T. Blanksvärd, "Effect of cut-out openings on the axial strength of concrete walls," *Journal of Structural Engineering,* vol. 142, no. 11, p. 04016100, 2016.

[26] A. A. M. Ali, I. S. Saleh, and A. S. Kawoosh, "Structural Behavior of Axially Loaded Shear Walls with Openings," *International Journal of Civil Engineering Technology,* vol. 9, no. 1, pp. 578-596, January 2018.

[27] L. M. Massone, G. Muñoz, and F. Rojas, "Experimental and numerical cyclic response of RC walls with openings," *Engineering Structures,* vol. 178, pp. 318-330, 2019.

[28] H. A. Hagag, M. H. Agamy, and M. M. Eshak, "Lateral stiffness of shear walls with openings," *Al-Azhar University Civil Engineering Research Magazine,* vol. 43, no. 2, 2021.

[29] Z. Tafheem, H. Alwashali, M. Maeda, and M. Seki, "Experimental study of the influence of opening size and additional reinforcement around opening on seismic performance of reinforced concrete walls," *Asian Journal of Civil Engineering,* vol. 23, no. 4, pp. 551-572, 2022.

[30] M. Sakurai, H. Kuramoto, T. Matsui, and T. Akita, "Seismic performance of RC shear walls with multiopenings," in *14th world conference on Earthquake Engineering*, 2008.

[31] S. M. Khatami, A. Mortezaei, and C. B. Rui, "Comparing effects of openings in concrete shear walls under near-fault ground motions," in *15th World Conference on Earthquake Engineering*, 2012, vol. 1, pp. 173-182.

[32] M. Masood, I. Ahmed, and M. Assas, "Behavior of shear wall with base opening," *Jordan Journal of Civil Engineering,* vol. 6, no. 2, pp. 255-266, 2012.

[33] P. Hegde and S. Itti, "Effect of base opening in reinforced concrete shear wall," *International Journal of Civil Environmental Research,* vol. 6, 2014.

[34] B. H. Gandhi, "Effect of opening on behaviour of shear wall," *International Journal for Technological Research in Engineering,* vol. 3, no. 4, pp. 875-878, 2015.

[35] T. Aarthi Harini and G. S. Kumar, "Behavior of RC shear wall with staggered openings under seismic loads," *International journal for research in emerging science technology,* vol. 2, no. 3, pp. 91-96, 2015.

[36] A. Y. Hong, "Analysis of Squat Shears Wall with Different Dimensions and Positions of Opening Under Different Type of Static Load," M. Sc. Thesis, University Malaysia Pahang, 2015.

[37] V. A. Itware, U. B. Kalwane, and Applications, "Effects of openings in shear wall on seismic response of structure," *Journal of Engineering Research,* vol. 5, no. 7, pp. 41-45, 2015.

[38] Y. Yasrebinia and M. Poursharifi, "Seismic Assessment of Concrete Shear Wall with Rectangular Openings in Near Fault Earthquake," 2016.

[39] A. Kankuntla, P. Sangave, and R. Chavan, "Effects of openings in shear wall," *IOSR Journal of Mechanical Civil Engineering,* vol. 13, no. 1, pp. 1-6, 2016.

[40] E. Montazeri, N. Panahshahi, and B. Cross, "Nonlinear finite element analysis of reinforced concrete shear walls with staggered openings under seismic loads," in *Structures Congress 2018*, 2018, pp. 281-291: American Society of Civil Engineers Reston, VA.

[41] A. Morsy and Y. Ibrahim, "Parametric Study for Performance of RC Wall with Opening using Analytical FE Model," *Athens Journal of Technology Engineering,* vol. 6, no. 1, pp. 31-62, 2019.

[42] H. Alimohammadi, M. D. Esfahani, and M. L. Yaghin, "Effects of openings on the seismic behavior and performance level of concrete shear walls," *International Journal of Engineering Applied Sciences,* vol. 6, no. 10, pp. 34-39, 2019.

[43] S. S. Chaudhary and S. Parekar, "Stress distribution of different shapes of opening in shear wall," *International Journal for Modern Trends in Science Technology ISSN,* pp. 2455-3778, 2019.

[44] A. M. Fares, "The impact of RC shear wall openings at the lateral stiffness of the cantilever shear walls," *Research on Engineering Structures Materials,* vol. 7, no. 1, pp. 51-63, 2021.

[45] R. Bush, A. Shirkol, J. Sruthi, and A. Kumar, "Study of seismic analysis of asymmetric building with different shapes of staggered openings and without openings in Shear Wall," *Materials Today: Proceedings,* vol. 64, pp. 964-969, 2022.

[46] M. Kumar and V. Keshav, "Effect of Shape and Size of Openings in Shear Walls on Lateral Deformations in Shear Walled Framed Structures," in *ASPS Conference Proceedings*, 2022, vol. 1, no. 3, pp. 901-907.

[47] K. Praveen and V. R. Chethan, "Analysis of Multistoried Building with Different Shear Wall Opening Condition using ETABS," *International Journal of Engineering Research Technology,* vol. 11, no. 11, November 2022.

[48] H. HASSAN, N. SAEED, and A. MANGURI, "NATURAL FREQUENCY OF RC WALLS WITH VARIOUS SIZES AND LOCATIONS OF OPENING," *Journal of Duhok University,* vol. 26, no. 2, pp. 772-783, 2023.

[49] *Iraqi Standard Specification, Portland cement, I. Q. S. NO. 5, 1984.*

[50] *Standard Specification for Concrete Aggregates* ASTM C33/C33M-18,2018.

[51] *Requirements of the Used Fine and Coarse Aggregate in the Concrete Mixes,* 2017.

[52] *Standard Specification for Chemical Admixtures for Concrete,* ASTMC494/C494M-19, 2019.

[53] *Standard Specification for Silica Fume Used in Cementitious Mixtures,* ASTM C1240-20a, 2020.

[54] *Standard Specification for Carbon steel bars for the reinforcement of concrete,* BS 4449:1997.

[55] *Standard Test Method for Slump of Hydraulic-Cement Concrete,* ASTMC143-17, 2017.

[56] *Standard Practice for Making and Curing Concrete Test Specimens in the Field, ASTM C31/C31M-21a 2021.*

[57] *Methods for Determination of Compressive Strength of Concrete Cubes,* B.S. 1881: Part 116(1983), January 1983, pp. 1-8.

[58] *Standard Test Method for Splitting Tensile Strength of Cylindrical Concrete Specimens,* ASTM C496/C496M-17,2017.

[59] *Standard Specification for Ready-Mixed Concrete,* ASTM C94/C94M-23,2023

[60] *Standard Test Method for Diagonal Tension (Shear) in Masonry Assemblages,* ASTM E519/E519M, 2022.

[61] ACI Committee, "*Building code requirements for structural concrete (ACI 318-19) and commentary (ACI 318R-19)*," 2019: American Concrete Institute.

[62] R. Park, "Evaluation of ductility of structures and structural assemblages from laboratory testing," *J Bulletin of the new Zealand society for earthquake engineering,* vol. 22, no. 3, pp. 155-166, 1989.

[63] H. J. Jiang, Y. Ying, and B. Wang, "Experimental Investigation on Damage Behavior of RC Shear Walls," *Advanced Materials Research,* vol. 250, pp. 2407-2411, 2011.

[64] H. Zhang, J. Dong, Y. Duan, X. Lu, and J. Peng, "Seismic and Power Generation Performance of U-Shaped Steel Connected PV-Shear Wall under Lateral Cyclic Loading," *International Journal of Photoenergy,* vol. 2014, no. 1, p. 362638, 2014.

[65] H. Mamdouh, N. Zenhom, M. Hasabo, A. F. Deifalla, and A. Salman, "Performance of strengthened, reinforced concrete shear walls with opening," *Sustainability,* vol. 14, no. 21, p. 14366, 2022.

[66] D. F. Arafa, H. M. Salem, and M. E. Issa, "AN EXPERIMENTAL INVESTIGATION OF AN INNOVATIVE COUPLING TECHNIQUE OF CONCRETE SHEAR WALLS," *Journal of Al-Azhar University Engineering Sector,* vol. 11, no. 38, pp. 1-17, 2016.

الخلاصة

تبحث هذه الدراسة في تأثير الفتحات المتعددة على الأداء الإنشائي لجدران القص الكونكريتية المسلحة. تم إجراء برنامج تجريبي على تسعة عشر عينة جدار قص مربعة الشكل، طول ضلع كل منها 600 ملم. شملت الدراسة فحص تأثير حجم وشكل الفتحات (مربعة ودائرية)، سمك الجدار عند 80 و100 و120 ملم، مقاومة الخرسانة عند 30 و45 و60 ميجا باسكال، ونمط التسليح القطري حول الفتحات.

أظهرت النتائج أن زيادة حجم الفتحات في جدران القص الخرسانية المسلحة يؤدي إلى انخفاض في سعة التحمل النهائية للجدران. وعند نسب فتحات تبلغ 7.1%، 11.1%، 16.0%، و21.8%، تبيّن أن الجدران ذات الفتحات المربعة تُظهر انخفاضًا في سعة التحمل يصل إلى 81% عند نسبة 21.8%، في حين تنخفض السعة بنسبة 76% للفتحات الدائرية. كما يتضح أن شكل الفتحة يلعب دورًا مهمًا في سعة التحمل، حيث تتميز الفتحات الدائرية بتأثير أقل في السعة بالمقارنة مع الفتحات المربعة عند النسب المنخفضة للفتحات (7.1%، 11.1%، و16.0%). علاوة على ذلك، فإن زيادة سمك الجدار من 80 مم إلى 120 مم عند نسبة فتحة 16.0% تُحسّن سعة التحمل بنسبة تصل إلى 39% للفتحات المربعة و58% للفتحات الدائرية. وبالمثل، فإن زيادة قوة الخرسانة من 30 إلى 60 ميجا باسكال ترفع من سعة التحمل بنسبة 33% للفتحات المربعة و17% للفتحات الدائرية. تشير هذه النتائج إلى أن الجدران ذات الفتحات الدائرية تستفيد على نحو أكبر من زيادة السمك، في حين تحقق الجدران ذات الفتحات المربعة استفادة أكبر عند زيادة مقاومة الخرسانة من ناحية سعة التحمل.

وبالنسبة إلى المطيلية وامتصاص الطاقة، فإن حجم وشكل الفتحات يؤثران في نحو ملحوظ على هذه الخصائص. حيث عند نسبة فتحة تبلغ 21.8%، تسببت الفتحات المربعة في زيادة المطيلية بنسبة 23% وخفض امتصاص الطاقة بنسبة 81%، في حين أدت الفتحات الدائرية إلى زيادة المطيلية بنسبة 10% وانخفاض امتصاص الطاقة بنسبة 66%. بالإضافة إلى ذلك، أدت زيادة سمك الجدار عند نسبة فتحة 16.0% إلى تحسن ملحوظ في المطيلية بنسبة 34% للفتحات المربعة و4% للفتحات الدائرية، بينما ارتفع امتصاص الطاقة بنسبة 160% للفتحات المربعة و104% للفتحات الدائرية. ثم إنَّ زيادة قوة الخرسانة من 30 إلى 60 ميجا باسكال أدت إلى تحسين المطيلية بنسبة 11% للفتحات المربعة و19% للفتحات الدائرية، وزيادة في امتصاص الطاقة بنسبة 77% للفتحات المربعة و29% للفتحات الدائرية. بالإضافة إلى ذلك، أظهر النموذج الأول الذي يحتوي على تسليح قطري حول الفتحات الدائرية بنسبة 7.1% زيادة في المطيلية بنسبة 12% وارتفاعًا في امتصاص الطاقة بنسبة 80%، مما يعكس تحسينات ملحوظة بالمقارنة مع النموذج الثاني.

كما توضح الدراسة تأثير الفتحات في الجساءة القصية للجدران. حيث يُلاحظ أن الجدار بنسبة فتحة مربعة تبلغ 21.8% اظهر انخفاض في الجساءة بنسبة تصل إلى 74%، بينما يؤدي وجود فتحة دائرية بنفس النسبة إلى تقليل الجساءة بنسبة 80%. ويُظهر تأثير شكل الفتحة على الجساءة أن الفتحات الدائرية تؤدي إلى انخفاض أقل في الجساءة مقارنةً بالفتحات المربعة، خصوصاً عند نسب فتحات 7.1%، 11.1%، و16.0%. كذلك، أدت زيادة سمك الجدار عند نسبة فتحة 16.0% إلى تحسين الجساءة القصية بنسبة 18% للفتحات المربعة و50% للفتحات الدائرية. ثم إنَّ زيادة قوة الخرسانة عززت الجساءة بنسبة 51% للفتحات المربعة و35% للفتحات الدائرية عند رفع القوة من 30 إلى 60 ميجا باسكال.

قُيِّم تأثير التسليح القطري أيضاً، للجدران ذات الفتحات الدائرية بنسبة فتحة 7.1%. وقد أظهر النموذج الأول، الذي يتضمن طبقتين من التسليح التقليدي مع تسليح قطري، تحسناً في سعة التحمل النهائية بنسبة 20% وزيادة طفيفة في الجساءة بنسبة 4%. بينما حقق النموذج الثاني، الذي يحتوي على طبقة واحدة من التسليح التقليدي مع تسليح قطري، زيادة بنسبة 2% في سعة التحمل لكنه أظهر انخفاضًا بنسبة 5% في الجساءة بالمقارنة مع التسليح التقليدي.

جمهورية العراق
وزارة التعليم العالي والبحث العلمي
كلية الهندسة/ جامعة ميسان
قسم الهندسة المدنية

التصرف الإنشائي لجدران القص الخرسانية المسلحة ذات الفتحات مشبكة الشكل

رسالة
مقدمة الى كلية الهندسة في جامعة ميسان
كجزء من متطلبات الحصول على درجة الماجستير في علوم الهندسة المدنية / الانشاءات

اعداد الطالب
علي محمود عباس
بكالوريوس هندسة مدني 2018

بأشراف
الاستاذ الدكتور: سعد فهد رسن
الاستاذ المساعد الدكتور: حيدر عبد راضي

تشرين الثاني 2024